

INFLUENCE OF SCAFFOLD PROPERTIES
ON CELLULAR COLONIZATION
FOR TISSUE ENGINEERING

By

YAN HUANG

Bachelor of Science
Beijing Technology and Business University
Beijing, China
1996

Master of Science
Beijing University of Chemical Technology
Beijing, China
1999

Submitted to the Faculty of the Graduate College
Of the Oklahoma State University in
partial fulfillment of the
requirements for
the Degree of
DOCTOR OF PHILOSOPHY
May 2005

INFLUENCE OF SCAFFOLD PROPERTIES
ON CELLULAR COLONIZATION
FOR TISSUE ENGINEERING

Dissertation Approved:

Sundararajan V. Madhally

Dissertation Advisor

Randy S. Lewis

Guoliang Fan

Bahram H. Arjmandi

A. Gordon Emslie

Dean of the Graduate College

ACKNOWLEDGEMENTS

I am indebted to many people whose support I have received while researching and drafting this dissertation. Without their help this work would not have been possible. Among them I would like to express my deepest gratitude to my advisor, Dr. Sundar Madihally, for his excellent guidance, concern, and patience. His insight, precision, and dedication will continue to influence all my future work. I would also like to thank my committee members Dr. Lewis, Dr. Arjmandi, Dr. Fan, and Dr. Lin for their valuable suggestions. Thank you Mbonda and Stella for your important contributions, Dr. Lucas for your assistance in tissue sectioning, Phoebe for your assistance in confocal microscopy, and Eric for your advice on culturing stem cells.

The departmental staff have been more than kind and helpful. Eileen, Carolyn, Genny, Cara, Sam, and Emory: you have been invaluable; from package handling to paperwork, your role merits special mention. To our lab manager, Robert, your help saved me from infinite hardships in the laboratory. Aparna, Ali and Deva: your companionship has meant a lot to me. Last, but certainly not least, I would like to thank my family and friend Rustin for their support and encouragement.

TABLE OF CONTENTS

Chapter	Page
1. INTRODUCTION	1
2. BACKGROUND	10
2.1. Tissue engineering	10
2.2. Cell sources	12
2.3. Scaffolds	21
2.3.1. Natural matrices	21
2.3.2. Synthesized matrices	22
2.3.3. Scaffold processing	30
2.3.4. Scaffold properties	31
2.4. Cell-matrix interaction	35
2.4.1. Cell adhesion on 2D	35
2.4.2. Chemical stimulus	38
2.4.3. Mechanical stimulus	39
2.4.4. Cell interactions in 3D scaffolds	43
2.4.5. ES cell differentiation in 3D scaffolds	46
2.5. References	50
3. EFFECT OF SPATIAL ARCHITECTURE ON CELLULAR COLONIZATION	64
3.1. Introduction	64
3.2. Materials and methods	66
3.2.1. Formation of 2D membranes and 3D scaffolds for cell culture	67
3.2.2. Chitosan/PLGA scaffolds fabrication	67
3.2.3. Cell culture and seeding	68
3.2.4. Morphology characterization	69
3.2.5. Evaluation of cytoskeletal organization and viability	69
3.2.6. Cell proliferation analysis	70
3.2.7. Evaluation of DMPC internalization	71
3.2.8. Material stiffness evaluation	71
3.2.9. Statistical analysis	72
3.3. Results	72
3.3.1. Characterization of 3D chitosan scaffolds	72
3.3.2. Influence of 3D architecture on the morphology of HUVECs	74
3.3.3. Influence of 3D architecture on the proliferation of HUVECs	76

Chapter	Page
3.3.4. Influence of 3D architecture on the morphology of MEFs.....	78
3.3.5. Altering the structural features of chitosan with PLGA	80
3.3.6. Influence of emulsification on morphology of HUVECs	82
3.3.7. Cells are functional and alive.....	82
3.3.8. Alteration in material stiffness.....	85
3.4. Discussion.....	86
3.5. Conclusion	92
3.6. References.....	93
4. IN VITRO CHARACTERIZATION OF CHITOSAN-GELATIN SCAFFOLDS FOR TISSUE ENGINEERING	97
4.1. Introduction.....	97
4.2. Materials and methods	99
4.2.1. Formation of 2D membranes and 3D scaffolds	100
4.2.2. Stabilizing Chitosan and Chitosan-gelatin Scaffolds.....	100
4.2.3. Mechanical testing measurement.....	101
4.2.4. Degradation Characterization	101
4.2.5. Cell culture and seeding.....	102
4.2.6. Parallel-plate flow chamber system	103
4.2.7. Morphological analysis.....	105
4.2.8. Immunofluorescence staining.....	105
4.2.9. Flow cytometric analysis of PECAM-1	106
4.2.10. Statistical analysis.....	106
4.3. Results.....	106
4.3.1. Morphology of chitosan and chitosan-gelatin cylindrical scaffolds ...	106
4.3.2. Stabilizing chitosan and chitosan-gelatin scaffolds	107
4.3.3. Mechanical properties of chitosan-gelatin blends.....	110
4.3.4. Degradation kinetics of 3D scaffolds.....	113
4.3.5. Evaluation of cell activity	115
4.3.6. Cell adhesion on different membranes	115
4.3.7. Effect of shear stress on morphological changes of ECs.....	117
4.3.8. Cytoskeleton reorganization	119
4.3.9. PECAM-1 expression	123
4.4. Discussion.....	125
4.5. Conclusion	128
4.6. References.....	130
5. INFLUENCE OF MATRIX ARCHITECTURE ON ES CELL DIFFERENTIATION	135
5.1. Introduction.....	135
5.2. Materials and methods	137
5.2.1. Scaffold formation	137

Chapter	Page
5.2.2. Cell culture.....	138
5.2.3. Morphological analysis.....	138
5.2.4. Flow cytometry.....	139
5.2.5. Immunostaining.....	139
5.2.6. Statistical analysis.....	140
5.3. Results.....	140
5.3.1. EC differentiation in conditioned medium.....	140
5.3.2. Differentiation of ES cell on different substrates.....	142
5.3.3. 3D ES cell differentiation.....	145
5.4. Discussion.....	149
5.5. Conclusion.....	151
5.6. References.....	152
6. CONCLUSIONS AND RECOMMENDATIONS.....	154
6.1. Conclusions.....	154
6.1.1. Influence of architecture in the absence of cell-binding domain.....	155
6.1.2. Influence of architecture in the presence of cell-binding domain.....	156
6.1.3. Influence of matrix on ES cell differentiation.....	156
6.2. Recommendations.....	157
6.2.1. Study on the absorption and deposition of ECM components.....	157
6.2.2. Evaluation of stiffness of material in the surface.....	157
6.2.3. Cell behavior study on spatially well-defined patterns in 3D system...	158
6.2.4. Characterization of surface wettability and charge.....	158
6.2.5. Exploration on cellular signal transmitting structures in 3D culture...	160
6.3. References.....	161

LIST OF TABLES

Table	Page
2.1. Current methods used to differentiate ES towards ECs.....	20
2.2. Chemical structures and characteristics of natural and synthetic polymers	23
2.3. Molecular compositions in 2D and 3D cell-matrix adhesions.....	47
3.1. Stiffness properties of various architectures.....	87
4.1. Stiffness properties of blends.....	112
4.2 Comparison of parameters describing cell morphology change.....	122

LIST OF FIGURES

Figure	Page
1.1. Scheme showing three important scaffold properties.....	5
1.2. Research scheme showing scopes of this study.....	7
2.1. Principle of tissue engineering.....	11
2.2. Schematic demonstration of blood vessels (top) and an arterial wall in cross-section (bottom).....	13
2.3. Diagram of mouse ES cells differentiation stages.....	17
2.4. Diagram of ES differentiation defined by markers and committed lineages promoted by certain cytokines.....	17
2.5. Schematic showing ES cells differentiation into ECs protocols.....	19
2.6. Chitosan in its protonated form in solution: the positive charge is from the amine groups on the chain backbone.....	28
2.7. Scanning electron micrographs of mesh PLA and PLA coated with PLGA.....	28
2.8. Cells respond to distinct physical and biochemical properties of ECM.....	40
2.9. EC responses to shear stress in molecular mechanism.....	45
3.1. <i>In situ</i> scaffold formation.....	73
3.2. Effect of 3D architecture on spreading of HUVECs.....	75
3.3. Cellular organization and proliferation of HUVECs.....	77
3.4. Effect of 3D architecture on spreading of MEFs.....	79
3.5. Influence of emulsification on surface topology and shape of HUVECs.....	81
3.6. HUVECs are viable and functional after 2 days.....	83

Figure	Page
3.7. Influence of emulsification on shape of MEFs	84
3.8. Schematic showing the cell colonization characteristics on different architectures	88
4.1. Schematic of perfusion system consisted of parallel plate chamber.....	104
4.2. Microarchitecture of chitosan-gelatin scaffolds.....	108
4.3. Effect of neutralization method on chitosan-gelatin scaffolds	109
4.4. Mechanical properties.....	111
4.5. Degradation characteristics of chitosan-gelatin scaffolds.....	114
4.6. Activity of MEFs in 3-D matrices	116
4.7. Effect of blending on the spreading of HUVECs	118
4.8. Effect of shear stress on the spreading of HUVECs	120
4.9. Effect of shear stress on actin assembly and PECAM-1 expression	124
5.1. Effect of EC medium on ES cell differentiation after two weeks of incubation	141
5.2. Histogram profiles of CD31 and Flk-1 expression showing ES differentiation after sixteen days incubation in EC medium.....	143
5.3. ES cells were differentiated on different substrates with the absence of LIF.....	144
5.4. Effects of different substrates on ES cell differentiation	146
5.5. Flow cytometric analysis of ES cells on different substrates after 12 days of differentiation.....	147
5.6. Phase contrast (A) and fluorescence micrographs stained with actin (B), showing ES cells within 3D chitosan matrices	148
6.1. Schematic showing the adsorption of proteins to the surfaces (A) and evaluation of influence of scaffold stiffness on cell behavior	159

LIST OF ABBREVIATIONS

2D: two dimensional

3D: three dimensional

ACL: anterior cruciate ligament

AFM: atomic force microscopy

ALP: alkaline phosphatase

BAEC: bovine aortic EC

bFGF: basic vascular endothelial growth factor

BMC: bone marrow cells

BrdU: bromodeoxyuridine

CFDA-SE: carboxyfluorescein diacetate-succinimidyl ester

CM: compression molding

CVD: cardiovascular disease

DAG: diacylglycerol

DD: degree of deacetylation

DMEM: Dulbecco's modified Eagle medium

DMPC: 1,2-dimyristoyl-sn-glycero-3-phosphocholine

DMSO: dimethyl sulfoxide

DPB: dense peripheral band

EB: embryoid bodies

EC: endothelial cells

ECGF: endothelial cell growth factor

ECGS: EC growth supplement

ECM: extracellular matrix

EDTA: ethylenediaminetetraacetic acid

EGF: epidermal growth factor

EGM: EC growth medium

EPC: endothelial progenitor cell

ERK: extracellular signal-regulated kinase

ES: embryonic stem

EthD-1: ethidium homodimer

FACS: fluorescence-activated cell sorting

FAK: focal adhesion kinase

FBS: fetal bovine serum

FD: fiber depositing

FGF: fibroblast growth factor

GAG: glycosaminoglycans

HDF: human dermal fibroblasts

HSPC: hematopoietic stem/progenitor cells

HSVECs: human saphenous vein ECs

HUVEC: human umbilical vein endothelial cell

Hyp: (Gly)-proline (Pro)-hydroxy proline

ICAM: intercellular adhesion molecule-1

ICM: inner cell mass

IP3: inositol triphosphate

JNK: c-Jun NH₂-terminal kinase

LDL: acetylated-low-density lipoprotein

LIF: leukemia inhibitory factor

MACS: magnetic-activated cell sorting

MAP: mitogen-activated protein

MCP-1: monocyte chemoattractant protein-1

MEF: mouse embryonic fibroblast

MFB: myofibroblasts

MFs: actin microfilaments

MHC: major histocompatibility complex

MMPs: matrix metalloprotenases

MT: microtubules

MTOC: microtubule organizing center

MW: molecular weight

NFκB: nuclear factor kappa B

NOS: nitric oxide synthase

P3HB: hydroxybutyrate

PBS: phosphate buffered saline

PCL: polycaprolactone

PDGF: platelet-derived growth factor

PEG: polyethylene glycol

PET: polyethyleneterephthalate

PHA: polyhydroxyalkanoates

PHB: poly (hydroxybutyrate)

PLGA: poly lactide-co-glycolide

PMMA: poly (methyl methacrylate)

PPF-DA: poly (propylene fumarates)-diacrylate

PU: polyurethane

REDV: Arg-Glu-Asp-Val

RGD: arginine-glycine-aspartate

SDS: sodium dodecyl sulfate

SEM: scanning electron microscopy

SMC: smooth muscle cell

SSEA-1: stage-specific embryonic antigen-1

TCP: tissue culture plate

tPA: tissue plasminogen activator

UCB: umbilical cord blood

YIGSR: Tyr-Ile-Gly-Ser-Arg

CHAPTER 1

INTRODUCTION

Tissue loss or organ failure remains one of the devastating and costly issues in human health care; more than \$400 billion is spent on these patients each year in the United States (www.researchandmarkets.com). In most situations, therapy for dysfunctional organs requires transplantations. However, the need for organs far outnumbers the organs available, many people die while waiting for an organ transplant (US transplant net work). Cardiovascular diseases (CVD) remain No.1 killer in the US since 1918 according to the American Heart Association. There are about 64,400,000 Americans who have one or more types of CVD. In 2001, CVD accounted for 38 percent of all deaths of 1,408,000 cases. The pathology of CVD in most situations requires surgeries and replaceable tissues. Thus there is an overwhelming and growing need for substitutes to replace or repair damaged tissues or organs. Current therapies involve autografting from the patient, allografting from a donor, xenografting from animal resources and artificial medical devices. Several problems associated with autografting include lack of availability of sufficient or suitable tissues or organs for multiple surgeries due to the pathological state of the patients. Allografting raises the problem of immunological rejection, whereas xenografting adds the potential risk of disease transmission. Medical devices, such as the artificial heart, have problems of infection, lack of biocompatibility and limited durability (Shieh and Vacanti 2005). While all

therapies have a significant impact on improving health, new approaches that seek to overcome the limitations need to be developed.

Tissue engineering has emerged as a new field of regenerating tissues or organs, utilizing specific combination of cells and scaffolds with the goal to repair or restore tissue or organ functions. The principle approach is to grow cells in three dimensional (3D) scaffolds; the scaffolds guide cells to proliferate, organize and produce their own extracellular matrix (ECM), further facilitating tissue or organ functions *in vitro*; and constructed cell seeded scaffold composites can be later used as for *in vivo* transplantation (Griffith and Naughton 2002). Tissue engineering strategies differ from other therapies in that the engineered tissue becomes an integrated part of the body, providing a potentially permanent and specific cure of the disease.

The pre-requisite for *in vitro* tissue engineering is to incorporate living cells with elicited function within the scaffold so that the cells can express desired phenotypic characteristics of targeted tissues. Although some of the tissue engineered products including skin grafts, cartilage substitutes, and heart valves are already in the market, the mechanism of how cells interact with material is not fully realized and investigated. Failures resulting from insufficient cell ingrowth within the scaffold are due to poor cell-material interactions. Cell interaction with the surrounding ECM plays a critical role in regulating cellular activities including cell proliferation, migration, differentiation, and apoptosis (Ranucci and Moghe 2001; Beningo, Lo et al. 2002; Schwartz and Ginsberg 2002). Cells attach to ECM via transmembrane proteins (integrins) which link ECM to the cytoskeleton (actin) through focal adhesions composed of a complex set of proteins including focal adhesion kinase (FAK) (Hynes and Zhao 2000). Chemical and

mechanical signals from ECM are transmitted to the cell cytoplasm and nucleus through the complex transduction processes. These signals subsequently influence cell morphology and activity. Scaffold characteristics (i.e. materials and structures), therefore, play a significant role in influencing signal transmitting structures and cellular behavior. The variations in material can greatly alter surface chemistry (i.e. wettability), and mechanical strength. Materials containing cell-binding sequences (i.e. adhesive peptides) can facilitate cell adhesion and growth while materials without cell-binding domain have relatively weak interaction with cells. Substrate stiffness is another important parameter in regulating cell spreading. The substrate should have sufficient rigidity to withstand cell tractional forces when cells are attaching.

A majority of the cell-material interactions have been studied in two dimensional (2D) matrices. However, 2D studies can not be directly transcribed to 3D conditions as a number of factors are changing. For example, cells cultured on 2D matrices spread on a single flat plane unlike 3D matrices which provide spatial advantages for cell attachment as well as cell-cell organization. Interestingly, it is not clearly understood how the microarchitecture influences cell colonization. Factors such as material stiffness, pore sizes, void fractions, and surface features in 3D system are different from 2D matrix. How these factors and the interplay of these scaffold properties affect cellular colonization and function need to be explored to understand the mechanisms involved. This will provide a basis for designing scaffolds that can elicit appropriate cellular responses and lead to successful regeneration of tissues.

The cell sources compose another important component in tissue engineering. When autologous cells are not available due to the morbidity of the sites and concerns of

infection and immunogenicity of allogenic or xenogenic cells, embryonic stem (ES) cells serve as a potential cell source due to their self-renewal characteristic and potential to differentiate into any cell type. Recent studies have shown *in vivo* function of cells derived from ES cells in animal model. Mouse ES (mES) derived neural progenitors promote recovery from Parkinson's disease in a rat model (Kim, Auerbach et al. 2002) probably by interacting with the host to produce myelin in the brain and spinal cord (Brustle, Jones et al. 1999). Unlike many ES cells, CCE cell lines derived from 129/sv mouse strain have been modified to grow on gelatin-coated surfaces without the presence of fibroblast feed-layer. This modification minimizes fibroblasts complexity in the culture.

This research is focused on how the scaffolds properties (pore size/structure), stiffness and chemical compositions (i.e. cell-binding domain) can affect cellular activity by monitoring cell-matrix interactions (**Figure 1.1**). Chitosan (a polysaccharide) based matrices were used to understand the influence of various factors. Also, three different cell types representing different cellular characteristics were used to understand the influence of cells from different origins.

1) Human umbilical vein endothelial cells (HUVECs) line the lumen of the blood vessel, act as barrier for transport of molecules, and are exposed to haemodynamic conditions such as flow and pressure variations.

2) Mouse embryonic fibroblasts (MEFs) present in connective tissues, synthesize collagen which contributes to increased tissue strength and are not exposed to haemodynamic flow.

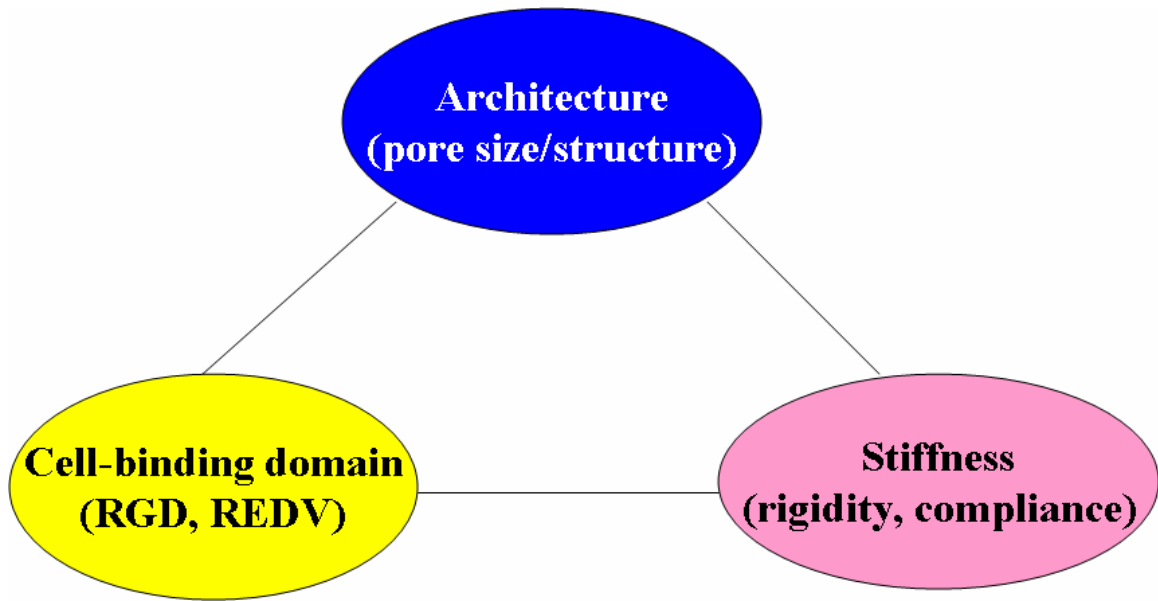


Figure 1.1. Scheme showing three important scaffold properties.

3) Murine embryonic stem (mES) cells provide a good model for an *in vitro* differentiation and proliferation study.

The underlying hypothesis of this study is: ***“architecture plays a dominant role in regulating cellular colonization and spreading in 3D scaffold rather than the presence of cell-binding domain in materials. However, cell-binding domain is important in 2D membranes”***. The scheme of research used to test this hypothesis is summarized in **Figure 1.2**.

Specific aim 1: To investigate the influence of scaffold architecture without cell binding domain on cellular colonization.

Chitosan and poly (lactide-co-glycolide) (PLGA) were used to study the influence of spatial architecture on cellular colonization. Since these materials don't contain cell-binding domain, cell adhesion to these materials tend to be non-receptor-mediated. The way scaffolds are synthesized can greatly change the scaffold properties such as architecture (i.e. pore size, structure), wettability, and compliance. Also, the blending of synthetic polymer PLGA with different molecular weight (MW) into chitosan scaffolds can alter scaffold architecture as well as chemical cues. To characterize the influence of these factors, cytoskeletal organization, morphology and proliferation in response to 2D, 3D chitosan and PLGA-chitosan scaffolds were compared. Further, the stiffness of 2D, 3D chitosan, and PLGA-chitosan scaffolds were analyzed (described in chapter 3).

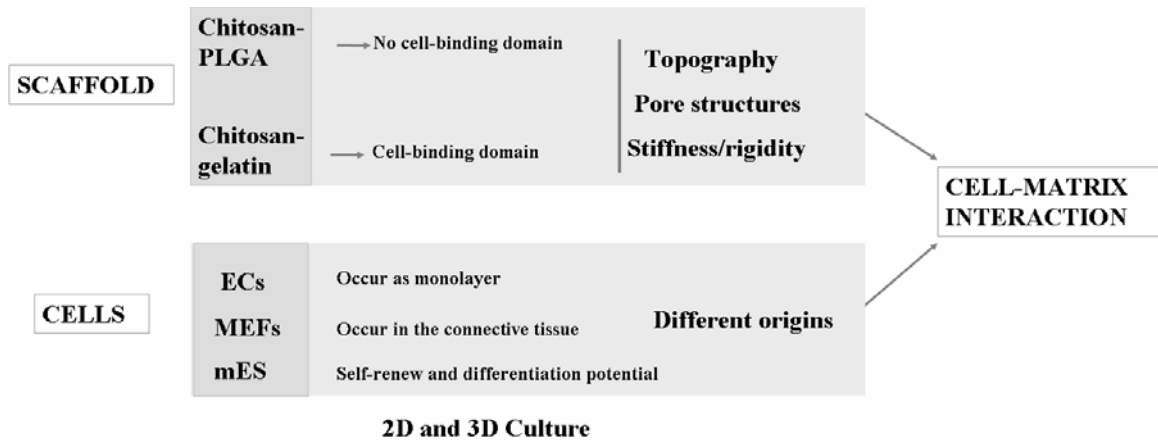


Figure 1.2. Research scheme showing scopes of this study.

Specific aim 2: To study the influence of spatial architecture in the presence of cell-binding domain (gelatin) on cellular activity.

Gelatin which contains cell-binding domain was blended with chitosan to study the effects of spatial architecture on cellular activities in the presence of cell-binding domain. Blending gelatin with chitosan can greatly affect cell-matrix interaction as well as scaffold properties (i.e. pore size, degradation characteristics and mechanical properties). Since the cellular function and structure in response to shear stress is different from the cells under the static conditions, it is important to investigate how the cells behave when exposed to shear stress in order to further understand cell-gelatin/chitosan interactions (discussed in chapter 4).

Specific aim 3: To study the influence of matrix architecture on mES cell morphology and differentiation.

mES was used to analyze *in vitro* EC differentiation potential under the stimulus of defined growth factors and varied matrix components. The effect of EC medium on ES cell differentiation into EC was studied, suggesting an important role of cytokines in regulating differentiation signal and process. Further, the influence of chitosan on ES cell differentiation was evaluated: the cell morphology of ES cells grew on chitosan and chitosan-gelatin was compared with gelatin; mES cells were also seeded into 3D chitosan matrices, and the cell organization was studied (described in chapter 5).

This study showed a significant influence of scaffold properties presented in 2D and 3D forms on cellular colonization (described in chapter 6). The conclusions are summarized in chapter 6 along with recommendations for future studies.

REFERENCES

www.researchandmarkets.com/reportinfo.asp?report_id=39127&cat_id=106

US transplant net work www.ustransplant.org

Beningo, K. A., C. M. Lo, et al. (2002). "Flexible polyacrylamide substrata for the analysis of mechanical interactions at cell-substratum adhesions." Methods Cell Biol **69**: 325-39.

Brustle, O., K. N. Jones, et al. (1999). "Embryonic stem cell-derived glial precursors: a source of myelinating transplants." Science **285**(5428): 754-6.

Griffith, L. G. and G. Naughton (2002). "Tissue engineering--current challenges and expanding opportunities." Science **295**(5557): 1009-14.

Hynes, R. O. and Q. Zhao (2000). "The evolution of cell adhesion." J Cell Biol **150**(2): F89-96.

Kim, J. H., J. M. Auerbach, et al. (2002). "Dopamine neurons derived from embryonic stem cells function in an animal model of Parkinson's disease." Nature **418**(6893): 50-6. Epub 2002 Jun 20.

Ranucci, C. S. and P. V. Moghe (2001). "Substrate microtopography can enhance cell adhesive and migratory responsiveness to matrix ligand density." J Biomed Mater Res **54**(2): 149-61.

Schwartz, M. A. and M. H. Ginsberg (2002). "Networks and crosstalk: integrin signalling spreads." Nat Cell Biol **4**(4): E65-8.

Shieh, S. J. and J. P. Vacanti (2005). "State-of-the-art tissue engineering: from tissue engineering to organ building." Surgery **137**(1): 1-7.

CHAPTER 2

BACKGROUND

2.1. TISSUE ENGINEERING

Tissue engineering has emerged as a novel field exploring a vast array of living cells which can restore, maintain, or enhance tissues and organs. The constructed tissues provide a potential alternative for tissue or organ replacements and treatments (Griffith and Naughton 2002). The principal therapeutic approach for treating damaged tissues involves: (i) establishing biopsied cells or stem cells (autologous, allogeneic and xenogeneic); (ii) placing the cells into 3D biocompatible scaffolds (both natural or synthetic) with various shapes and structures in a static or dynamic culture environment such as a bioreactor which can provide mechanical stimulations as well as sufficient nutrients (the seeded cells can proliferate and organize to produce their own ECM under the guidance of scaffolds); and (iii) implanting the constructed scaffolds at the injured location. While in the host, the scaffolds are degraded, reabsorbed, or metabolized to restore, maintain or improve tissue functions (**Figure 2.1**).

There are three key elements in tissue engineering: i) cell source (cell component), ii) scaffolds and iii) regulations of cell-material interactions. Based on the tissue being developed, specified cells and scaffolds are chosen and designed. In this research, our interests focus on vascular applications. Each element involved in tissue engineering will be discussed in the context of vascular applications.

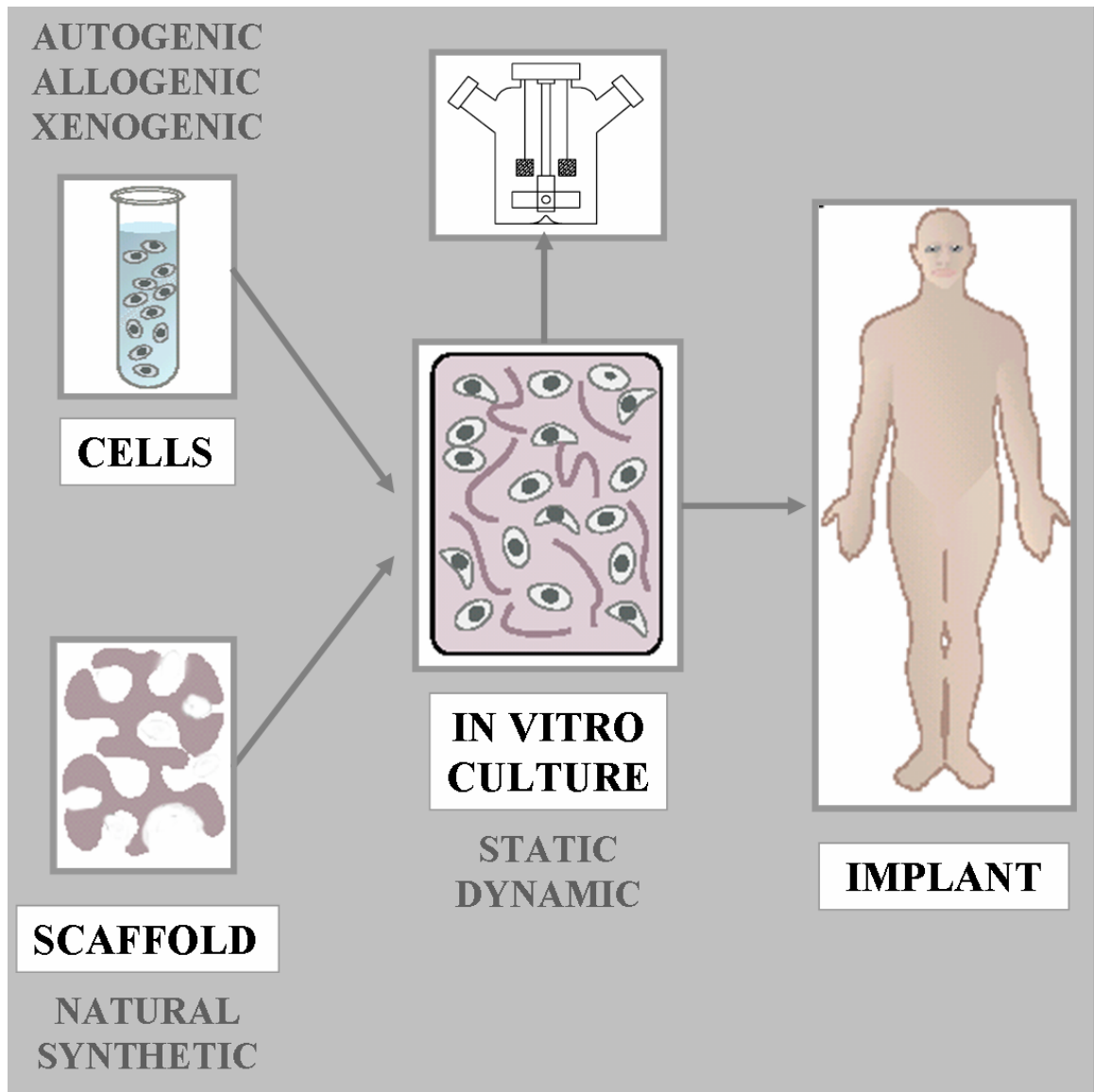


Figure 2.1. Principle of tissue engineering.

2.2. CELL SOURCES

Mature cells

An important consideration in tissue engineering is the cell sources required for colonizing the biodegradable matrices. Cells typically seeded *in vitro* are tissue specific mature cells and can be isolated from different tissues, such as keratinocytes, ECs, fibroblasts, chondrocytes, hepatocytes and cardiomyocytes. Most autologous cells used in vascular tissue engineering are shown in **Figure 2.2**. Cell sources should be a) easily accessible, b) able to expand without losing phenotype and tissue-specific functional characteristics, and c) least immunologic to the host (Shieh and Vacanti 2005). Primary cells derived from the patient (autogenic cells) are the ideal sources since they avoid immunological problems. However, these cells are often hard to harvest in sufficient quantities due to the patient's pathology state. Primary cells from donors (allogeneic cells) or other species (xenogeneic cells) can give rise to the problems of immune rejection by the patient and disease transmission. Hence, they have restricted usage. In addition, due to the limited number of cells that can be obtained and the time-consuming requirements to expand cells *in vitro*, further improvement to attain higher efficacy for harvesting cells is needed for further clinical application (Mooney 2001).

Immature cells and adult stem cells

To address the limitations of cell sources, other alternative sources have been investigated. Recent studies have shown that endothelial progenitor cells (EPC) obtained from peripheral blood provide a suitable cell source for lining vascular grafts. These bone marrow-derived EPCs home in on sites of endothelial injury (Kaushal, Amiel et al. 2001; He, Shirota et al. 2003).

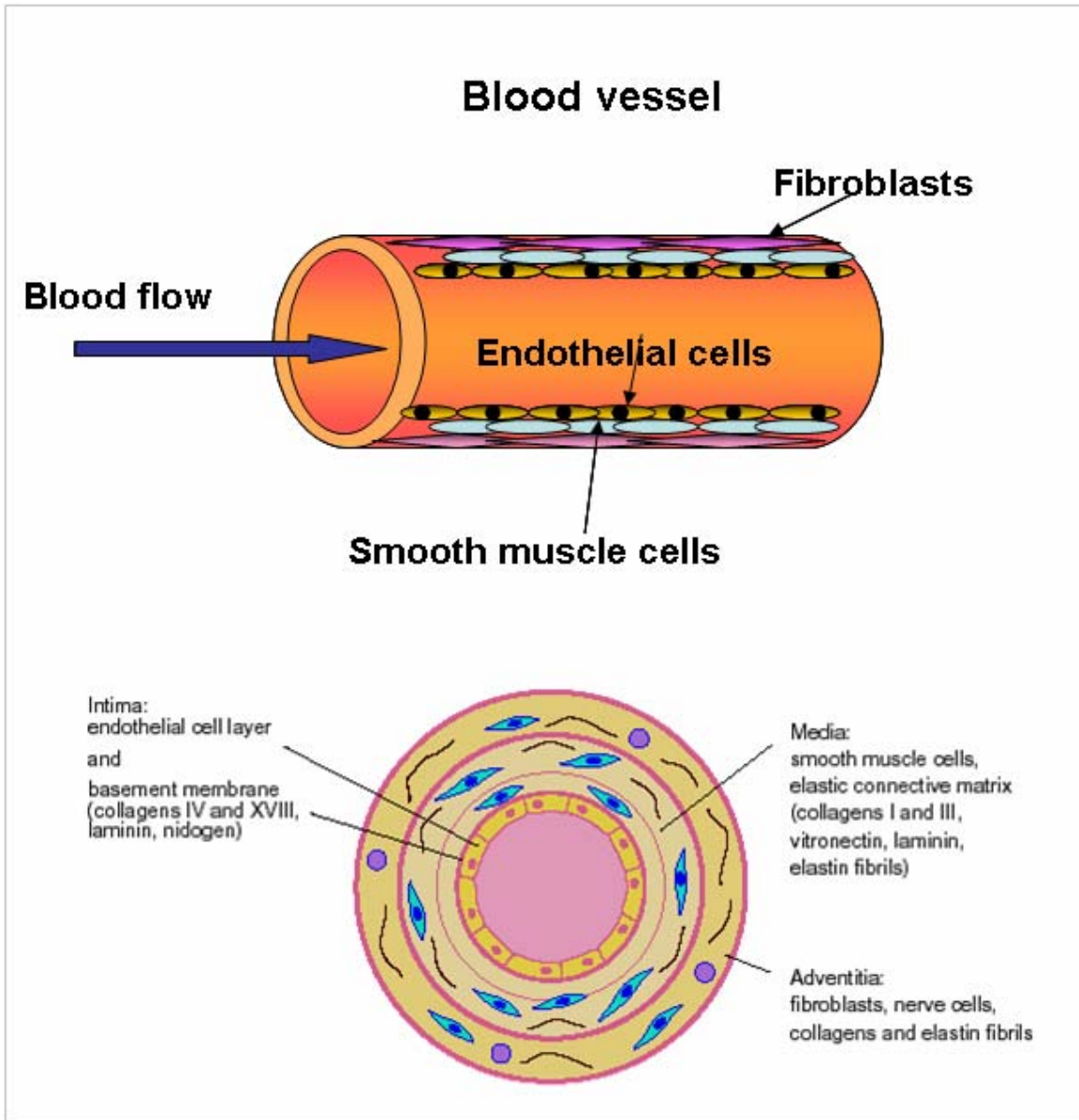


Figure 2.2. Schematic demonstration of blood vessels (top) and an arterial wall in cross-section (bottom).

The advantages of using EPCs are their accessibility and simplicity in recapitulating vascular structures. To acquire the more optimized quality and quantity of EPCs; several issues remain to be addressed such as identification of a specific marker, EPC purification and evaluation of EPC transdifferentiation in vitro (Mooney 2001; He, Shirota et al. 2003).

Comparable to these adult-derived progenitor cells, stem cells are primitive cells with the capacity of self-renewal and differentiation potential. There are three kinds of stem cells: adult stem cells derived from adult or fetal tissues, ES cells derived from very early blastocyst stage embryos (Mummery 2004) and cells derived from umbilical cords (neonatal stem cells). Adult stem cells including mesenchymal, hematopoietic, neural, muscle and hepatic stem cells are being actively investigated (Hori, Inoue et al. 2004; Mayer, Bertram et al. 2005; Sartori, Spiezia et al. 2005). Bone marrow cells are the most studied adult stem cells and have been used for decades in the successful treatment for blood-related disorders. Recently, bone marrow stem cells have also been explored with the potential to differentiate into mesenchymal lineages such as adipocytic, chondrocytic, or osteocytic lineages (Shieh and Vacanti 2005). There has been an increasing use of human umbilical cord blood (UCB) as an alternative to bone marrow and hematopoietic stem/progenitor cells (HSPC). A number of cord blood transplantations have been performed to date for treatment of various disorders including malignant diseases, bone marrow failures, hemoglobinopathies and inborn errors of metabolism (Gluckman 2000). But problems associated with the isolation and differentiation compose a number of technical obstacles for the production of the large number of desirable cells needed to create tissue.

Embryonic stem (ES) cells

ES cells have emerged as a potential source for tissue engineering. ES cells are pluripotent cell lines with the capacity of unlimited self-renewal and differentiation potential. The first mES cell lines were isolated from inner cell mass (ICM) (Evans and Kaufman 1981). The promise of these cells lies in their ability to self-renew indefinitely *in vitro* without losing their ability to differentiate into every cell type of every organ of the mouse (Keller 1995). ES cell differentiation is discussed in detail below.

The established ES cell lines show the ability to differentiate into multiple lineages (Martin and Evans 1975). Pluripotent mES cells can be maintained in undifferentiated state either on feed layer of mitotically inactivated embryonic fibroblasts or on gelatin coated surfaces in the presence of leukemia inhibitory factor (LIF) *in vitro* (Keller 1995). Without these conditions, the ES cells can form 3D spherical cellular aggregates, termed embryoid body (EB). Since its isolation, ES cells have heralded a breakthrough for development biology in providing a unique tool to genetic engineering for introducing gene knock-outs and genome manipulation. Also, ES research makes it possible for the study of mechanisms underlying embryonic development and cell lineage specification. Using ES cells in tissue engineering applications has been an alternative option with the development of human ES cells in 1998 (Thomson, Itskovitz-Eldor et al. 1998).

ES cells have special characteristics from other cells or cell lines. They exhibit high nuclear to cytoplasm ratio, shorter G1 cell cycle phase and grow in compact, multilayered colonies (Savatier, Huang et al. 1994). The differentiation stage of mES cell can be marked by expression of stage-specific embryonic antigen-1 (SSEA-1) and germ line-specific transcription factor Oct-4 (Solter and Knowles 1978; Scholer, Hatzopoulos et al.

1989). Both markers can be expressed at high levels in undifferentiated state while downregulated upon differentiation. They also have a high alkaline phosphatase (ALP) activity and high telomerase activity (Prelle, Zink et al. 2002).

When ES cells are plated in liquid or methyl cellulose containing media, or directly seeded on stromal cells in “hanging drops”, they can facilitate formation of EB (Keller 1995). Cells in EB undergo differentiation with formation of an outer layer of endoderm-like cells, development of an ectodermal rim and generation of mesodermal cells (Wobus, Guan et al. 2001) (**Figure 2.3**). By manipulation of the differentiation stimuli, enriched cell populations for cardiomyocytes (Muller, Fleischmann et al. 2000), haematopoietic lineages (Nishikawa, Nishikawa et al. 1998); (Choi, Kennedy et al. 1998) and neural lineages (Schuldiner, Eiges et al. 2001; Murashov, Pak et al. 2004) from EB can be achieved. The methods used to induce differentiation include addition of chemical inducers (i.e. retinoic acid) (Dinsmore, Ratliff et al. 1996), conditioned medium (Levenberg, Golub et al. 2002; Kaufman, Lewis et al. 2004), cytokines (Vittet, Prandini et al. 1996; Lieber, Keller et al. 2003) and coculture with other cells (Nishikawa, Nishikawa et al. 1998; Fair, Cairns et al. 2003). Changing the ECM components can also induce ES cell differentiation into various cell types. Some of the factors used for restricting lineage differentiation are summarized in **Figure 2.4**.

EC differentiation

In close association with hemopoietic precursor cells are the differentiation of ECs within blood islands of the yolk sac (Risau 1995). This finding led to the hypothesis that ECs and blood cells may share the common precursor. Flk-1, one of the receptors for VEGF, is the earliest differentiation marker for endothelial and blood cells. Flk-1⁺VE-

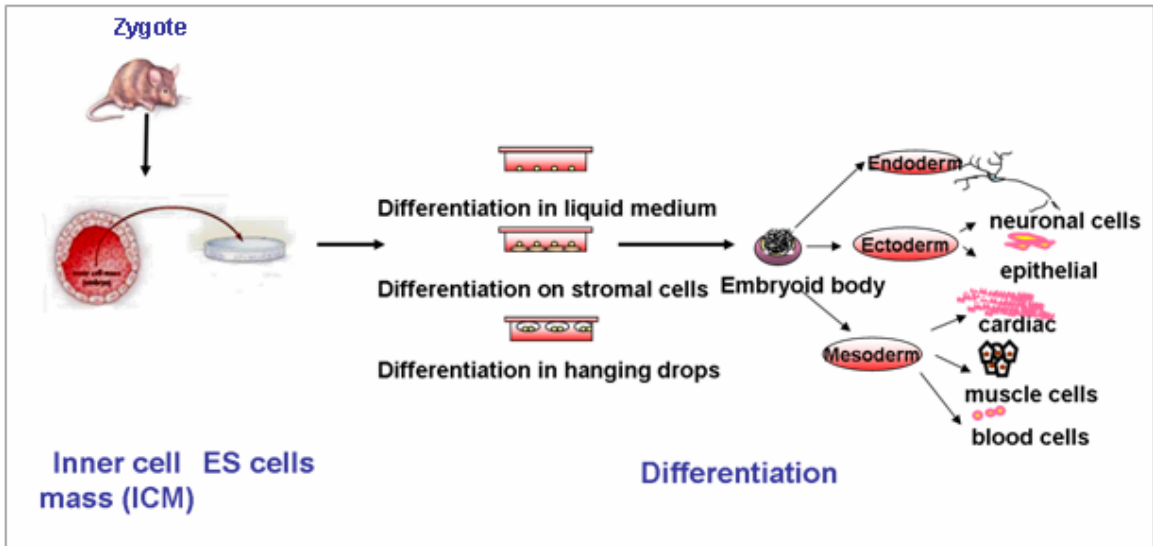


Figure 2.3. Diagram of mouse ES cells differentiation stages.

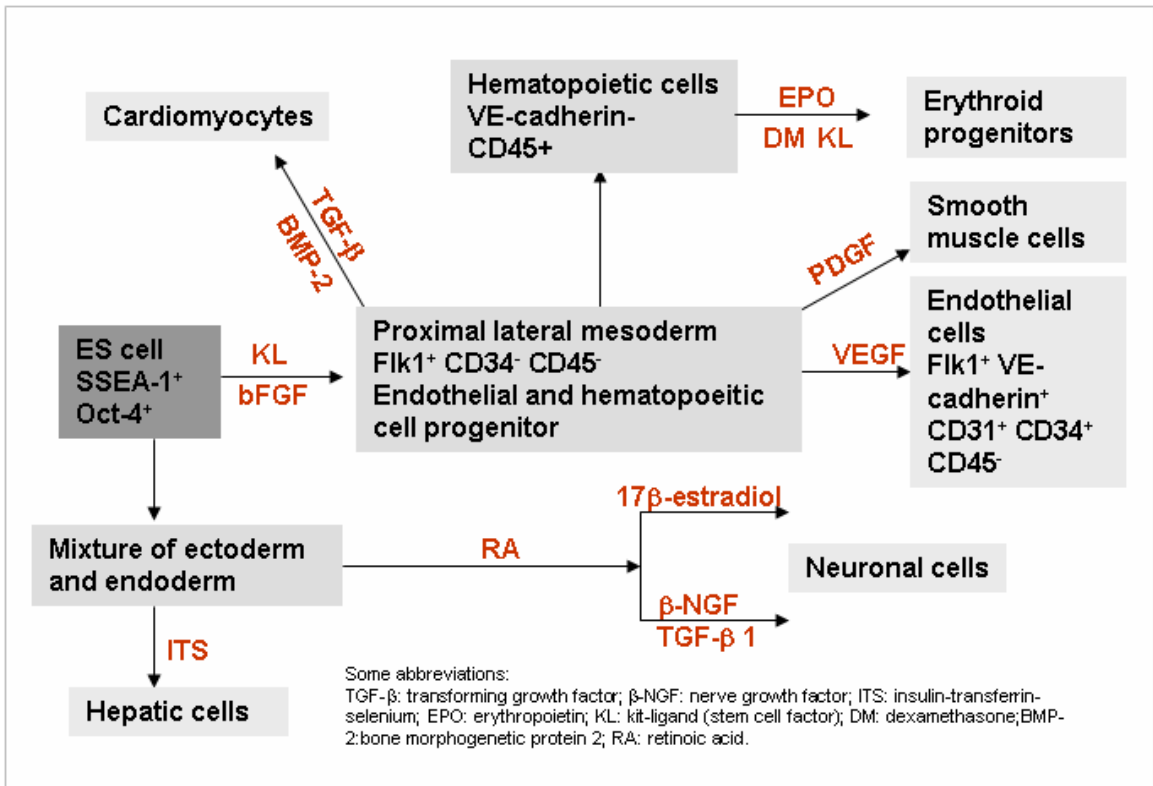


Figure 2.4. Diagram of ES differentiation defined by markers and committed lineages promoted by certain cytokines.

cadherin⁺ cells could be the diverging point of hemopoietic and EC lineages (Nishikawa, Nishikawa et al. 1998) (**Figure 2.5**). Further, Flk-1⁺ cells can give rise to both ECs and blood cells *in vitro* (Yamashita, Itoh et al. 2000). By controlling the level and type of cytokines, the ES cells can be directed to differentiate into ECs. A higher percentage of ECs can be obtained using combined growth factors (Saito, Ugai et al. 2002).

Particularly, VEGF has been found to promote the differentiation of Flk-1⁺ cells (Nishikawa, Nishikawa et al. 1998). More purified ECs are achieved when ES cells are cultured with EC growth medium (EGM-2) with combined growth factors, and this method has been used by many researchers (Levenberg, Golub et al. 2002; McCloskey, Lyons et al. 2003; Kaufman, Lewis et al. 2004). Earlier studies on EC differentiation followed the step of EB formation, where EB provided a suitable model to study the mechanism involved in vasculogenesis (Vittet, Prandini et al. 1996). The study of Nishikawa et al. (Nishikawa, Nishikawa et al. 1998) challenged that the differentiation of EB is pre-requisite for EC differentiation. They circumvented the intermediate step of 3D differentiation of EB, allowing direct 2D monolayer differentiation. Not only did this method improve differentiation efficiency, the functions of derived EC cells are comparable to the specific matured cells by expressing many EC surface antigens and genes (McCloskey, Lyons et al. 2003). Type IV collagen supports Flk-1⁺ cell differentiation more efficiently (Nishikawa, Nishikawa et al. 1998; Hirashima, Kataoka et al. 1999). Since both matured ECs and ES cells in embryonic development are constantly exposed to shear stress, mechanical stimuli also influence EC differentiation (Yamamoto, Sokabe et al. 2004). The current protocols differentiating ES cells into ECs are demonstrated in **Figure 2.5** and summarized in **Table 2.1**.

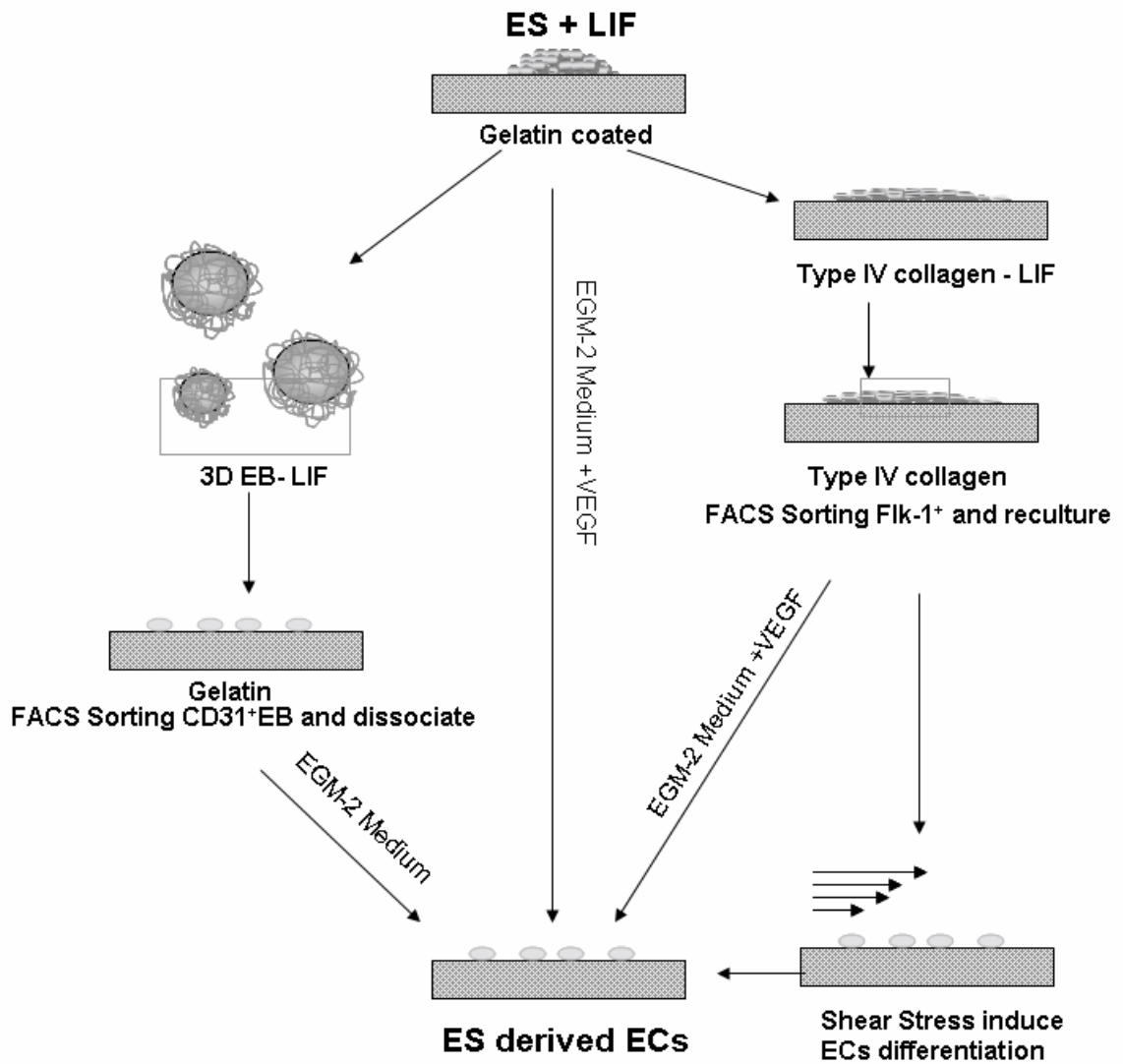


Figure 2.5. Schematic showing ES cells differentiation into ECs protocols.

Cell line	Differentiation method	Markers	Reference
129/sv-derived CCE, CJ7, R1	Plated on 1% methylcellulose-containing medium in Petri dishes up to 11 days, further supplemented with 50 ng/mL VEGF, 2 U/mL erythropoietin EPO, 100 ng/mL FGF, 210 ng/mL, murine interleukin-6 (IL-6).	PECAM-1, Flk-1, and VE-cadherin	Vittet, Prandini et al. 1995
CCE ES from Dr. Evans MJ)	Cultured on IV collagen-coated dishes in a minimal essential medium with 10% FCS, 5×10^{-5} mol/L, 2-mercaptoethanol, Flk-1 ⁺ VE-cadherin ⁺ E-cadherin ⁺ cells induced Flk-1 ⁺ cells, recultured 10 cells/mm ² on feeder layer with mFit-1, hVEGF, human placenta growth factor (PlGF), 20 ug/mL VE-cadherin.	FLK-1, E-cadherin, CD34, VE-cadherin, and DiI-Ac-LDL staining	Hirashima, Kataoka et al. 1999
CCE ES from Dr. Evans	Transferred to gelatin-coated dishes to remove MEFs, 10 ⁴ cells transferred to each well of IV collagen-coated 6-well dishes in aMEM with 10% FCS and 5×10^{-5} M B-mercaptoethanol for 4 days to induce Flk-1 ⁺ , further Flk-1 ⁺ E-cadherin ⁺ cell sorted on type IV collagen and on OP9 stromal cell layer.	Platelet-derived growth factor receptor (PDGFR), Flk-1, VE-cadherin, Ter 119, and CD45	Nishikawa, Nishikawa et al. 1998
CCE ES from Dr. Evans	Plated 2×10^4 cells flk-1 ⁺ on IV collagen coated 24-well dishes in differentiation medium. Flk-1 ⁺ cells on serum-free with VEGF (50 ng/mL), PDGF. Before 3D culture, Flk-1 ⁺ cells in 50 ng/mL VEGF medium on uncoated Petri dishes for 12h, in collagen I gel 3D culture with 10% FCS and 50 ng/mL VEGF to form tube structures.	Flk-1, VE-cadherin, CD31, CD34, endoglin, and acetyl-LDL	Yamashita, Itoh et al. 2000
E-1, E-2	ES (P18) 10 ⁴ per well in medium with 10% FBS, 10 ng/mL stem cell factor (SCF), 10 ng/mL bFGF, 10 ng/mL oncostatin M (OSM) for 10 days; EC like cells cultured another 7-10 days.	GATA-4, Flk-1, and GAPDH	Saito, Ugai et al. 2002
hES(H9clone)	To form EBs, cells were grown in Petri dishes in medium without LIF and bFGF. Isolated CD31 ⁺ cells grew on plate coated with 0.1% gelatin in EGM-2 for 6 passages.	CD31, CD34, VE-cadherin, Flk-1, GATA-2/3, and AC133/CD133	Levenberg, Golub et al. 2002
Rhesus monkey ES (R366.4 cell line)	Differentiated in EGM-2 for 29 days, subcultured and expanded.	CD31, VE-cadherin, VWF, Flk-1 and CD34	Kaufman, Lewis et al. 2004
ES-D3	ES were transferred to collagen type IV-coated dishes, sorted Flk-1 ⁺ cells, replated in EGM-2 medium with 50 ng/mL VEGF.	CD31, Flk-1, E-cadherin, and CD34	McCloskey, Lyons et al. 2003

Table 2.1. Current methods used to differentiate ES cells towards ECs.

Many other somatic cell types have also been derived from mES or hES cells, such as neuronal cells (Rolletschek, Chang et al. 2001; Schuldiner, Eiges et al. 2001), hematopoietic cells (Kaufman, Hanson et al. 2001), cardiomyocytes (Sachinidis, Fleischmann et al. 2003), chondrocytes (Kramer, Hegert et al. 2000), insulin-secreting cells (Soria, Roche et al. 2000), hepatocytes (Fair, Cairns et al. 2003) and adipocytes (Dani, Smith et al. 1997).

2.3. SCAFFOLDS

2.3.1. Natural matrices

Decellularized biological scaffolds which have decreased antigenicity are being explored for regenerating vascular tissues. A decellularized scaffold is obtained by removing cells with their surface antigens by treating with detergents and enzymes, leaving a well-preserved acellular matrix which provides support for cell ingrowth and tissue regeneration (Xue and Greisler 2003). Allogenic acellular scaffolds have decreased antigenicity and thus are used as a primary choice for decellularized scaffolds. Decellularized human saphenous vein scaffold was developed using sodium dodecyl sulfate (SDS) to remove cells (Schaner, Martin et al. 2004). After treatment of the natural vein, it was found that the ECM component of collagen and elastin remained unchanged, while achieving adequate mechanical strength (burst and suture-holding). Xenogeneic acellular scaffolds have been used when there is a limited supply of human materials. Human ECs and myofibroblasts (MFB) were seeded on decellularized porcine matrix and cultured under pulsatile flow conditions. Although ECs grew into monolayers, there was partial endothelialization (Teebken, Bader et al. 2000), similar to other studies (Schaner, Martin et al. 2004). Xenogeneic acellular scaffolds also have the

disadvantage of eliciting significant chronic inflammation and interspecies immunogenicity (Xue and Greisler 2003).

2.3.2. Synthesized matrices

An alternative to natural matrices is to synthesize scaffolds using different material processing techniques. Both natural and synthetic materials have been used in tissue engineering application. While natural materials have the benefits of facilitating cell adhesion and repopulation by providing critical signals, they lack tailorability of mechanical properties. On the contrary, synthetic materials possess advantages of easy control of microstructure, strength and degradation rate, but they lack required cell signals (Xue and Greisler 2003). Chemical structures and characteristics of several polymers are summarized in **Table 2.2**. A few of the widely investigated materials are discussed below.

Collagens are a family of structural proteins reinforcing a variety of animal tissues including skin, bone, and tendon. Type I collagen is a major component of most connective tissues and present in the arterial wall (Xue and Greisler 2003). Extracellular collagen may be degraded by several matrix metalloprotenases (MMPs) (Tam, Wu et al. 2002). Collagen contains integrin-binding domains which can facilitate cell adhesion. Considering its unique biological properties, collagen has been extensively used in vascular tissue engineering. Weinberg and Bell first constructed complete biological blood conduits using collagen as support to embed bovine SMC and fibroblasts (Weinberg and Bell 1986). Collagen failed to show requisite mechanical strength despite reinforcing with Dacron. To improve the mechanical properties of collagen scaffolds, a number of techniques have been used including cyclical strain at a frequency of 1Hz

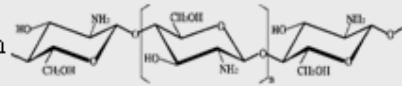
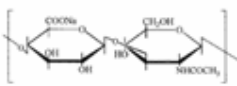
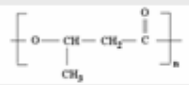
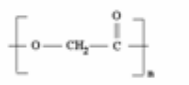
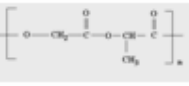
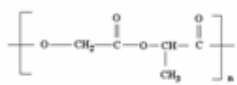
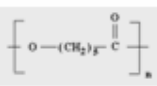
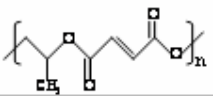
	Materials	Characteristics
Natural	Chitosan 	Analog to GAG; cationic nature; minimal immune response; can be degraded by lysozyme; easy to process and blend with other materials (Suh and Matthew 2000).
	Collagen	Contains integrin-binding domains; weak mechanical properties (Weinberg and Bell 1986).
	Gelatin	Contains high levels of amino acid sequence of Gly-Pro-Hyp; can be modulated through many function groups (Mao, Zhao et al. 2003).
	Hyaluronan 	Degradation rate can be tailored; does not elicit any inflammatory response; difficult to modify to specified application (Turner, Kielty et al. 2004).
	Fibrin	Provides binding sites for cell receptors; needs to be blended with other materials to produce good mechanical properties (Akassoglou and Strickland 2002).
	PHB 	Highly crystalline, brittle and have very long degradation time (Griffith 2002).
	Decellularized matrix	Has ECM components as well as required mechanical strength; limited supply; lack of enough bioactivity; may elicit immunoresponsive inflammation (Xue and Greisler 2003).
Synthetic	PGA 	Highly crystalline and is hydrophilic; relatively better biocompatibility than PLA (Seal, Otero et al. 2001).
	PLA 	Hydrophobic; high mechanical strength (Xue and Greisler 2003).
	PLGA 	Degradation rate can be monitored; toxic degradation products (Hasirci, Lewandrowski et al. 2001).
	PCL 	Low melting temperature; long degradation time (Gunatillake and Adhikari 2003).
	PPF 	Properties rely on the synthesis process; used in bone tissue engineering (Gunatillake and Adhikari 2003).

Table 2.2. Chemical structures and characteristics of natural and synthetic polymers used in tissue engineering.

(Seliktar, Black et al. 2000). Significant increases in ultimate stress, material modulus and circumferential orientation was compared with static conditions.

Gelatin, a partially denatured derivative of collagen, has also been used to generate scaffolds. Gelatin is widely found in nature, and can be extracted from collagen found in fish, bovine bone and porcine skin. Gelatin contains high levels of amino acid sequences of glycine (Gly)-proline (Pro)-hydroxy proline (Hyp) and a unique protein structure that provides a wide range of functional properties (Mao, Zhao et al. 2003). The physicochemical properties of gelatin can be suitably modulated due to the existence of many functional groups. Gelatin has been shown to activate macrophages and has high hemostatic effect (Mao, Zhao et al. 2003). Although the vascular application is not extensively investigated, gelatin is blended with chitosan as artificial skin and cartilage applications due to the ability to form a polyelectrolyte complex (Mao, Zhao et al. 2003; Xia, Liu et al. 2004).

Chitosan is a polysaccharide derived from N-deacetylation of chitin, the second largest polysaccharide in nature. Chitin is present in the outer shells of crustaceans. Chitosan is composed of β (1-4) linked 2-acetamido-2-deoxy-D-glucose and 2-amino-2-deoxy-D-glucose units (**Table 2.2**). Chitosan is a semi-crystalline polymer, and the crystallinity of chitosan is dependent on the degree of deacetylation. Because structurally analogous to glycosaminoglycans (GAG), chitosan produces properties similar to ECM. Since GAG has specific interactions with growth factors/proteins, chitosan may share similar activity. Chitosan is insoluble in water or organic solvents but soluble in aqueous acids (pH < 6.3), which provides convenience for processing chitosan into different

shapes. Due to the protonation of the free amine groups on the chain backbone (**Figure 2.6**), chitosan exhibits a high charge density in solution. The cationic nature and high charge density allow favorable interactions with negatively charged cells as well as antibacterial activity. Chitosan is widely investigated in wound dressing (Risbud, Hardikar et al. 2000) and drug delivery systems. The biocompatibility and biodegradability of chitosan makes it a promising application in tissue engineering (Suh and Matthew 2000). Chitosan has shown biological support towards diverse cell types including ECs, chondrocytes, osteoblasts, hepatocytes, and Schwann cells. In addition, chitosan has minimal immune reaction and its stimulatory effect can induce local cell proliferation. Chitosan can be degraded by lysozyme, a naturally occurring enzyme *in vivo*. The biodegradation time is determined by the amount of residual acetyl content, a parameter that can be easily varied. Another significant feature of chitosan is that it can be processed into porous structures with orientated direction (Madihally and Matthew 1999). Due to the active amino groups, chemical modification of chitosan can produce materials with a variety of physical and mechanical properties. Polysaccharide scaffolds were synthesized by crosslinking arabinogalactan, dextran and amylose with chitosan to create a cell compatible environment (Ehrenfreund-Kleinman, A.J. et al. 2003). Chitosan is also blended with collagen, alginate, GAGs and synthetic polymers (i.e. PLGA, PCL) to fabricate suitable scaffolds (Mei, Chen et al. 2005). In all, the pH dependent solubility, the easy process ability under mild condition, the modification reactivity, the biodegradability, and biocompatibility make chitosan an excellent candidate for use as porous scaffolds in tissue engineering.

Hyaluronan (HyA), a large linear GAG, is composed of repeating disaccharide of D-N-acetylglucos-amine- β -D-Glucuronic acid (Lee and Spicer 2000). It is negatively charged, acting as a polyelectrolyte in solution, and as a lubricant (Tadmor, Chen et al. 2002). Although HyA is involved in mediating cell adhesion as an ECM component, it lacks control on the degradation rate (Seal, Otero et al. 2001). Thus, many applications have focused on more hydrophobic HYAFF-11, which is formed from esterification of all free carboxylic groups with benzyl alcohol from HyA (Turner, Kielty et al. 2004). Since esterification produces an increased hydrophobic polymer, the degradation rate can be tailored through hydrophobicity control (Seal, Otero et al. 2001). HYAFF-11 has been shown to support human venous ECs attachment, proliferation, and ECM synthesis (Turner, Kielty et al. 2004). However, due to the weak mechanical properties, long-term studies are needed to further evaluate the application used as vascular grafts.

Fibrin has been used for cartilage repair (Westreich, Kaufman et al. 2004). Upon injury, fibrinogen self-assembles to become 3D fibrin hydrogel (Seal, Otero et al. 2001). Fibrin can bind to different integrin receptors to regulate cytokine gene expression as well as regulate inflammation. Since fibrinogen can be obtained from the patient's own blood, use of fibrin minimizes immunogenic concerns. Another advantage of fibrin is that fibrin can be degraded by cell-associated enzymatic system. Despite these advantages, fibrin scaffolds failed to keep shape integrity by significant reduction in size after *in vitro* incubation and weak compression modulus (Ting, Sims et al. 1998), suggesting a need for further modifications.

Polyhydroxyalkanoates (PHA) are polyesters produced by biological processes (in microorganisms) and the molecular weight of these polymers can be tailored by varying

bacterial strain and media composition (Griffith 2002). The most widely studied and the simplest among these polyesters is polyhydroxybutyrate (P3HB). Most of these homopolymers are highly crystalline, brittle and have a very long degradation time (up to years). Thus they are not suitable for scaffolding materials unless blended with other materials compensating for the disadvantages.

Poly glycolic acid (PGA) and poly lactic acid (PLA) are the most investigated synthetic bioresorbable polyesters in tissue engineering. PGA is a rigid thermoplastic material with high crystallinity and is hydrophilic (Seal, Otero et al. 2001). Common processing techniques can be used to fabricate PGA into various forms such as woven or non-woven mesh (**Figure 2.7**), which can provide a 3D matrix for cell attachment due to high porosity (>95 %). In addition, degradation rates and mechanical properties can be altered by varying processing methods. PLA is more hydrophobic than PGA due to an extra methyl group in the lactide molecule. Because lactic acid is a chiral molecule, PLA has D-PLA and L-PLA stereoisomeric forms. Possessing high mechanical strength, L-PLA is more frequently used in tissue engineering (Xue and Greisler 2003). However, its application has been limited because of its stiffness and hydrophobicity. Many research groups introduced polyethylene glycol (PEG) to enhance the hydrophilicity and flexibility of PLLA (Wan, Chen et al. 2003; Lai, Liao et al. 2004).

PLGA is the copolymer of glycolic acid and lactic acid. Various ratios of PLGA have been investigated. 50:50 PLGA is widely investigated in various tissue engineering applications, since it is amorphous, and degrades faster. The degradation of PLGA is via random hydrolysis of ester bonds. In addition, the degradation rate can be tuned by the copolymer ratio and molecular weight (Gunatillake and Adhikari 2003). However, the

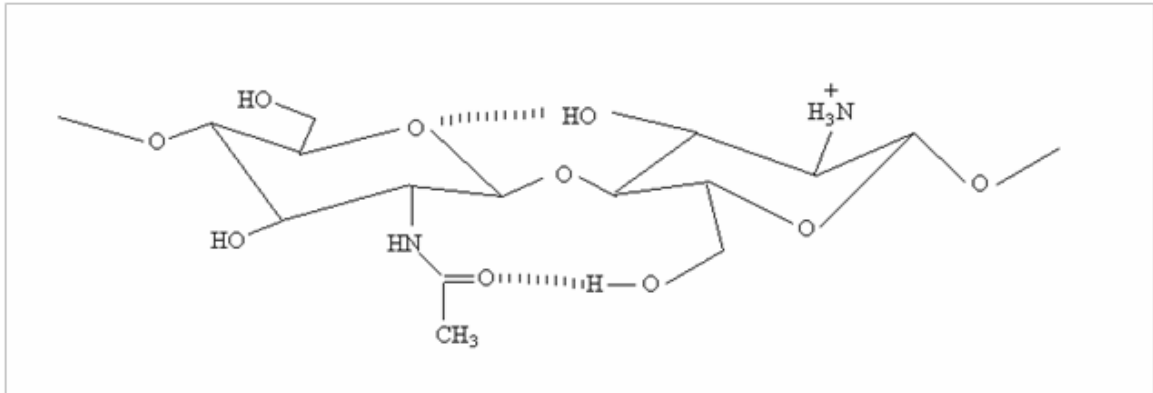


Figure 2.6. Chitosan in its protonated form in solution: the positive charge is from the amine groups on the chain backbone.

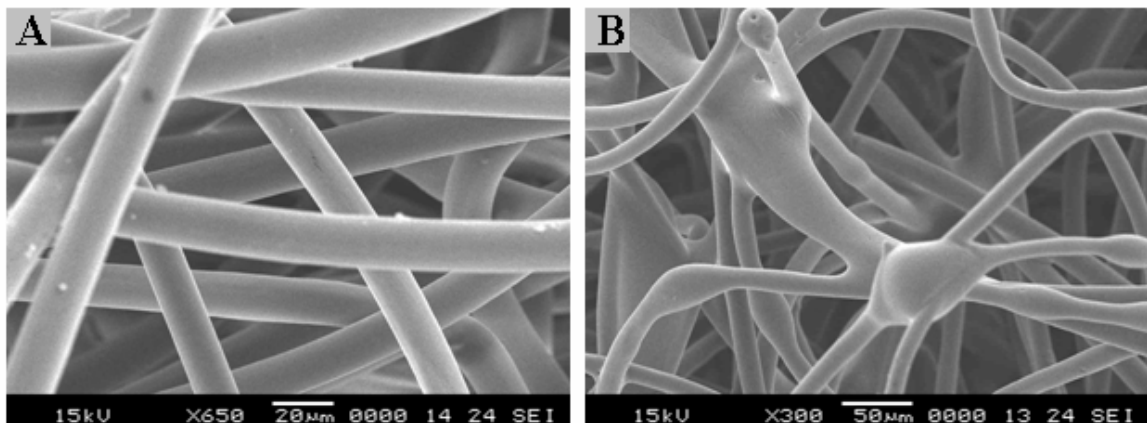


Figure 2.7. Scanning electron micrographs of mesh PLA (A) and PLA coated with PLGA (B).

biocompatibility of these materials is a problem because the synthetic polymers don't possess cell-anchoring sites and the toxic acid degradation products elicit inflammatory responses (Hasirci, Lewandrowski et al. 2001).

Poly (caprolactone) (PCL) is an aliphatic polyester and is considered as a non-toxic and biocompatible material (Gunatillake and Adhikari 2003). The ring-opening polymerization of ϵ -caprolactone produces a semicrystalline polymer with a glass transition temperature of about $-60\text{ }^{\circ}\text{C}$ and low melting temperature of $59\text{-}64\text{ }^{\circ}\text{C}$. Due to its low melting point, it can be blended with a range of other polymers (Gunatillake and Adhikari 2003). PCL has a degradation time of the order of two to three years which make it unsuitable for short term implants (Middleton and Tipton 2000). The rate of degradation can be altered by copolymerization with other polymers. Copolymers of ϵ -caprolactone with d, l-lactide have been synthesized to accelerate the degradation rate (Pitt, Gratzl et al. 1981).

Poly (propylene fumarates) (PPF) based polymers have been developed as injectable materials for orthopedic applications. The advantages of injectable materials are that the materials can be injected directly into cavities of irregular shape and size in a minimally invasive manner, thus avoiding any long-term stress-shielding effects around the wound site (Timmer, Ambrose et al. 2003). PPF can be photo cross-linked with poly(propylene fumarate)-diacrylate (PPF-DA) by free radical polymerization to form solid polymeric networks with high compressive strength at fracture site suitable for consideration for bone replacement (Fisher, Dean et al. 2002). The degradation of PPF produces fumaric acid and propylene glycol and the degradation time is dependent on the polymer structures (Gunatillake and Adhikari 2003). When tested in rats, a mild

inflammatory response initially occurred although a high compressive strength was achieved (Peter, Miller et al. 1998).

Other synthetic polymers such as polyanhydrides, tyrosine-derived polycarbonates, polyurethanes and polyphosphazenes have also been investigated as biodegradable polymers (Gunatillake and Adhikari 2003). Although the degradation rate and mechanical properties can be readily controlled, they lack the ability to modulate cellular activity. Surface modifications which incorporate cell adhesive components on the materials have been extensively investigated (Teebken and Haverich 2002; Yoon, Song et al. 2004).

2.3.3. Scaffold processing

Several techniques have been developed to fabricate porous scaffolds, including solvent casting/particulate leaching (Lee, Kim et al. 2004), fiber bonding (unwoven meshes) (Mooney, Baldwin et al. 1996), gas foaming (Riddle and Mooney 2004), and phase separation/emulsification (Chun, Cho et al. 2004). PGA mesh scaffolds have been formed using fiber bonding method, which involves joining PGA fibers in PLLA solution at the cross-point above the melting temperature followed by dissolving PLLA to create porous structures (Mikos, Bao et al. 1993). Another method to fabricate porous scaffolds is to introduce porogen such as salt (NaCl) into the process (particulate leaching). The leaching of salt from a polymer composite can form pores within scaffolds, the pore sizes are dependent on the size and amount of salt crystals and are difficult to control. Gas porogen has been used as alternative to eliminate the use of organic solvents (gas foaming). But the pores created in this method are not interconnected, limiting cell seeding and migration (Mooney, Baldwin et al. 1996).

Another technique to fabricate porous scaffolds is using phase separation. A homogeneous system with multicomponents can become thermodynamically unstable and separate into more than one phase under lower temperature. The polymer-rich phase solidifies after the solvent is removed, leaving porous structures. The pore size and structures can be easily controlled by freezing temperature, the ratio of polymer solution to water, and the solvents. Phase separation method is advantageous over other methods since it eliminates the extra washing/leaching step.

Besides these processes, scaffolds with different interconnecting pore structures were developed by compression molding (CM) and fiber depositing (FD) (Miot, Woodfield et al. 2005) and scaffolds with nanofibers can be produced using electrospinning process (Li, Laurencin et al. 2002; Lee, Shin et al. 2005). Recently, solid freeform fabrication (SFF) has been developed to create scaffolds from direct control using computer-generated models. This technique involves constructing 3D scaffolds by a series of cross-section layers (Sachlos, Reis et al. 2003). Systems using SFF currently are 3D printing, stereolithography, fused deposition modeling and phase-change jet printing. SFF allows exact control of the internal microstructure and tissue shape; however, problems such as residue removal and poor mechanical strength arise. The intertwining of SFF with other methods has promising potential to create optimized scaffolds.

2.3.4. Scaffold properties

Scaffolds form the template for cell colonization and should have the following basic properties: (1) biocompatible, bioresorbable and biodegradable during tissue regeneration process, (2) porous with an interconnected network to enable rapid tissue

ingrowth through pores, and to allow unimpaired diffusion of nutrients, oxygen and wastes, (3) suitable surface properties (wettability, stiffness, and compliance) to support cell attachment, proliferation and differentiation, and (4) provide sufficient mechanical strength to withstand stresses at the site of implantation (Vacanti, Morse et al. 1988).

Influence of scaffold properties on mature cell behavior

The architecture of the tissue-engineered scaffold is an important design consideration that can modulate cellular behavior for further clinical application. A highly porous scaffold is desirable, since it can support the growth of tissue for the necessary nutrients transport. The major architecture features include pore size, porosity, fiber orientation, pore interconnectivity, topography and scaffold stiffness.

Pore size is the determinate factor for tissue ingrowth, because pore sizes affect cell binding, migration, depth of cellular ingrowth, cell morphology and phenotypic expression (O'Brien, Harley et al. 2005). Importantly, appropriate pore size provides structural advantages to allow cells to spread into the pores through “bridges” from adjacent cells. There is an “optimum size range” for supporting cell ingrowth. Outside this range, cells fail to spread and form networks. The optimal pore size range depends on the materials as well as cell types (Teebken and Haverich 2002), and a lot of cells have preference to pore size which is bigger than the cell size. For example, a minimum pore size of 150 μm and 200-250 μm are suggested for bone and soft tissues (Cooper, Lu et al. 2005). Vascular SMCs were found to preferentially bind to pore sizes ranging from 63 to 150 μm while dermal fibroblasts (mFb) showed no selectivity to pore sizes tested in L-PLA scaffolds (Zeltinger, Sherwood et al. 2001). Proliferation of human dermal fibroblasts (HDF) were found to be limited in the pore size of 500-1000 μm in PLGA-

PCL mesh due to the difficulty for the cells to cross large bridging distances (Ng, Khor et al. 2004). Pore sizes not only affect cell growth, but also affect scaffolds properties, such as elasticity of microporous scaffolds increased with the number of pores within the scaffolds (Doi, Nakayama et al. 1996).

Porosity also plays an important role in regulating cell adhesion and migration. High porosity provides a high surface area for cell-matrix interactions, sufficient space for ECM regeneration, uniform and efficient cell seeding (Agrawal and Ray 2001). Many scaffolds with the porosity >90% were found to support cell proliferation (Freed, Vunjak-Novakovic et al. 1994; Ishaug-Riley, Crane-Kruger et al. 1998). Higher porosity could also lead to increased cell adhesion (Marois, Sigot-Luizard et al. 1999). Pore interconnectivity increases the overall surface area for cell attachment and facilitates cell ingrowth in the scaffolds. Increased interconnectivity and porosity also affect the deposition of ECM elements (Miot, Woodfield et al. 2005).

Fiber orientation within a scaffold could also affect tissue regeneration. Scaffolds made of oriented PCL nanofibers (700 nm in diameter) were found to promote phenotypic differentiation of chondrocytes compared with 2D nonporous membranes (Li, Laurencin et al. 2002). This study did not investigate the influence of fiber orientation. However, another study showed that significantly more collagen was synthesized by fibroblasts on aligned nanofibers than randomly orientated fibers despite similar proliferation (Lee, Shin et al. 2005). Cells seeded on oriented fibrous structures tended to maintain phenotypic shape and had guided growth according to nanofiber orientation. A hypothesis is that spindle-shaped and oriented fibroblasts in the direction of aligned fibers mimic *in vivo* condition better and thus produce more ECM. Further studies are

necessary to understand the mechanisms involved in these cell-matrix and cell-cell interactions.

Topography of scaffold surface significantly influences spreading characteristics and activity of cells. The existence of grooves may inhibit cell movement to bend its cytoskeleton (Clark, Connolly et al. 1987) or reshape its actin filaments to adjust to the new topography (Walboomers, Croes et al. 1999). Curtis proposed a term “topographic reaction” to describe that cells react as a response to substratum in microscale through changes in cell orientation, motility, and adhesion (Curtis and Wilkinson 1999). ECs cultured on 15, 30, 60 μm wide collagen strips showed complete alignment on 15 μm wide strips and migration along the strip. It was found that focal adhesions in cells on 15 μm wide strips were oriented with their lamellipodial protrusion and the direction of cell migration (Li, Bhatia et al. 2001). Roughness can significantly increase cell migration area (Lampin, Warocquier et al. 1997). Surface topographies at even small scale can affect cell activities. HUVEC adhesion and growth were significantly enhanced in membranes with higher roughness (Chung, Liu et al. 2003). However, the mechanisms for enhanced cell behavior are not completely understood.

Scaffold stiffness is another factor that could affect cell behavior. Cellular function of various cell types are influenced by stiffness of the substrate (Lee, Grodzinsky et al. 2001; Freyman, Yannas et al. 2002; Sieminski, Hebbel et al. 2004). Cells show reduced spreading and disassembly of actin even when soluble adhesive ligands are present in weak gels (Pelham and Wang 1997; Lo, Wang et al. 2000); muscle cell spreading could fit a hyperbolic curve when $E < E_{\text{Muscle}}$ (12 ± 4 kPa) (Engler, Griffin et al. 2004). This could be via the response of tractional forces between cell and materials; scaffold should

be able to withstand cell contractional forces (Sieminski, Hebbel et al. 2004). Maximum tractional force generated by a cell could be as much as 10-15% of substrate modulus (Lo, Wang et al. 2000). The degree of anisotropy of the substratum determines the elongation of cells. Cells on circular deformable collagen gels show significantly less elongation than cells on rectangular gels except at the edges. In contrast, ECs adopt elongation in the direction of narrow strips and less in the direction perpendicular to the strips of rigid tissue culture plates (Thoumine, Ziegler et al. 1995). Further, the rigidity of the scaffolds may affect the formation of ECM which can affect cellular activity (Wozniak, Modzelewska et al. 2004). Quantification of orientation correlation function between two cells showed that cell tractions can affect coalignment of adjacent cells. The stiffness of the matrix that fits cell spreading may be tissue specific with different cell types requiring different stiffness. The effect of stiffness on cellular behavior may be related to changes in adhesive proteins and tyrosine phosphorylation (Pelham and Wang 1997).

2.4. CELL-MATRIX INTERACTION

When cells are seeded onto various materials, they begin to interact with the material, receiving signals to synthesize proteins, remodel the scaffolds and grow into the scaffolds. Understanding how the cells interact with the scaffolds and respond to various stimuli is important to design scaffolds which favor cell ingrowth and successful tissue regeneration.

2.4.1. Cell adhesion on 2D

Cells attach to ECM through transmembrane integrins and communicate from inside of the cells to the outside environment. Integrins are composed of α , β subunits, to

link ECM to the cytoskeleton through focal adhesions (Hynes and Zhao 2000). $\alpha_v\beta_1$, $\alpha_5\beta_1$ and $\alpha_v\beta_3$ are important members of the integrin family in cell survival and proliferation. Integrins bind to ECM proteins via RGD, YIGSR or REDV binding sequences. RGD is the most widely studied cell adhesive oligopeptide which can be found in fibronectin, laminin, collagen and vitronectin. RGD has been applied to incorporate into different surfaces to improve cell adhesion and spreading (Drumheller and Hubbell 1994; Burdick and Anseth 2002). The viability of HUVECs on the GRGD grafted surfaces increased with the increased GRGD concentration (Chung, Lu et al. 2002). Different peptides may preferentially support adhesion of certain cell types. REDV has been shown to allow EC adhesion but not fibroblasts, smooth muscle cells or platelets (Hubbell, Massia et al. 1991). Developing surface modifications with selected proteins to facilitate specific cellular attachment can be another strategy to regulate tissue regeneration. However, cell migration, proliferation and ECM production on surfaces modified with adhesive ligands of RGDS were found to be lower than non-coated surfaces (Mann and West 2002). 3D PLGA scaffolds with the inner pore surface modified with GRGDY showed more proliferation and more efficient differentiation of mouse bone marrow cells relative to unmodified scaffolds (Yoon, Song et al. 2004). Thus, presence of cell adhesive ligands on the surface of 3D scaffold may improve cell-material as well as cell-cell interactions. A more complete understanding of cell material interaction is needed to allow the scaffold to elicit appropriate cellular responses.

Once integrins bind to ECM they cluster and form focal adhesion complexes with cytoskeletal proteins like talin, vinculin and α -actinin but low levels of tensin. Further, a variety of cellular signaling pathways such as tyrosine phosphorylation of focal adhesion

kinase (FAK) and paxillin are activated (Burrige, Petch et al. 1992; Short, Talbott et al. 1998; Sastry and Burrige 2000). The focal adhesions are dynamic structures, which assemble, disperse and turn over when cells migrate. Adhesion sites may disappear and new sites form, cells constantly probe and reprobe the substratum (Davies, Barbee et al. 1997). FAK plays an essential role in regulating cytoskeleton assembly and focal adhesion turn over during cell migration. Fibrillar adhesions are another kind of adhesions, where integrin associates with fibronectin fibrils. Fibrillar adhesions consist of elongated fibrils or dots and demonstrate high levels of tensin with little phosphotyrosine (Zaidel-Bar, Cohen et al. 2004).

Cell-cell and cell-matrix interactions are very important in maintaining cell integrity and restoration (Lee and Gotlieb 2003). Two cytoskeletal proteins i) actin microfilaments (MFs) and ii) microtubules (MT) are important in repairing and maintaining the structural integrity. MFs have two distributions in the cells: one located in the central part (stress fibers) and the other at the periphery as a continuous dense peripheral band (DPB). DPB is more associated with cell-cell adhesion while stress fibers are important in cell-substratum adhesion (Lee and Gotlieb 2003). MT polymerization is associated with local destabilization of focal adhesions, thus the state of MT may regulate focal adhesion assembly and affect organization of stress fibers (Sastry and Burrige 2000). All together, MFs, MT and their associated adheren junctions and focal adhesions are important regulators of adhesion, spreading, migration and cell integrity.

2.4.2. Chemical stimulus

Tissue or organ regeneration is driven by the combined action of a variety of soluble factors. Understanding the roles of these soluble factors provide useful tool to construct the engineered tissue. Although the role of certain growth factors in human EC proliferation remains unclear, the importance of growth factors and attachment factors have been appreciated to stimulate cell proliferation and maintain long-term subculture *in vitro*, by interaction with specific cell-membrane receptors. Among these factors, the most important are fibroblast growth factor (FGF), EC growth supplement (ECGS), EC growth factor (ECGF), epidermal growth factor (EGF), and platelet-derived growth factor (PDGF). Especially basic FGF (bFGF, also called FGF-2, and known as heparin-binding growth factor) can induce the proliferation of ECs, fibroblasts and smooth muscle cells. Heparin can stabilize growth factor activity by preventing proteolytic degradation of FGF molecules and inhibits intimal hyperplasia in the presence of heparin-binding growth factors such as ECGF and FGF (Weinstein and Wenc 1986). VEGF can increase EC proliferation and could be a primary regulator for vasculogenesis. VEGF could also increase vascular permeability, along with promoting endothelial migration (Yancopoulos, Davis et al. 2000). However, the usage of growth factors must be regulated in spatial and quantitative manner, in order to prevent side effects such as tumor formation (Yancopoulos, Davis et al. 2000).

Due to the instability of many growth factors *in vivo*, an approach is to deliver them to the scaffold and releasing them at controlled and sustained rates for extended period of time. The release rate can be regulated by the degradation rate of the scaffold. This strategy mimics the natural mechanism of vascular wall healing; bFGF is gradually

released and ECs proliferate at the site (Wissink, Beernink et al. 2000). Heparin immobilized bFGF-loaded biomaterials (Wissink, Beernink et al. 2000) or in ECGF enmeshed matrix (Santhosh Kumar and Krishnan 2001) show improved EC adhesion and proliferation.

2.4.3. Mechanical stimulus

ECs separate blood from the underlying SMCs and are constantly exposed to hemodynamic forces. ECs undergo dramatic morphological changes in response to fluid shear stress. These changes include cytoskeleton reorientation, cell elongation, cell alignment in the direction of flow. Flow in long straight blood vessels is mostly laminar, and the shear stress (τ) can be approximated using Poiseuille's law as $\tau = 4\mu Q/\pi R^3$, where μ is blood viscosity, Q is volumetric flow and R is the vessel radius. Shear stress that ECs experience are location-dependent: a normal artery has a bigger range of 10-70 dyn/cm² than normal vein which is in the range of 1-6 dyn/cm² (Malek, Alper et al. 1999). But at curvatures or bifurcations, the flow becomes more turbulent. The gene expression and mechanotransduction are different in response to different flow patterns (Brooks, Lelkes et al. 2004).

Mechanotransduction to shear stress

ECs convert mechanical stimulation to biochemical signals through complex mechanotransduction mechanism, as shown in **Figure 2.8**. ECs respond to laminar steady shear stress by early electrophysiological changes in membrane potential and an increase in intracellular calcium concentration (Powell 2003). These changes drive potassium channel activation, generation of inositol triphosphate (IP3) and diacylglycerol (DAG), and G protein activation. Shear stress activates the extracellular signal-regulated

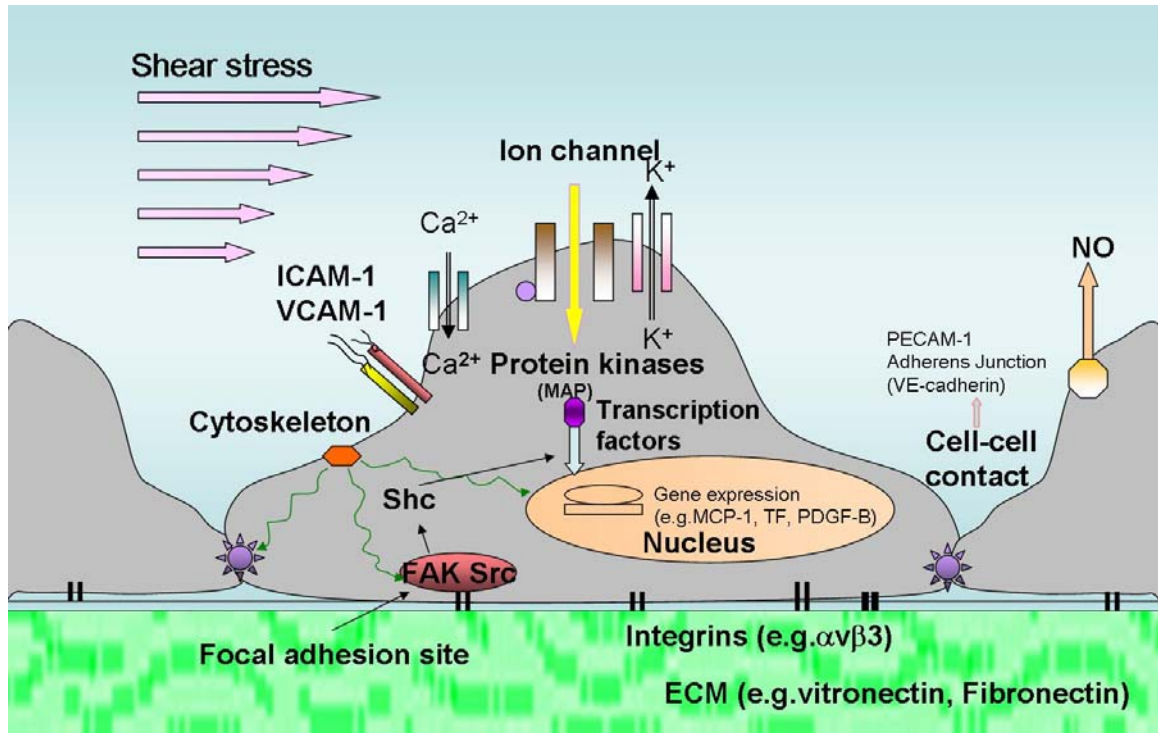


Figure 2.8. EC responses to shear stress in molecular mechanism.

kinase (ERK) and c-Jun NH2-terminal kinase (JNK) signal transduction pathways and induce the transcriptional activation of many immediate early genes through FAK signaling (Li, Kim et al. 1997). Signaling cascades occur within several minutes to one hour including activation of mitogen-activated protein kinase (MAP kinase) and nuclear factor kappa B (NFκB) and structural changes in cytoskeleton. Changes in gene regulation of nitric oxide synthase (NOS), tissue plasminogen activator (tPA), intercellular adhesion molecule-1 (ICAM), monocyte chemoattractant protein-1 (MCP-1), and PDGF-B follow within hours. These changes further alter cytoskeleton, remodel focal adhesion sites, and align cells in the flow direction (Davies, Barbee et al. 1997). Integrins and cell junction complexes play crucial roles in transduction by interacting with receptor tyrosine kinases, phosphatases and regulators of gene transcription (Masuda, Kogata et al. 2004; McCue, Noria et al. 2004). Platelet/endothelial cell adhesion molecule-1 (PECAM-1, CD 31) localizes at the cell-cell junction and establishes homophilic binding via extracellular domain (Albelda and Buck 1990). There is growing evidence that PECAM-1 interacts with the underlying cytoskeleton physically and functionally; it may regulate assembly of F-actin at the cell periphery, in association with changes in cell shape and spreading (Newman and Newman 2003). PECAM-1 is also involved in integrin activation and may induce integrin clustering or conformational changes (Newman and Newman 2003). The assembly of PECAM-1 may undergo rapid changes and serve as mechanosensor that activates a tyrosine kinase in response to fluid shear stress (Osawa, Masuda et al. 2002; Kaufman, Albelda et al. 2004).

Cell morphology alteration and reorganization

Shear-induced EC morphology changes integrate with cell adhesion junction complexes, and regulate cellular function to counteract the effect of shear stress (McCue, Noria et al. 2004). Reorganization of actin has been demonstrated to interact with the redistribution and levels of focal adhesion complexes such as vinculin, talin, and integrins (Girard and Nerem 1995). In response to shear stress, the cytoskeletal elements may achieve cell motility by depolymerization and repolymerization, demonstrated by DPB and thick stress fibers. The alteration in cytoskeleton leads to further change in cell shape and size (Galbraith, Skalak et al. 1998). With longer exposure to flow, more stable architectural arrangement of microfilament can be developed which is exhibited by actin reorientation, alignment and elongation in the direction of flow. The change in cytoskeleton does not occur monotonically; instead, the changes in elongation and alignment undergo several distinct stages (Galbraith, Skalak et al. 1998; Dieterich, Odenthal-Schnittler et al. 2000). In phase I, cells remain on attached surfaces and resist downstream movement by enhancement of basal stress fibers and DPB. In phase II, cells show increased motility, DPB disappears, and nucleus and microtubule organizing center (MTOC) are relocated. Cells elongate as characterized by plasma membrane protrusions. Also, cells orient in the direction of flow and then elongate.

Another change is that cells exhibit flattened profile after shear stress (Barbee, Mundel et al. 1995). After 24 h exposure to 12 dyn/cm^2 shear stress, the cell heights increase slightly relative to non-flow conditioned cells. However, the surface undulations (streamlining of cells) decrease significantly in flow-aligned cells. Subsequently, flow

perturbations due to the undulating surface produce cell-scale variations in shear stress magnitude and gradients.

There are heterogeneities in cell morphological responses to shear stress. The discrepancy in cell behaviors observed may associate with cell origin, cell passage number, media used and levels/magnitude of shear stress. However, the most important variable is the confluency of the culture and the substrates that cells attach (McCue, Noria et al. 2004). Cell alignment occurs more slowly in more confluent cultures than in less confluent cultures. HUVECs incubated for 1 h exhibit alignment after 4 h exposure to medium flow (Sirois, Charara et al. 1998) while the process occurs after a longer time in post-confluent cells (Noria, Xu et al. 2004). This could be due to surrounding cell geometry, which can affect shear stress distribution. The substrates also affect cell morphology and function (McCue, Noria et al. 2004). If the substrate contain adhesive ECM, cells are more likely to resist shear stress due to stronger interaction with the surface. When grafts are coated with substrates such as gelatin, fibrin glue and fibronectin, seeded cells can resist shear stress without detachment to the graft material in the physiologic ranges of shear stress (Heilshorn, DiZio et al. 2003). Shear stress also changes the synthesis and deposition of ECM including fibronectin, laminin, collagen and vitronectin (Thoumine, Nerem et al. 1995).

2.4.4. Cell interactions in 3D scaffolds

Cells could respond differently in attachment, morphology, migration and proliferation on a 3D matrix than 2D membrane. In 2D substrata, cultured cells are restricted to spread and attach to a flat plane while 3D matrices provide spatial advantages for cells attachment. Also, cells assume different cellular adhesion responses,

depending on different cell types and matrices. Many cell types such as fibroblasts, mesenchymal, epithelial and neural crest cells attached to 3D matrices show distinct adhesions from 2D culture (Yamada, Pankov et al. 2003; Wozniak, Modzelewska et al. 2004).

Biophysical and surface properties (discussed in 2.3.4) significantly influence cell adhesion, signaling and functions in 3D environment, unlike 2D environment. These different characteristics of matrix are demonstrated in **Figure 2.9**. The chemical (molecular) composition in 2D matrix plays a dominant role in controlling cell spreading and attachment, as discussed in 2.4.1. In addition, 2D cell culture is performed on ECM-coated glass slide or tissue culture plate (TCP) which provide a rigid support for cell adhesion. Thus cell attachment on these substrata is dependent on the recognition of cell binding proteins. On the other hand, 3D matrix provides substrate for cell attachment as well as traction. Due to the lack of very rigid matrix, the architecture and mechanical properties of the matrix become dominant factors influencing cell interaction with the matrix. As discussed in scaffold properties (2.3.4), the rigidity of the matrix and the spatial structures of 3D matrix (i.e. pore sizes) play an important role in cell adhesion by guiding cell organization (Yamada, Pankov et al. 2003).

Further, the 3D architecture could distribute binding sites differently than 2D architecture (Yamada, Pankov et al. 2003; Friedl 2004). 3D focal adhesions appear distinct from 2D focal adhesions on a rigid 2D matrix and were termed as “3D matrix adhesions” to separate them from 2D counterparts. In addition to proteins present in focal adhesions on 2D matrices, cells may have cytoskeletal adaptor proteins on 3D matrix (Cukierman, Pankov et al. 2001; Yamada, Pankov et al. 2003). There are

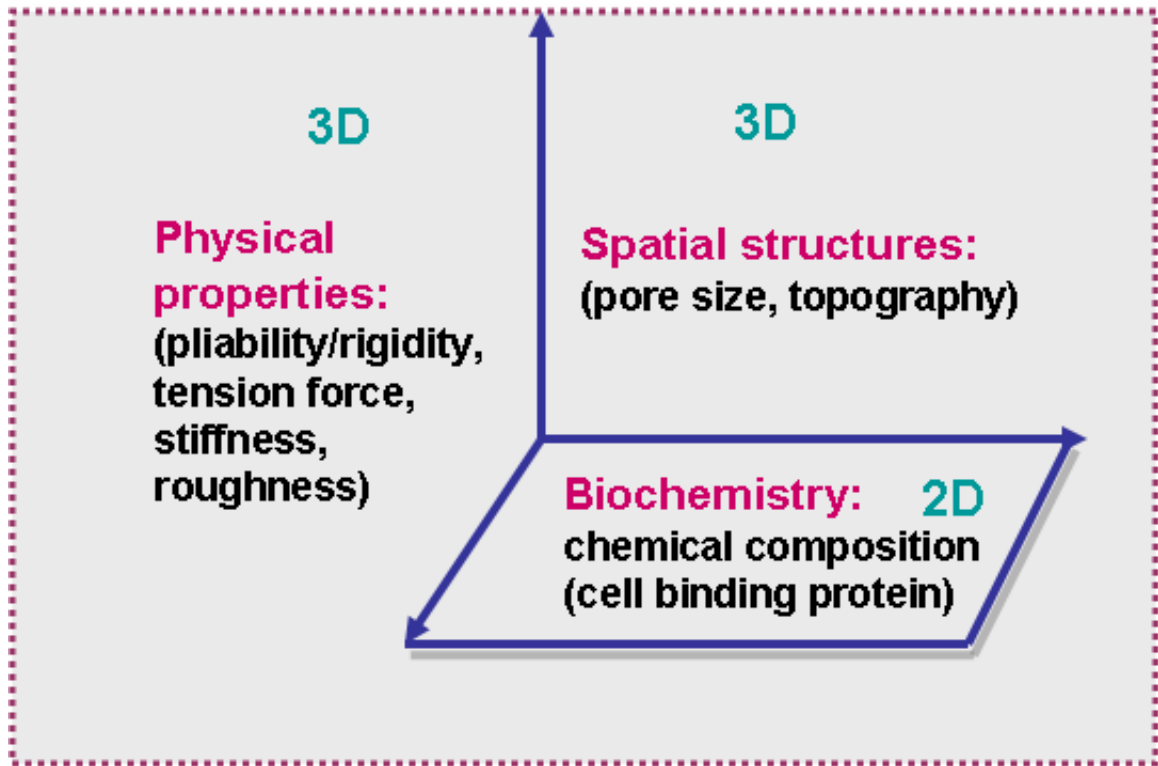


Figure 2.9. Cells respond to distinct physical and biochemical properties of ECM (modified from Yamada, Pankov et al. 2003).

similarities and differences in specific type of integrin. Also, FAK in 3D matrix adhesion is poorly phosphorylated at its major tyrosine phosphorylation site for cell adhesion (**Table 2.3**). Such discrepancy in cell adhesion between 2D vs. 3D causes different signal transduction, subsequent altered cell morphology and rearrangement. In response to different physical and chemical signals from surrounding 3D matrix, cells can synthesize ECM components and the degradation of matrix can create spatial advantages for cell expansion and forward migration unlike 2D architecture. Further, cells take “collective patterning” in ECM: the collective invasion is guided and maintained by a subset of cells at the leading edge which interact with ECM and traction, while other cells follow a more passive mode in retaining cell-cell contacts (Friedl 2004). Although cells exhibit different behaviors in 2D vs. 3D environment, cells may utilize already existing conveniences for cell adhesion. In other words, cells seek the best adhesion which they can find to facilitate cell growth and attachment. 3D matrix provides spatial as well as physical advantages beside adhesive interactions presented on rigid 2D matrix. Better understanding of cellular function in 2D vs. 3D can help us design scaffolds which mimic natural ECM with desired properties.

2.4.5. ES cell differentiation in 3D scaffolds

Concurrent with the development of tissue engineering, more concepts have been introduced in ES cell differentiation. Many reports on ES cell differentiation are focused in 2D monolayer cultures; however, these systems are limited for formation of higher-order structures which is essential in transplantation application. 3D scaffolds provide physical cues of porous structures, mechanical strength to guide cell colonization as well as chemical cues of cell-binding sites to support cell attachment and spreading.

Moleculars involved in adhesion	Focal adhesion (2D)	3D matrix adhesion (3D focal adhesion)
α_5 integrin	-	+
β_1 integrin	+	+
β_3 integrin	+	-
Paxillin	+	+
Talin	+	+
Vinculin	+	+
FAK	+	+
Phospho-FAK (Y ³⁹⁷)	+	-

Table 2.3. Molecular compositions in 2D and 3D cell-matrix adhesions.

“+” represents existence and “-” represents deficiency Yamada, Pankov et al. 2003).

Considering these advantages, 3D scaffolds with specific features (i.e. pore structures, micro-pattern) may be applied to direct maturation and specialization of differentiated cell types. Researchers have addressed the supporting function of scaffolds in directing ES cell differentiation in hES, mES and rhesus monkey ES (rmES) (Chen, Revoltella et al. 2003; Levenberg, Huang et al. 2003; Chaudhry, Yao et al. 2004). hES cell differentiation was directed in 3D PLGA/PLLA (1:1) in presence of defined growth factors (Levenberg, Huang et al. 2003). Not only the structures with the characteristics of neural, cartilage or liver formed, 3D vessel-like network was observed. Interestingly, comparison of hES differentiation on matrigel and polymer scaffolds showed that matrigel failed to support cell growth and 3D organization, probably attributed partially to the difference in stiffness of the materials. More specified organization as well as homogeneity were formed within polymer scaffolds compared with EBs (Levenberg, Huang et al. 2003). The properties of the scaffolds can affect ES cells differentiation differently. For example, rmES showed more migration behavior in collagen porous sponge; however, these cells developed more tissue-like structures in collagen gel, which had different topology but same chemical cues (Chen, Revoltella et al. 2003). 3D differentiation system has shown promise in using ES cells to generate tissue constructs useful for organ transplantation.

In all, there are several critical factors in regulating and directing ES cell differentiation into specific cell type (not including genetic monitoring): cell culture media components (especially growth factors); cell-cell contacts (coculture with other cells, cell-cell aggregates); cell-matrix interaction (ECM coat protein in 2D culture, matrices structure in 3D culture) and mechanical stimuli (shear stress). The factors

affecting matured cells (i.e. ECs) can also play a significant role in affecting ES cell differentiation. Before ES cell can be actually used in cell and tissue therapy in humans, there are still a lot of concerns involved in clinical applications such as purification and lineage selection, immunological compatibility, safety and ethnic issues.

2.5. REFERENCES

- Agrawal, C. M. and R. B. Ray (2001). "Biodegradable polymeric scaffolds for musculoskeletal tissue engineering." J Biomed Mater Res **55**(2): 141-50.
- Albelda, S. M. and C. A. Buck (1990). "Integrins and other cell adhesion molecules." Faseb J **4**(11): 2868-80.
- Barbee, K. A., T. Mundel, et al. (1995). "Subcellular distribution of shear stress at the surface of flow-aligned and nonaligned endothelial monolayers." Am J Physiol **268**(4 Pt 2): H1765-72.
- Brooks, A. R., P. I. Leikes, et al. (2004). "Gene expression profiling of vascular endothelial cells exposed to fluid mechanical forces: relevance for focal susceptibility to atherosclerosis." Endothelium **11**(1): 45-57.
- Burdick, J. A. and K. S. Anseth (2002). "Photoencapsulation of osteoblasts in injectable RGD-modified PEG hydrogels for bone tissue engineering." Biomaterials **23**(22): 4315-23.
- Burridge, K., L. A. Petch, et al. (1992). "Signals from focal adhesions." Curr Biol **2**(10): 537-9.
- Chaudhry, G. R., D. Yao, et al. (2004). "Osteogenic Cells Derived From Embryonic Stem Cells Produced Bone Nodules in Three-Dimensional Scaffolds." J Biomed Biotechnol **2004**(4): 203-210.
- Chen, S. S., R. P. Revoltella, et al. (2003). "Multilineage differentiation of rhesus monkey embryonic stem cells in three-dimensional culture systems." Stem Cells **21**(3): 281-95.
- Choi, K., M. Kennedy, et al. (1998). "A common precursor for hematopoietic and endothelial cells." Development **125**(4): 725-32.
- Chun, K. W., K. C. Cho, et al. (2004). "Controlled release of plasmid DNA from biodegradable scaffolds fabricated using a thermally-induced phase-separation method." J Biomater Sci Polym Ed **15**(11): 1341-53.

- Chung, T. W., D. Z. Liu, et al. (2003). "Enhancement of the growth of human endothelial cells by surface roughness at nanometer scale." Biomaterials **24**(25): 4655-61.
- Chung, T. W., Y. F. Lu, et al. (2002). "Growth of human endothelial cells on photochemically grafted Gly-Arg-Gly-Asp (GRGD) chitosans." Biomaterials **23**(24): 4803-9.
- Clark, P., P. Connolly, et al. (1987). "Topographical control of cell behaviour. I. Simple step cues." Development **99**(3): 439-48.
- Cooper, J. A., H. H. Lu, et al. (2005). "Fiber-based tissue-engineered scaffold for ligament replacement: design considerations and in vitro evaluation." Biomaterials **26**(13): 1523-32.
- Cukierman, E., R. Pankov, et al. (2001). "Taking cell-matrix adhesions to the third dimension." Science **294**(5547): 1708-12.
- Curtis, A. and C. Wilkinson (1999). "New depths in cell behaviour: reactions of cells to nanotopography." Biochem Soc Symp **65**: 15-26.
- Dani, C., A. G. Smith, et al. (1997). "Differentiation of embryonic stem cells into adipocytes in vitro." J Cell Sci **110**(Pt 11): 1279-85.
- Davies, P. F., K. A. Barbee, et al. (1997). "Spatial relationships in early signaling events of flow-mediated endothelial mechanotransduction." Annu Rev Physiol **59**: 527-49.
- Dieterich, P., M. Odenthal-Schnittler, et al. (2000). "Quantitative morphodynamics of endothelial cells within confluent cultures in response to fluid shear stress." Biophys J **79**(3): 1285-97.
- Dinsmore, J., J. Ratliff, et al. (1996). "Embryonic stem cells differentiated in vitro as a novel source of cells for transplantation." Cell Transplant **5**(2): 131-43.
- Doi, K., Y. Nakayama, et al. (1996). "Novel compliant and tissue-permeable microporous polyurethane vascular prosthesis fabricated using an excimer laser ablation technique." J Biomed Mater Res **31**(1): 27-33.

- Drumheller, P. D. and J. A. Hubbell (1994). "Polymer networks with grafted cell adhesion peptides for highly biospecific cell adhesive substrates." Anal Biochem **222**(2): 380-8.
- Ehrenfreund-Kleinman, T., D. A.J., et al. (2003). "Polysaccharide Scaffolds Prepared by Crosslinking of Polysaccharides with Chitosan or Proteins for Cell Growth." J Bioact Compat Polym **18**(5): 323-338.
- Engler, A. J., M. A. Griffin, et al. (2004). "Myotubes differentiate optimally on substrates with tissue-like stiffness: pathological implications for soft or stiff microenvironments." J Cell Biol **166**(6): 877-87.
- Evans, M. J. and M. H. Kaufman (1981). "Establishment in culture of pluripotential cells from mouse embryos." Nature **292**(5819): 154-6.
- Fair, J. H., B. A. Cairns, et al. (2003). "Induction of hepatic differentiation in embryonic stem cells by co-culture with embryonic cardiac mesoderm." Surgery **134**(2): 189-96.
- Fisher, J. P., D. Dean, et al. (2002). "Photocrosslinking characteristics and mechanical properties of diethyl fumarate/poly(propylene fumarate) biomaterials." Biomaterials **23**(22): 4333-43.
- Freed, L. E., G. Vunjak-Novakovic, et al. (1994). "Biodegradable polymer scaffolds for tissue engineering." Biotechnology (N Y) **12**(7): 689-93.
- Freyman, T. M., I. V. Yannas, et al. (2002). "Fibroblast contractile force is independent of the stiffness which resists the contraction." Exp Cell Res **272**(2): 153-62.
- Friedl, P. (2004). "Dynamic imaging of cellular interactions with extracellular matrix." Histochem Cell Biol **122**(3): 183-90. Epub 2004 Jul 16.
- Galbraith, C. G., R. Skalak, et al. (1998). "Shear stress induces spatial reorganization of the endothelial cell cytoskeleton." Cell Motil Cytoskeleton **40**(4): 317-30.
- Girard, P. R. and R. M. Nerem (1995). "Shear stress modulates endothelial cell morphology and F-actin organization through the regulation of focal adhesion-associated proteins." J Cell Physiol **163**(1): 179-93.

- Gluckman, E. (2000). "Current status of umbilical cord blood hematopoietic stem cell transplantation." Exp Hematol **28**(11): 1197-205.
- Griffith, L. G. (2002). "Emerging design principles in biomaterials and scaffolds for tissue engineering." Ann N Y Acad Sci **961**: 83-95.
- Griffith, L. G. and G. Naughton (2002). "Tissue engineering--current challenges and expanding opportunities." Science **295**(5557): 1009-14.
- Gunatillake, P. A. and R. Adhikari (2003). "Biodegradable synthetic polymers for tissue engineering." Eur Cell Mater **5**: 1-16; discussion 16.
- Hasirci, V., K. Lewandrowski, et al. (2001). "Versatility of biodegradable biopolymers: degradability and an in vivo application." J Biotechnol **86**(2): 135-50.
- He, H., T. Shirota, et al. (2003). "Canine endothelial progenitor cell-lined hybrid vascular graft with nonthrombogenic potential." J Thorac Cardiovasc Surg **126**(2): 455-64.
- Heilshorn, S. C., K. A. DiZio, et al. (2003). "Endothelial cell adhesion to the fibronectin CS5 domain in artificial extracellular matrix proteins." Biomaterials **24**(23): 4245-52.
- Hirashima, M., H. Kataoka, et al. (1999). "Maturation of embryonic stem cells into endothelial cells in an in vitro model of vasculogenesis." Blood **93**(4): 1253-63.
- Hori, Y., S. Inoue, et al. (2004). "Effect of culture substrates and fibroblast growth factor addition on the proliferation and differentiation of rat bone marrow stromal cells." Tissue Eng **10**(7-8): 995-1005.
- Hubbell, J. A., S. P. Massia, et al. (1991). "Endothelial cell-selective materials for tissue engineering in the vascular graft via a new receptor." Biotechnology (N Y) **9**(6): 568-72.
- Hynes, R. O. and Q. Zhao (2000). "The evolution of cell adhesion." J Cell Biol **150**(2): F89-96.

- Ishaug-Riley, S. L., G. M. Crane-Kruger, et al. (1998). "Three-dimensional culture of rat calvarial osteoblasts in porous biodegradable polymers." Biomaterials **19**(15): 1405-12.
- Kaufman, D. A., S. M. Albelda, et al. (2004). "Role of lateral cell-cell border location and extracellular/transmembrane domains in PECAM/CD31 mechanosensation." Biochem Biophys Res Commun **320**(4): 1076-81.
- Kaufman, D. S., E. T. Hanson, et al. (2001). "Hematopoietic colony-forming cells derived from human embryonic stem cells." Proc Natl Acad Sci U S A **98**(19): 10716-21. Epub 2001 Sep 04.
- Kaufman, D. S., R. L. Lewis, et al. (2004). "Functional endothelial cells derived from rhesus monkey embryonic stem cells." Blood **103**(4): 1325-32. Epub 2003 Oct 16.
- Kaushal, S., G. E. Amiel, et al. (2001). "Functional small-diameter neovessels created using endothelial progenitor cells expanded ex vivo." Nat Med **7**(9): 1035-40.
- Keller, G. M. (1995). "In vitro differentiation of embryonic stem cells." Curr Opin Cell Biol **7**(6): 862-9.
- Kramer, J., C. Hegert, et al. (2000). "Embryonic stem cell-derived chondrogenic differentiation in vitro: activation by BMP-2 and BMP-4." Mech Dev **92**(2): 193-205.
- Lai, W.-C., W.-B. Liao, et al. (2004). "The effect of end groups of PEG on the crystallization behaviors of binary crystalline polymer blends PEG/PLLA." Polymer **45**(9): 3073-3080.
- Lampin, M., C. Warocquier, et al. (1997). "Correlation between substratum roughness and wettability, cell adhesion, and cell migration." J Biomed Mater Res **36**(1): 99-108.
- Lee, C. H., H. J. Shin, et al. (2005). "Nanofiber alignment and direction of mechanical strain affect the ECM production of human ACL fibroblast." Biomaterials **26**(11): 1261-70.

- Lee, C. R., A. J. Grodzinsky, et al. (2001). "The effects of cross-linking of collagen-glycosaminoglycan scaffolds on compressive stiffness, chondrocyte-mediated contraction, proliferation and biosynthesis." Biomaterials **22**(23): 3145-54.
- Lee, J. Y. and A. P. Spicer (2000). "Hyaluronan: a multifunctional, megaDalton, stealth molecule." Curr Opin Cell Biol **12**(5): 581-6.
- Lee, S. H., B. S. Kim, et al. (2004). "Thermally produced biodegradable scaffolds for cartilage tissue engineering." Macromol Biosci **4**(8): 802-10.
- Lee, T. Y. and A. I. Gotlieb (2003). "Microfilaments and microtubules maintain endothelial integrity." Microsc Res Tech **60**(1): 115-27.
- Levenberg, S., J. S. Golub, et al. (2002). "Endothelial cells derived from human embryonic stem cells." Proc Natl Acad Sci U S A **99**(7): 4391-6. Epub 2002 Mar 26.
- Levenberg, S., N. F. Huang, et al. (2003). "Differentiation of human embryonic stem cells on three-dimensional polymer scaffolds." Proc Natl Acad Sci U S A **100**(22): 12741-6. Epub 2003 Oct 15.
- Li, S., S. Bhatia, et al. (2001). "Effects of morphological patterning on endothelial cell migration." Biorheology **38**(2-3): 101-8.
- Li, S., M. Kim, et al. (1997). "Fluid shear stress activation of focal adhesion kinase. Linking to mitogen-activated protein kinases." J Biol Chem **272**(48): 30455-62.
- Li, W. J., C. T. Laurencin, et al. (2002). "Electrospun nanofibrous structure: a novel scaffold for tissue engineering." J Biomed Mater Res **60**(4): 613-21.
- Lieber, J. G., G. M. Keller, et al. (2003). "The in vitro differentiation of mouse embryonic stem cells into neutrophils." Methods Enzymol **365**: 129-42.
- Lo, C. M., H. B. Wang, et al. (2000). "Cell movement is guided by the rigidity of the substrate." Biophys J **79**(1): 144-52.
- Madhally, S. V. and H. W. Matthew (1999). "Porous chitosan scaffolds for tissue engineering." Biomaterials **20**(12): 1133-42.

- Malek, A. M., S. L. Alper, et al. (1999). "Hemodynamic shear stress and its role in atherosclerosis." Jama **282**(21): 2035-42.
- Mann, B. K. and J. L. West (2002). "Cell adhesion peptides alter smooth muscle cell adhesion, proliferation, migration, and matrix protein synthesis on modified surfaces and in polymer scaffolds." J Biomed Mater Res **60**(1): 86-93.
- Mao, J., L. Zhao, et al. (2003). "Study of novel chitosan-gelatin artificial skin in vitro." J Biomed Mater Res **64A**(2): 301-8.
- Marois, Y., M. F. Sigot-Luizard, et al. (1999). "Endothelial cell behavior on vascular prosthetic grafts: effect of polymer chemistry, surface structure, and surface treatment." Asaio J **45**(4): 272-80.
- Martin, G. R. and M. J. Evans (1975). "Differentiation of clonal lines of teratocarcinoma cells: formation of embryoid bodies in vitro." Proc Natl Acad Sci U S A **72**(4): 1441-5.
- Masuda, M., N. Kogata, et al. (2004). "[Crucial roles of PECAM-1 in shear stress sensing of vascular endothelial cells]." Nippon Yakurigaku Zasshi **124**(5): 311-8.
- Mayer, H., H. Bertram, et al. (2005). "Vascular endothelial growth factor (VEGF-A) expression in human mesenchymal stem cells: Autocrine and paracrine role on osteoblastic and endothelial differentiation." J Cell Biochem **18**: 18.
- McCloskey, K. E., I. Lyons, et al. (2003). "Purified and proliferating endothelial cells derived and expanded in vitro from embryonic stem cells." Endothelium **10**(6): 329-36.
- McCue, S., S. Noria, et al. (2004). "Shear-induced reorganization of endothelial cell cytoskeleton and adhesion complexes." Trends Cardiovasc Med **14**(4): 143-51.
- Mei, N., G. Chen, et al. (2005). "Biocompatibility of Poly(epsilon-caprolactone) scaffold modified by chitosan--the fibroblasts proliferation in vitro." J Biomater Appl **19**(4): 323-39.
- Middleton, J. C. and A. J. Tipton (2000). "Synthetic biodegradable polymers as orthopedic devices." Biomaterials **21**(23): 2335-46.

- Mikos, A. G., Y. Bao, et al. (1993). "Preparation of poly(glycolic acid) bonded fiber structures for cell attachment and transplantation." J Biomed Mater Res **27**(2): 183-9.
- Miot, S., T. Woodfield, et al. (2005). "Effects of scaffold composition and architecture on human nasal chondrocyte redifferentiation and cartilaginous matrix deposition." Biomaterials **26**(15): 2479-89.
- Mooney, D. (2001). "Nimble progenitors rescue vascular grafts." Nat Med **7**(9): 996-7.
- Mooney, D. J., D. F. Baldwin, et al. (1996). "Novel approach to fabricate porous sponges of poly(D,L-lactic-co-glycolic acid) without the use of organic solvents." Biomaterials **17**(14): 1417-22.
- Muller, M., B. K. Fleischmann, et al. (2000). "Selection of ventricular-like cardiomyocytes from ES cells in vitro." Faseb J **14**(15): 2540-8.
- Mummery, C. (2004). "Stem cell research: immortality or a healthy old age?" Eur J Endocrinol **151**(Suppl 3): U7-12.
- Murashov, A. K., E. S. Pak, et al. (2004). "17beta-Estradiol enhances neuronal differentiation of mouse embryonic stem cells." FEBS Lett **569**(1-3): 165-8.
- Newman, P. J. and D. K. Newman (2003). "Signal transduction pathways mediated by PECAM-1: new roles for an old molecule in platelet and vascular cell biology." Arterioscler Thromb Vasc Biol **23**(6): 953-64. Epub 2003 Apr 10.
- Ng, K. W., H. L. Khor, et al. (2004). "In vitro characterization of natural and synthetic dermal matrices cultured with human dermal fibroblasts." Biomaterials **25**(14): 2807-18.
- Nishikawa, S. I., S. Nishikawa, et al. (1998). "Progressive lineage analysis by cell sorting and culture identifies FLK1+VE-cadherin+ cells at a diverging point of endothelial and hemopoietic lineages." Development **125**(9): 1747-57.
- Noria, S., F. Xu, et al. (2004). "Assembly and reorientation of stress fibers drives morphological changes to endothelial cells exposed to shear stress." Am J Pathol **164**(4): 1211-23.

- O'Brien, F. J., B. A. Harley, et al. (2005). "The effect of pore size on cell adhesion in collagen-GAG scaffolds." Biomaterials **26**: 433-441.
- Osawa, M., M. Masuda, et al. (2002). "Evidence for a role of platelet endothelial cell adhesion molecule-1 in endothelial cell mechanosignal transduction: is it a mechanoresponsive molecule?" J Cell Biol **158**(4): 773-85. Epub 2002 Aug 12.
- Pelham, R. J., Jr. and Y. Wang (1997). "Cell locomotion and focal adhesions are regulated by substrate flexibility." Proc Natl Acad Sci U S A **94**(25): 13661-5.
- Peter, S. J., S. T. Miller, et al. (1998). "In vivo degradation of a poly(propylene fumarate)/beta-tricalcium phosphate injectable composite scaffold." J Biomed Mater Res **41**(1): 1-7.
- Pitt, C. G., M. M. Gratzl, et al. (1981). "Aliphatic polyesters II. The degradation of poly (DL-lactide), poly (epsilon-caprolactone), and their copolymers in vivo." Biomaterials **2**(4): 215-20.
- Powell, J. (2003). Comprehensive Vascular and Endovascular Surgery, 1000 Illustrations.
- Prelle, K., N. Zink, et al. (2002). "Pluripotent stem cells--model of embryonic development, tool for gene targeting, and basis of cell therapy." Anat Histol Embryol **31**(3): 169-86.
- Riddle, K. W. and D. J. Mooney (2004). "Role of poly(lactide-co-glycolide) particle size on gas-foamed scaffolds." J Biomater Sci Polym Ed **15**(12): 1561-70.
- Risau, W. (1995). "Differentiation of endothelium." Faseb J **9**(10): 926-33.
- Risbud, M. V., A. A. Hardikar, et al. (2000). "pH-sensitive freeze-dried chitosan-polyvinyl pyrrolidone hydrogels as controlled release system for antibiotic delivery." J Control Release **68**(1): 23-30.
- Rolletschek, A., H. Chang, et al. (2001). "Differentiation of embryonic stem cell-derived dopaminergic neurons is enhanced by survival-promoting factors." Mech Dev **105**(1-2): 93-104.

- Sachinidis, A., B. K. Fleischmann, et al. (2003). "Cardiac specific differentiation of mouse embryonic stem cells." Cardiovasc Res **58**(2): 278-91.
- Sachlos, E., N. Reis, et al. (2003). "Novel collagen scaffolds with predefined internal morphology made by solid freeform fabrication." Biomaterials **24**(8): 1487-97.
- Saito, S., H. Ugai, et al. (2002). "Isolation of embryonic stem-like cells from equine blastocysts and their differentiation in vitro." FEBS Lett **531**(3): 389-96.
- Santhosh Kumar, T. R. and L. K. Krishnan (2001). "Endothelial cell growth factor (ECGF) enmeshed with fibrin matrix enhances proliferation of EC in vitro." Biomaterials **22**(20): 2769-76.
- Sartori, M. T., L. Spiezia, et al. (2005). "Role of fibrinolytic and clotting parameters in the diagnosis of liver veno-occlusive disease after hematopoietic stem cell transplantation in a pediatric population
Urokinase Plasminogen Activator, uPa Receptor, and Its Inhibitor in Vernal Keratoconjunctivitis." Thromb Haemost **93**(4): 682-9.
- Sastry, S. K. and K. Burridge (2000). "Focal adhesions: a nexus for intracellular signaling and cytoskeletal dynamics." Exp Cell Res **261**(1): 25-36.
- Savatier, P., S. Huang, et al. (1994). "Contrasting patterns of retinoblastoma protein expression in mouse embryonic stem cells and embryonic fibroblasts." Oncogene **9**(3): 809-18.
- Schaner, P. J., N. D. Martin, et al. (2004). "Decellularized vein as a potential scaffold for vascular tissue engineering." J Vasc Surg **40**(1): 146-53.
- Scholer, H. R., A. K. Hatzopoulos, et al. (1989). "A family of octamer-specific proteins present during mouse embryogenesis: evidence for germline-specific expression of an Oct factor." Embo J **8**(9): 2543-50.
- Schuldiner, M., R. Eiges, et al. (2001). "Induced neuronal differentiation of human embryonic stem cells." Brain Res **913**(2): 201-5.
- Seal, B. L., T. C. Otero, et al. (2001). "Polymeric biomaterials for tissue and organ regeration." Materials Science and Engineering **34**: 147-230.

- Seliktar, D., R. A. Black, et al. (2000). "Dynamic mechanical conditioning of collagen-gel blood vessel constructs induces remodeling in vitro." Ann Biomed Eng **28**(4): 351-62.
- Shieh, S. J. and J. P. Vacanti (2005). "State-of-the-art tissue engineering: from tissue engineering to organ building." Surgery **137**(1): 1-7.
- Short, S. M., G. A. Talbott, et al. (1998). "Integrin-mediated signaling events in human endothelial cells." Mol Biol Cell **9**(8): 1969-80.
- Sieminski, A. L., R. P. Hebbel, et al. (2004). "The relative magnitudes of endothelial force generation and matrix stiffness modulate capillary morphogenesis in vitro." Exp Cell Res **297**(2): 574-84.
- Sirois, E., J. Charara, et al. (1998). "Endothelial cells exposed to erythrocytes under shear stress: an in vitro study." Biomaterials **19**(21): 1925-34.
- Solter, D. and B. B. Knowles (1978). "Monoclonal antibody defining a stage-specific mouse embryonic antigen (SSEA-1)." Proc Natl Acad Sci U S A **75**(11): 5565-9.
- Soria, B., E. Roche, et al. (2000). "Insulin-secreting cells derived from embryonic stem cells normalize glycemia in streptozotocin-induced diabetic mice." Diabetes **49**(2): 157-62.
- Suh, J. K. and H. W. Matthew (2000). "Application of chitosan-based polysaccharide biomaterials in cartilage tissue engineering: a review." Biomaterials **21**(24): 2589-98.
- Tadmor, R., N. Chen, et al. (2002). "Thin film rheology and lubricity of hyaluronic acid solutions at a normal physiological concentration." J Biomed Mater Res **61**(4): 514-23.
- Tam, E. M., Y. I. Wu, et al. (2002). "Collagen binding properties of the membrane type-1 matrix metalloproteinase (MT1-MMP) hemopexin C domain. The ectodomain of the 44-kDa autocatalytic product of MT1-MMP inhibits cell invasion by disrupting native type I collagen cleavage." J Biol Chem **277**(41): 39005-14. Epub 2002 Jul 26.

- Teebken, O. E., A. Bader, et al. (2000). "Tissue engineering of vascular grafts: human cell seeding of decellularised porcine matrix." Eur J Vasc Endovasc Surg **19**(4): 381-6.
- Teebken, O. E. and A. Haverich (2002). "Tissue engineering of small diameter vascular grafts." Eur J Vasc Endovasc Surg **23**(6): 475-85.
- Thomson, J. A., J. Itskovitz-Eldor, et al. (1998). "Embryonic stem cell lines derived from human blastocysts." Science **282**(5391): 1145-7.
- Thoumine, O., R. M. Nerem, et al. (1995). "Changes in organization and composition of the extracellular matrix underlying cultured endothelial cells exposed to laminar steady shear stress." Lab Invest **73**(4): 565-76.
- Thoumine, O., T. Ziegler, et al. (1995). "Elongation of confluent endothelial cells in culture: the importance of fields of force in the associated alterations of their cytoskeletal structure." Exp Cell Res **219**(2): 427-41.
- Timmer, M. D., C. G. Ambrose, et al. (2003). "Evaluation of thermal- and photo-crosslinked biodegradable poly(propylene fumarate)-based networks." J Biomed Mater Res A **66**(4): 811-8.
- Ting, V., C. D. Sims, et al. (1998). "In vitro prefabrication of human cartilage shapes using fibrin glue and human chondrocytes." Ann Plast Surg **40**(4): 413-20; discussion 420-1.
- Turner, N. J., C. M. Kielty, et al. (2004). "A novel hyaluronan-based biomaterial (Hyaff-11) as a scaffold for endothelial cells in tissue engineered vascular grafts." Biomaterials **25**(28): 5955-64.
- Vacanti, J. P., M. A. Morse, et al. (1988). "Selective cell transplantation using bioabsorbable artificial polymers as matrices." J Pediatr Surg **23**(1 Pt 2): 3-9.
- Vittet, D., M. H. Prandini, et al. (1996). "Embryonic stem cells differentiate in vitro to endothelial cells through successive maturation steps." Blood **88**(9): 3424-31.
- Walboomers, X. F., H. J. Croes, et al. (1999). "Contact guidance of rat fibroblasts on various implant materials." J Biomed Mater Res **47**(2): 204-12.

- Wan, Y., W. Chen, et al. (2003). "Biodegradable poly(L-lactide)-poly(ethylene glycol) multiblock copolymer: synthesis and evaluation of cell affinity." Biomaterials **24**(13): 2195-203.
- Weinberg, C. B. and E. Bell (1986). "A blood vessel model constructed from collagen and cultured vascular cells." Science **231**(4736): 397-400.
- Weinstein, R. and K. Wenc (1986). "Growth factor responses of human arterial endothelial cells in vitro." In Vitro Cell Dev Biol **22**(9): 549-56.
- Westreich, R., M. Kaufman, et al. (2004). "Validating the subcutaneous model of injectable autologous cartilage using a fibrin glue scaffold." Laryngoscope **114**(12): 2154-60.
- Wissink, M. J., R. Beernink, et al. (2000). "Endothelial cell seeding of (heparinized) collagen matrices: effects of bFGF pre-loading on proliferation (after low density seeding) and pro-coagulant factors." J Control Release **67**(2-3): 141-55.
- Wobus, A. M., K. Guan, et al. (2001). "In vitro differentiation of embryonic stem cells and analysis of cellular phenotypes." Methods Mol Biol **158**: 263-86.
- Wozniak, M. A., K. Modzelewska, et al. (2004). "Focal adhesion regulation of cell behavior." Biochim Biophys Acta **1692**(2-3): 103-19.
- Xia, W., W. Liu, et al. (2004). "Tissue engineering of cartilage with the use of chitosan-gelatin complex scaffolds." J Biomed Mater Res **71B**(2): 373-80.
- Xue, L. and H. P. Greisler (2003). "Biomaterials in the development and future of vascular grafts." J Vasc Surg **37**(2): 472-80.
- Yamada, K. M., R. Pankov, et al. (2003). "Dimensions and dynamics in integrin function." Braz J Med Biol Res **36**(8): 959-66. Epub 2003 Jul 23.
- Yamamoto, K., T. Sokabe, et al. (2004). "Fluid Shear Stress Induces Differentiation of Flk-1-Positive Embryonic Stem Cells into Vascular Endothelial Cells In Vitro." Am J Physiol Heart Circ Physiol **2**: 2.

- Yamashita, J., H. Itoh, et al. (2000). "Flk1-positive cells derived from embryonic stem cells serve as vascular progenitors." Nature **408**(6808): 92-6.
- Yancopoulos, G. D., S. Davis, et al. (2000). "Vascular-specific growth factors and blood vessel formation." Nature **407**(6801): 242-8.
- Yoon, J. J., S. H. Song, et al. (2004). "Immobilization of cell adhesive RGD peptide onto the surface of highly porous biodegradable polymer scaffolds fabricated by a gas foaming/salt leaching method." Biomaterials **25**(25): 5613-20.
- Zaidel-Bar, R., M. Cohen, et al. (2004). "Hierarchical assembly of cell-matrix adhesion complexes." Biochem Soc Trans **32**(Pt3): 416-20.
- Zeltinger, J., J. K. Sherwood, et al. (2001). "Effect of pore size and void fraction on cellular adhesion, proliferation, and matrix deposition." Tissue Eng **7**(5): 557-72.

CHAPTER 3

EFFECT OF SPATIAL ARCHITECTURE ON CELLULAR COLONIZATION

3.1 INTRODUCTION

Tissue engineering has given promise for generating functionally replaceable tissue parts. Bioactive and bioresorbable scaffolds are used to support and guide the in-growth of cells. While supporting biological activity, scaffold transiently degrades allowing regeneration of tissue without any reminiscent foreign material in the long term (2000; Langer and Vacanti 1993; Schoen and Levy 1999). Scaffolds generated from natural (Chvapil 1977) and synthetic polymers or after removing the cellular components from xenogeneic tissues (Oberpenning et al. 1999) have been used with and without prior cell-seeding.

A number of studies have shown that chemical and mechanical properties of matrices such as edges, grooves, hydrophilicity, pore sizes, presence of adhesion domains, roughness/ nanotopographies, stiffness, and void fractions influence cellular processes in 2D or 3D matrices (Balgude et al. 2001; Curtis and Wilkinson 1999; Rajnicek et al. 1997; Ranucci and Moghe 2001; Salem et al. 2002; Zeltinger et al. 2001). The general dogma is that stimuli signaled through Arginine-Glycine-Aspartic acid (RGD) binding domain, integrins and focal adhesion points change the polymerization state of cytoskeletal actin, which subsequently results in changed cellular morphology and cellular activity (Giancotti and Ruoslahti 1999; Korff and Augustin 1999; Sastry and

Burridge 2000). Restraining cell spreading characteristics using micropatterned substrates, has also shown the influence of cell size on life or death (Chen et al. 1997). Majority of the *in vitro* studies are performed in two-dimension and/or substrates that have specific adhesion domains. Although many *in vivo* studies have shown that the microarchitecture of the biomaterials is the primary determinant in the foreign body response rather than chemical composition (Sieminski and Gooch 2000), it is not clear how the microarchitecture influences cell colonization.

The goal of this study was to understand the influence of architecture via presenting a substrate in multiple forms i.e., 2D membranes, 3D porous scaffolds, and in presence of other materials without affecting its inherent chemical characteristics. Chitosan, a derivative of naturally occurring chitin, was selected because a) it can be easily processed into beads, fibers, films, or scaffolds with regulated porous structure (Madhally and Matthew 1999) and b) it is a positively charged polysaccharide resembling glycosaminoglycans, present in the extracellular matrix. Although chitosan has no specific binding domain for integrin-mediated adhesion, it supports biological activity of diverse cell types and it has been a subject of many investigations in tissue engineering (Cai et al. 2002; Chung et al. 2002; Chupa et al. 2000; Lahiji et al. 2000; Mizuno et al. 2003; Zhu et al. 2002). In addition, chitosan is an anti-infective and biocompatible polymer metabolized into non-toxic D-glucosamines by lysozymes (Tomihata and Ikada 1997).

To alter the structural features of chitosan, blending with synthetic biodegradable poly-lactic-co-glycolic acid (50:50 PLGA) was considered. 50:50 PLGA is widely investigated in various tissue engineering applications although it has no integrin binding

domain for adhesion. Unlike chitosan, 50:50 PLGA is amorphous, degrades by hydrolysis, electroneutral, and hydrophobic. An emulsion system was used to blend the two polymers without altering the chemical nature of either polymer. Further, cells from two different origins were tested: i) human umbilical vein endothelial cells (HUVECs) which make-up the luminal lining and ii) mouse embryonic fibroblasts (MEFs) which are found in the connective tissue, synthesize collagen type I and III and tend to develop fibrous network (Shigemasa Y 1994). Cell spreading, proliferation, viability, endocytic activity, and cytoskeletal organization were analyzed on 2D chitosan, 3D chitosan and PLGA-chitosan scaffolds. These results show significant influence of spatial architecture on cell adhesion and cytoskeletal organization.

3.2. MATERIALS AND METHODS

Chitosan with 50-190kD MW and >310kD MW, unconjugated 1,2-Dimyristoyl-sn-Glycero-3-Phosphocholine (DMPC, 678Da) and Dulbecco's modified Eagle medium (DMEM) were obtained from Sigma Aldrich Chemical Co (St. Louis, MO). The degree of deacetylation of both chitosans were $\approx 85\%$. 19kD 50:50 PLGA was from Alkermes Inc. (Cambridge, MA). 75kD and 160kD 50:50 PLGA were from Birmingham Polymers, Inc. (Birmingham, AL). FITC-conjugated DMPC was obtained from Avanti Polar-Lipids (Alabaster, AL). Bromodeoxyuridine (BrdU) cell proliferation assay kit was obtained from EMD Biosciences, Inc., (San Diego, CA). Carboxyfluorescein diacetate-succinimidyl ester (CFDA-SE), LIVE/DEAD Assay Kit, and Alexa Fluor 488 phalloidin were obtained from Molecular Probes (Eugene, OR). HUVECs and endothelial growth medium-2 (EGM-2) Bulletkit were from Cambrex Biosciences (Walkersville, MD). MEFs were from American Tissue Culture Collection (Walkersville, MD).

3.2.1. Formation of 2D and 3D chitosan scaffolds for cell culture

Sterile 0.5% (w/v) chitosan solutions were prepared by autoclaving (at 121°C in a wet cycle for 20 min) chitosan suspension in water and then adding acetic acid equivalent to 0.5M in a laminar flow hood. To form 2D membranes, 24-well and 6-well tissue culture plates were layered with chitosan solution and dried in a biological laminar flow hood at room temperature; uncoated tissue culture-treated plastic surfaces were used as controls (henceforth referred to as control). To form 3D matrices, 300 µL of chitosan solutions was poured into tissue culture plates which were frozen at -20°C (in a freezer) or at -86°C (inside a freeze dryer). Samples were lyophilized for 24 hr using a Benchtop 6K lyophilizer (VirTis, Gardiner, NY). Dried samples were neutralized with 0.1 N NaOH for 30 min, washed four times with sterile phosphate buffered saline (PBS), and stored in PBS till subsequent cell seeding.

3.2.2. Formation of PLGA-chitosan scaffolds

Three percent (w/v) 19 kD, 75kD, and 160kD PLGA solutions were prepared by dissolving in chloroform. Chitosan solution of >310 kD MW was emulsified with chloroform or PLGA solution in the volume ratio of 3:1 with 0.2% (w/v) DMPC. To obtain 2D membranes, the emulsion was layered onto glass slides, air dried overnight at room temperature. To form 3D scaffolds, glass slides were converted into wells using silicon glue to form the wall and then emulsions were freeze dried similar to the procedure described above for 3D chitosan scaffolds. All scaffolds were neutralized prior to cell seeding, similar to the method described above for 2D and 3D chitosan scaffolds.

3.2.3. Cell culture and seeding

HUVECs were cultured in EGM-2 BulletKit medium (containing 2% fetal bovine serum (FBS), hydrocortisone, fibroblast growth factor-B, heparin, vascular endothelial growth factor, insulin-like growth factor-1, ascorbic acid, human epidermal growth factor, gentamicin) following vendors protocol. Cells between 2 and 8 passages were used in all the experiments.

MEFs were maintained in DMEM supplemented with 4 mM L-glutamine, 4.5 g/L glucose, 1.5g/L sodium bicarbonate, 100 U/mL penicillin-streptomycin, 2.5 µg/mL amphotericin B and 10 % FBS (Invitrogen Corp., Carlsbad, CA).

Both cultures were maintained at 37°C, 5% CO₂/ 95% air and fed with fresh medium every 48 h. Prior to cell seeding, cells were detached with 0.01% trypsin/ 10 µM EDTA (Invitrogen Corp., Carlsbad, CA), centrifuged and resuspended in medium. 10,000 and 25,000 cells per well were seeded onto 2D and 3D scaffolds respectively and incubated with 0.5 mL of growth medium. To achieve uniform distribution of cells in 3D scaffolds, a concentrated (500,000 cells/mL) cell suspension was placed at different locations on each sample. Then cells were distributed in the vertical direction by lateral shaking with the addition of growth medium summing up to 0.5 mL. To confirm uniform distribution of cells in the scaffold, few experiments were performed by staining the cells with a non-toxic metabolic stain CFDA-SE prior to seeding onto the scaffold. To stain cells, they were incubated in growth medium containing 2µM CFDA-SE at 37°C for 20 min followed by washing the excess stain with growth medium. In addition, histological analysis was performed to confirm the cell distribution in the porous structure of 3D scaffolds. For this purpose, samples were fixed in a 10% buffered formalin solution,

embedded in paraffin, 6 μm thick sections were cut, and stained with hematoxylin and eosin (H & E) (Madihally et al. 2003).

3.2.4. Morphology characterization

Morphologies were evaluated using an inverted microscope (Nikon TE2000, Melville, NY) outfitted with a CCD camera. Digital micrographs were captured from different locations. Cell spreading area, pore sizes, and shape factors (defined as $4\pi \times \text{area} / \text{perimeter}^2$; when the number is closer to 1, the cell shape is closer to a circle) were quantified using an image analysis software (Sigma Scan Pro, Chicago, IL). For each condition, more than 50 pores or cells were analyzed. Few samples were also analyzed using scanning electron microscope (SEM, Joel scanning microscope) to confirm the open pore architecture. For this purpose, samples were dried using a series of increasing concentrations of ethanol followed by a brief vacuum drying. Samples were sputter coated with gold at 40 mA prior to observing under SEM.

3.2.5. Evaluation of cytoskeletal organization and viability

Cell-containing scaffolds were fixed in 3.7 % formaldehyde for 15 min at room temperature. Cells were washed with PBS and permeabilized with -20°C ethanol for 30 min at -4°C , and then incubated with Alexa Fluor 488 phalloidin for 1 h at room temperature in the dark. Cell viability on emulsified samples was tested using LIVE/DEAD Assay Kit. After two days of culture, growth medium was replaced with the combined solution of calcein AM and ethidium homodimer (EthD-1) and incubated for 40 min. All the fluorescently-labeled cells were examined under a fluorescence microscope and digital images were captured.

3.2.6. Cell proliferation analysis

Cell growth was determined by MTT-Formazan assay by sacrificing culture plates at regular intervals. MTT-formazan assay was performed using a previously reported procedure for 2D membranes (Chupa et al. 2000) and a modified procedure for 3D scaffolds (Mosmann 1983). Modifications were made in order to minimize the background absorbance from 3D scaffolds. For 2D membranes, the growth medium was replaced with 0.5 mL of MTT (Sigma Chemical Co., Saint Louis) solution (2 mg/mL in PBS) followed by incubation for two hours at 37°C. Then MTT solution was discarded and dimethyl sulfoxide (DMSO) was added to dissolve formazan and the solution absorbance was measured at 540 nm. For 3D scaffolds, cells were detached from the scaffolds using trypsin-EDTA and transferred to 96 well plates. MTT solution was added and incubated for four hours at 37°C. Isopropanol was added and the absorbance was measured at 490 nm. Obtained values were plotted assuming an exponential growth rate i.e., $\ln(A/A_0) = \mu(t-t_0)$ where A_0 is the absorbance at initial time t_0 , A is the absorbance at certain time t (day) and μ is the specific growth rate (day^{-1} units). μ was determined in conditions where the regression coefficients were >0.95 . Calibration curves were developed by seeding cells onto 3D matrices formed at -20°C at four different densities (10000, 25000, 100000 and 300000 cells) and cultured for two days prior to analyses.

BrdU assay was also performed to confirm the growth behavior on different matrices using vendor's protocol for 2D cultures. However, for 3D cultures, modifications were made similar to MTT-assay. Briefly, BrdU was added to the wells and incubated for 24 h in 2D cultures. 3D cultures were incubated for 4 hr and cells were then detached using trypsin-EDTA and centrifuged. Cells were fixed and denatured, anti-

BrdU antibody was added and incubated for 1 h at room temperature followed by incubation with horseradish peroxidase-conjugated goat anti-mouse IgG for 30 min. Tetra-methylbenzidine was added and incubated for 15 min before stopping the reaction with sulfuric acid. The solution absorbance was measured at 450 nm.

3.2.7. Evaluation of DMPC internalization

DMPC was used as a stabilizer while forming PLGA-chitosan emulsions. To understand the fate of DMPC during cell culture, FITC-conjugated DMPC was used in preparing the emulsions. 2D and 3D PLGA-chitosan scaffolds were formed and HUVECs were seeded using the procedure described above. After two days of incubation, cells were harvested using trypsin-EDTA and the suspension was split into two parts. One part was incubated in a trypan blue solution for 5 min to quench the extracellular fluorescence. Both portions were resuspended in PBS supplemented with 1% FBS and washed twice. Cells incubated on unconjugated DMPC-containing scaffolds served as negative control. All samples were analyzed using a FACSCalibur (Becton-Dickinson, San Jose, CA) flow cytometer.

3.2.8. Material stiffness evaluation

Tensile properties of 2D membranes were measured by the method described previously (Raghavan et al. 2005; Sarasam and Madihally 2005). In brief, large samples were neutralized in 1N NaOH for 15 min and rinsed thoroughly under tap water and immersed in PBS for 30min prior to testing. Rectangular strips of approximately 60 mm×7.5 mm size were cut from each sample and pulled to break at a constant cross head speed of 5 mm/min using INSTRON 5842 (INSTRON Inc., Canton, MA) outfitted with a 100 N load cell.

For measuring the material stiffness in 3D cylindrical scaffolds, compression tests were performed at a rate of 5mm/min, similar to tensile tests were neutralized with alcohol and washed with PBS. All samples were tested in the wet state at 37°C using a custom-built environmental chamber. The stiffness (or elastic modulus) was calculated from the slope of the linear portion of the stress-strain curve.

3.2.9. Statistical analysis

All experiments were repeated three or more times with triplicate samples. The pore size and cell spreading characteristics were plotted as box plots to show the distribution in the data and significant differences between measured groups. At least 50 pores or cells were analyzed for each condition. Each box encompasses 25th to 75th percentiles, extending lines cover 90th and 10th percentiles, thin line is the median (50th percentile), and the thick line is the mean of the values. Values outside 95th and 5th percentiles were treated as outliers and are represented by dots. Significant differences between two groups were also evaluated using a one way analysis of variance (ANOVA) with 99% confidence interval. When $P < 0.01$, the differences were considered to be statistically significant.

3.3. RESULTS

3.3.1. Characterization of 3D chitosan scaffolds

First, thin scaffolds were formed directly inside 24-well plates (**Figure 3.1A**) by freeze-drying a 300 μ L volume of chitosan solution. This volume was selected on the basis of initial experiments which showed non-uniform coverage of the 24-well plate at lower volumes. Formed scaffolds were \sim 1 mm thick when dry. Although the thickness reduced to less than 0.3 mm after hydration, scaffolds maintained their porous structure

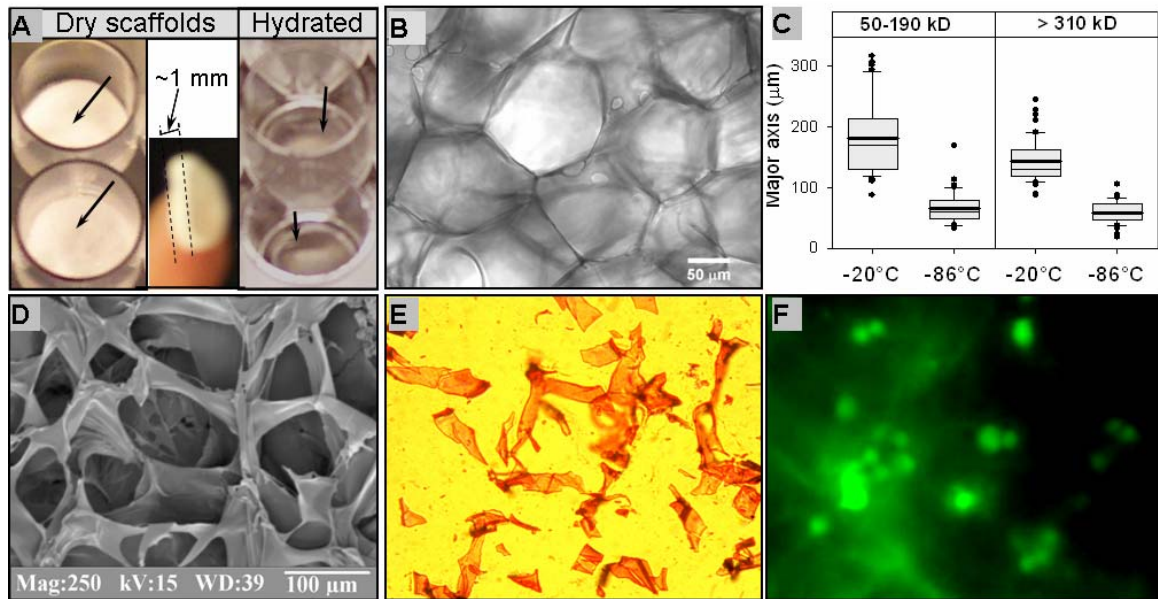


Figure 3.1. *In situ* scaffold formation. **Panel A.** The macroscopic view of 3D chitosan scaffold before and after hydration. **Panel B.** Phase contrast micrograph of a hydrated chitosan scaffold formed at -86°C. **Panel C.** Box plots showing the pore size distribution in chitosan scaffolds. **Panel D.** Scanning electron micrograph of 3D chitosan scaffold. **Panel E.** Micrograph of H/E stained cross section of 3D chitosan scaffold formed at -20°C. **Panel F.** Distribution of CFDA SE-stained HUVECs after 1 h of seeding onto a 3D chitosan scaffold.

with no significant changes during 15 days of incubation. When the hydrated scaffolds were examined under an inverted light microscope, porous structures were clearly noticeable (**Figure 3.1B**) in different layers. Evaluation of micrographs showed that pore sizes between 50 to 200 μm (**Figure 3.1C**) could be obtained by regulating the rate of cooling, similar to thick cylindrical scaffolds (Madihally and Matthew 1999); pore sizes were larger in scaffolds frozen at -20°C relative to samples frozen at -86°C . However, MW of chitosan did not significantly influence the size or the shape of the pores. To understand whether these pores are open to cell seeding and interconnected, scaffolds were analyzed via SEM and histology. These results showed that the pores are open to cell seeding (**Figures 3.1D**) and interconnected (**Figures 3.1E**).

3.3.2. Influence of 3D architecture on the morphology of HUVECs

To understand the influence of 3D matrix on cellular activity, HUVECs were seeded onto 2D and 3D chitosan matrices. First, cell seeding technique on 3D matrices was confirmed using CFDA-SE staining. These results showed the uniform distribution of cells in the 3D scaffold (**Figure 3.1F**). Next, comparison of cell spreading area showed significant reduction on 2D chitosan surfaces (**Figures 3.2A-C**) relative to control surfaces. Reduction in cell spreading was similar in both MWs of chitosan (**Figure 3.2F**). In addition, cells showed circular morphology rather than typical polygonal shape of HUVECs (**Figure 3.2G**). On the contrary, HUVECs on 3D matrices showed two distinct morphologies: i) rounded cells resembling 2D chitosan membranes; ii) polygonal cells, resembling control surface, but forming interconnected microstructures (**Figures 3.2D and 3.2E**). To understand the differences better, quantified data were grouped into two distributions. One group showed spreading area

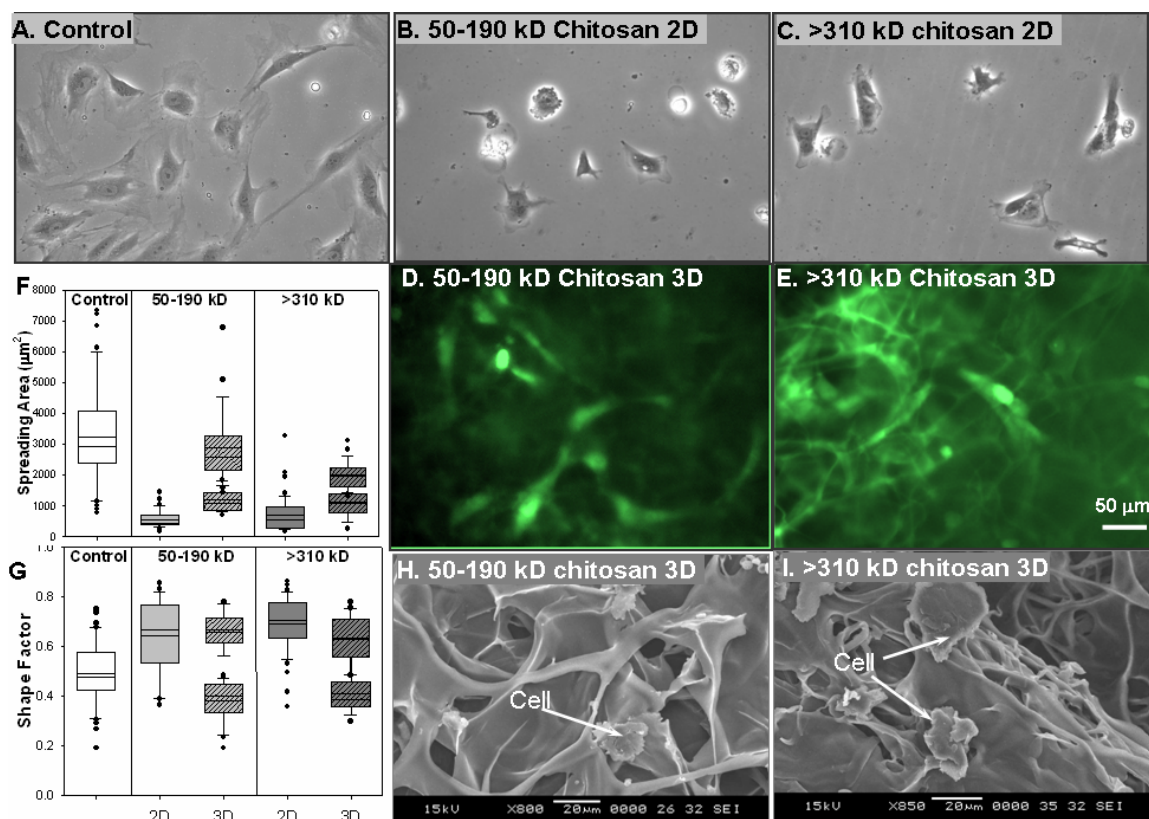


Figure 3.2. Effect of 3D architecture on spreading of HUVECs. Cells were cultured for 2 days in 2D and 3D chitosan scaffolds. **Panels A-C.** Phase contrast micrographs. **Panels D-E.** Fluorescence micrographs of CFDA-SE stained cells. **Panel F.** Box plots showing the distribution in the projected spreading area. **Panel G.** Box plots showing the distribution in the shape factor. **Panels H and I.** Scanning electron micrographs of HUVECs on 3D matrices.

resembling control and the other resembling 2D membranes. The actual spreading may even be more (up to 15% per cell) since cell spreading area was calculated using 2D projections. Similar dichotomy was observed in the shape of the cells and the lower shape factor corresponded to the larger surface area for the respective conditions.

Further analysis by SEM revealed (**Figures 3.2H and 3.2I**) that the cells on a flat surface within the 3D matrix showed a morphology similar to spreading on 2D membranes. Elongated spreading characteristics were presumed to be the cells colonized within the porous structure, although they could not be identified by this method. Next, cytoskeletal organization of HUVECs was probed via actin staining. On 2D membranes (**Figures 3.3B and 3.3C**), actin fibers were not well-distributed relative to control (**Figures 3.3A**) and showed bright spots. On the contrary, HUVECs on 3D scaffolds showed peripheral distribution of actin filaments in the spread cells (**Figures 3.3D and 3.3G**). Further, rounded cells that were out of focus confirmed that the two cell morphologies are in two different planes suggesting that cells colonized in the porous structure correspond to elongated cell shape.

3.3.3. Influence of 3D architecture on the proliferation of HUVECs

To characterize the influence of morphological changes on cellular colonization, cell culture was continued for up to seven days for 2D cultures and fifteen days for 3D cultures. These results showed an increase in polygonal cells with peripheral actin distribution on 3D chitosan scaffolds, particularly in 50-190 kD chitosan scaffold (**Figures 3.3E and 3.3H**). To confirm whether the cells are present inside the porous structure or not, scaffolds were analysed via histochemical technique. These results showed a significant number of cells inside the porous structure (**Figures 3.3F and 3.3I**)

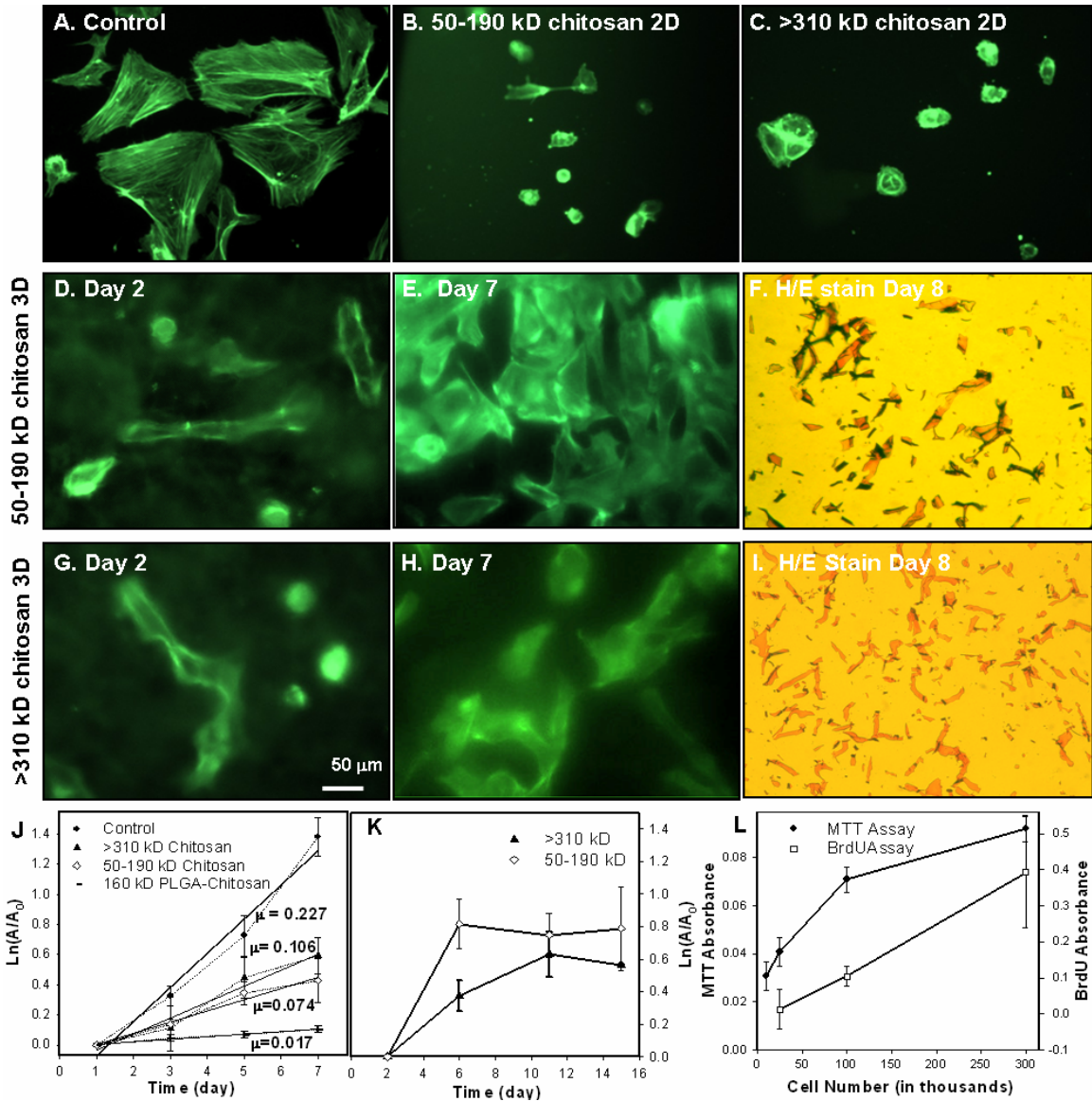


Figure 3.3. Cellular organization and proliferation of HUVECs. Micrographs were obtained after staining cells on various surfaces for actin. **Panel A.** Control. **Panel B.** 50-190 kD 2D chitosan membrane. **Panel C.** >310 kD 2D chitosan membrane. **Panels D-F.** 50-190 kD chitosan scaffolds. **Panels G-I.** >310 kD chitosan scaffolds. **Panel J.** Proliferation on 2D matrices. **Panel K.** Proliferation on 3D matrices. Error bars represent \pm SD. **Panels L.** Calibration curve.

distributed throughout the matrix.

Next, growth rate was analyzed in 2D and 3D scaffolds. These results showed that 50-190 kD 2D membranes (**Figure 3.3J**) were least supportive ($\mu=0.074 \text{ day}^{-1}$) relative to >310 kD 2D membranes ($\mu=0.106 \text{ day}^{-1}$) and the controls showed the maximum growth ($\mu=0.227 \text{ day}^{-1}$). Cell proliferation on 3D matrices was significantly different from 2D matrices. 50 -190 kD matrices showed a higher initial growth rate than >310 kD matrices (**Figure 3.3K**). However, cells on both the matrices reached a saturation point after which no significant changes were observed. Since the saturation region could be due to decreased mitochondrial activity at higher densities, the absorbance values from different time points were compared with a calibration curve (**Figure 3.3L**). All the values were located in the linear portion of the calibration curve indicating that the saturation region is not due to decreased MTT activity. Nevertheless, growth kinetics was also analyzed via the incorporation of BrdU into the DNA at few time points. These results supported the MTT-assay results on 2D and 3D matrices.

3.3.4. Influence of 3D architecture on the morphology of MEFs

To understand whether the influence of architecture is unique to HUVECs or not, activity of MEFs was tested. These results showed a similar reduction in spreading area of MEFs on 2D chitosan membranes (**Figures 3.4A-C**) and also typical spindle shape of fibroblasts was absent. The shape factor was on all 2D chitosan surfaces ($\sim 0.8 \pm 0.1$) which was significant different than on control surface ($\sim 0.4 \pm 0.1$). Further analysis via actin staining (**Figures 3.4D**) showed a significant reorganization in the cytoskeleton and reduction in the intracellular actin fibers on chitosan membranes relative to control. Also actin was localized in the perinuclear space of MEFs on 2D chitosan membranes rather

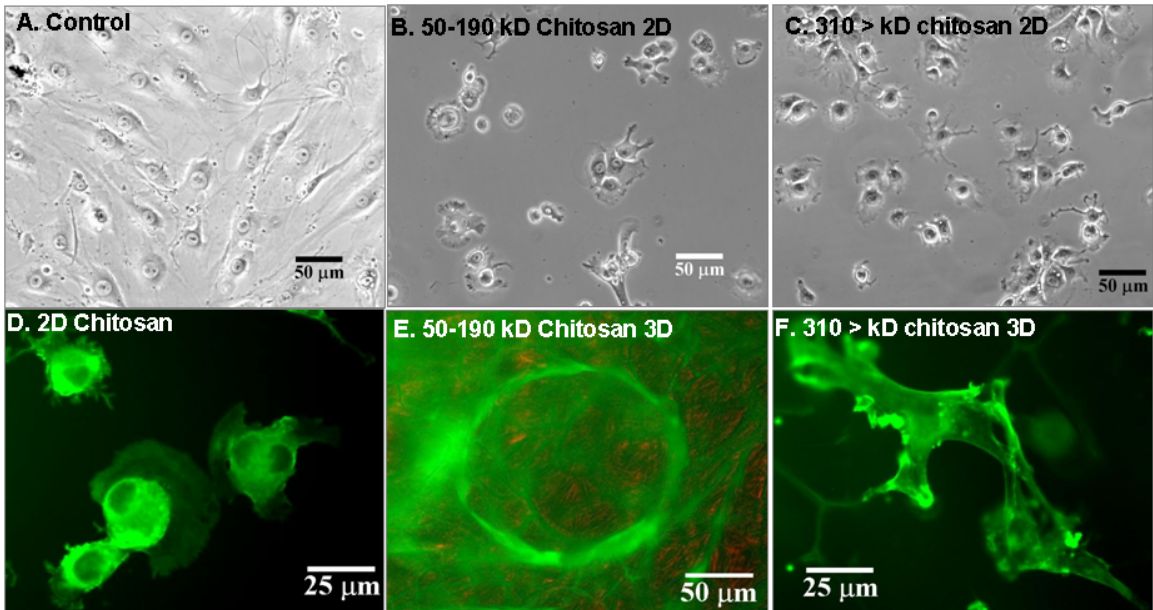


Figure 3.4. Effect of 3D architecture on spreading of MEFs. Cells were cultured for 2 days in 2D and 3D chitosan scaffold. **Panel A-C.** Phase contrast micrographs. **Panels D-F.** Fluorescence micrographs of actin staining.

than in the cytoplasmic region seen on controls. On the contrary, MEFs on 3D chitosan scaffolds showed well spread spindle shape (**Figures 3.4E and 3.4F**). Spreading appeared to be guided by the porous structure since a number of cellular structures mimicking the pore morphologies of the scaffold were observed (**Figure 3.4E**). Interestingly, actin did not accumulate in the perinuclear space and was distributed in the entire cytoplasm.

3.3.5. Altering the structural features of chitosan with PLGA

Next, the surface features of emulsified chitosan were studied using SEM. Obtained micrographs revealed the presence of PLGA particles in 2D surfaces (**Figures 3.5A-D**), probably due to preferential vaporization of chloroform relative to water. Quantification of these particles indicated that the size increased in tandem with PLGA MW (**Figure 3.6B**). In particular there was a significant increase from 19kD to 76kD PLGA.

Scaffolds formed from emulsions had a different porous structure relative to unemulsified scaffolds. Scaffolds formed from emulsified chitosan alone showed circular micropores in addition to the pores from the freeze-drying of ice, probably due to drying of chloroform. In PLGA-chitosan scaffolds, few PLGA particles were embedded in the matrix similar to 2D membranes (**Figures 3.5E-H**). However, majority of the PLGA was interdispersed within the matrix and could not be differentiated from chitosan. To assess any interaction among the components, thermogravimetric analysis was performed using differential scanning calorimetry. These results indicated no interaction among chitosan, PLGA and DMPC.

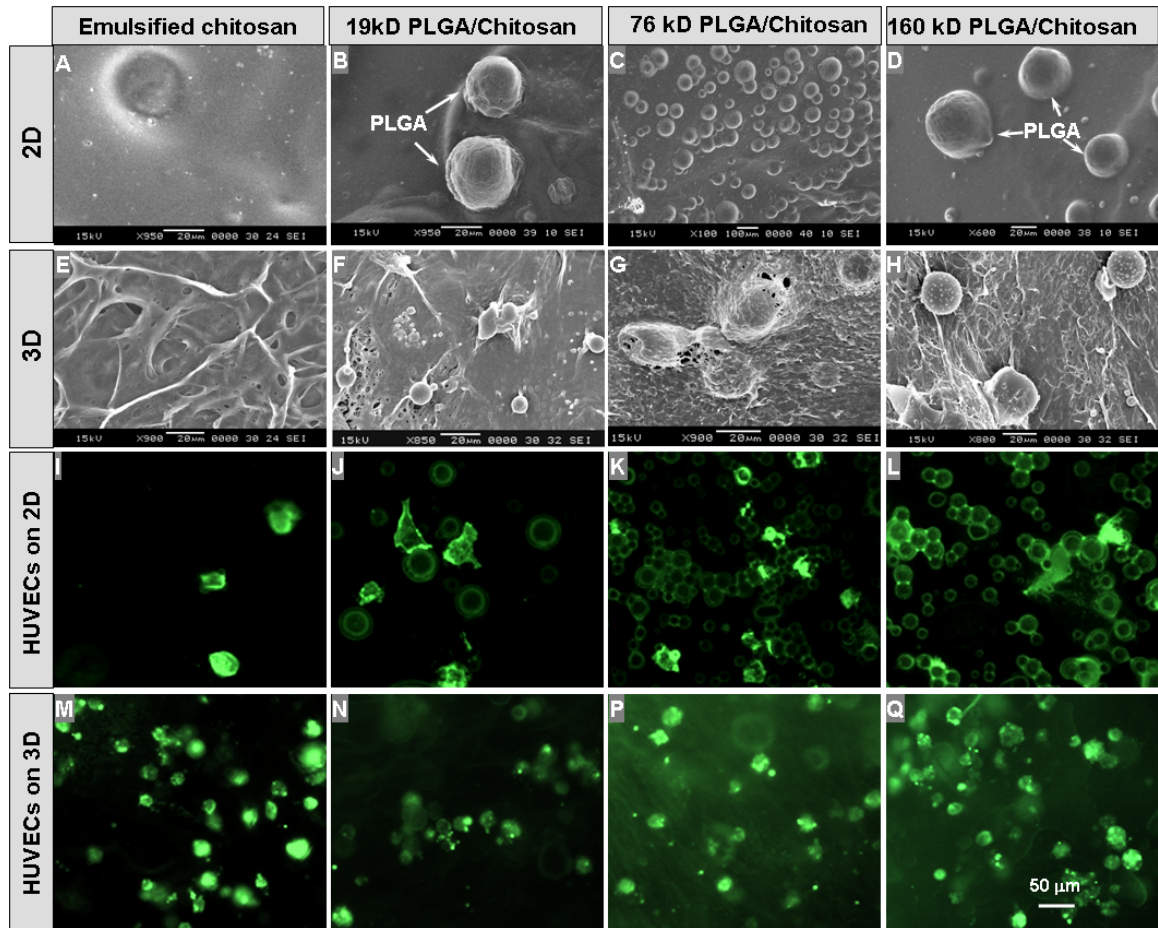


Figure 3.5. Influence of emulsification on surface topology and shape of HUVECs.

Panels A-H. Scanning electron micrographs of formed blends. **Panels I-Q.** Fluorescent micrographs of HUVECs cultured for 2 days on various surfaces prior to staining for actin.

3.3.6. Influence of emulsification on morphology of HUVECs

Responses of HUVECs on 2D and 3D PLGA-chitosan matrices were studied, similar to chitosan matrices. Actin stained HUVECs (**Figures 3.5I-Q**) showed a reduced cell spreading in emulsified 2D chitosan membranes (i.e., chitosan emulsified in chloroform in the presence or absence of DMPC without PLGA) but not significantly lower than the unemulsified chitosan membranes. Presence of 19kD particles did not affect cell spreading significantly (**Figure 3.6A**). However, the presence of 160kD PLGA on the surface affected cell spreading. Also, increase in the MW of PLGA progressively decreased cell spreading; cell spreading area on 19kD PLGA-chitosan was about 30% more than 160kD PLGA-chitosan.

In 3D matrices, emulsification significantly affected cell spreading. Compared with unemulsified 3D chitosan scaffolds, there was a four-fold reduction in cell spreading on emulsified chitosan scaffolds. Quantitatively, the spreading area was equivalent to the cells in suspension i.e., the minimum area occupied by a viable cell in the absence of any adhesive interactions. Thus, additional changes in the PLGA MW did not affect the spreading area any further. Similar effect of emulsification and presence of PLGA on spreading characteristics of MEFs were observed (**Figure 3.7**). MEFs showed significantly reduced spreading area and remained spherical on all the emulsified chitosan/ PLGA scaffolds.

3.3.7. Influence on cell viability and endocytic activity

The reduction in cell spreading could lead to decreased cellular activity. Thus, cell growth was analyzed on these scaffolds, similar to chitosan scaffolds. These results showed that growth rate was negligible on 2D 160 kD-PLGA-chitosan (**Figure 3.3J**)

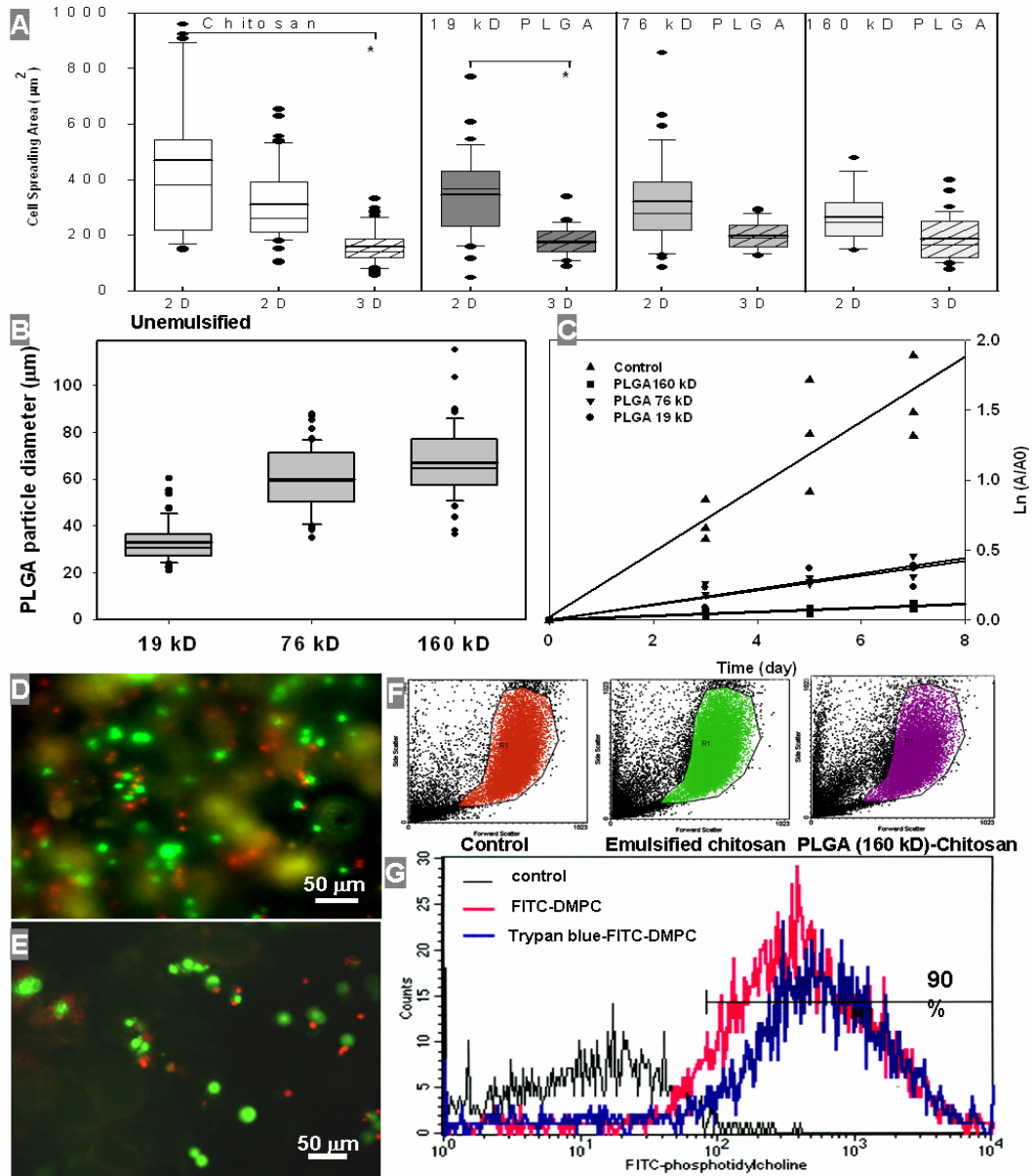


Figure 3.6. HUVECs are viable and functional after 2 days. **Panel A.** Box plots showing the distribution of spreading area. **Panel B.** Box plots showing the distribution of PLGA particle size. **Panel C.** Cell proliferation on 2D PLGA-chitosan. **Panel D and E.** Fluorescence micrographs showing the viability on 2D 19kD PLGA-chitosan membrane and 3D 160kD PLGA-chitosan scaffold, respectively. **Panel F.** Flow cytometric dots plots showing cell size and granularity. **Panel G.** Flow cytometric histograms showing the intracellular delivery of DMPC.

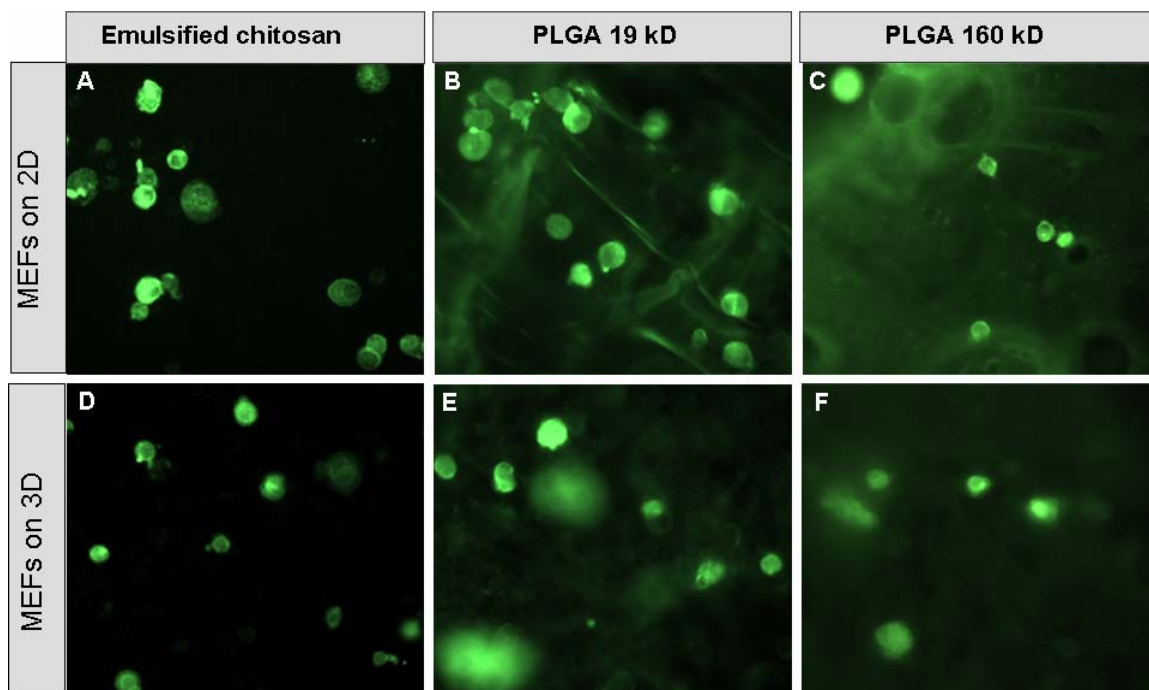


Figure 3.7. Influence of emulsification on shape of MEFs. Fluorescence micrographs of MEFs were stained for actin after 4 days in culture.

membranes relative to 2D chitosan membranes or controls. Similar growth rate constants were obtained for other 2D PLGA-chitosan membranes (**Figure 3.6C**). This could be due to altered morphology not conducive for cell growth (Folkman and Moscona 1978) or due to decreased viability. To confirm, viability of these cells was tested using LIVE/DEAD Assay kit after two days of culture. Quantification of micrographs (**Figures 3.6D and 3.6E**) showed nearly 71% (± 3) of green fluorescent (live) cells on 2D matrices and 63% (± 4) on 3D matrices. These numbers were comparable to control surfaces analyzed just after seeding. There were no significant differences in the cell size and granularity when analyzed using flow cytometry (**Figure 3.6F**).

Next, the endocytic activity of these cells was tested. If cells were functional, then they would internalize the phospholipid-stabilizer through the established endocytic pathway. For this purpose, membranes were formed by replacing unconjugated DMPC with FITC-conjugated DMPC and seeded HUVECs were analyzed via flow cytometry (**Figure 3.6G**). These results showed the presence of fluorescence in 90% of the cells exposed to FITC-DMPC compared to cells exposed to unconjugated DMPC. Since this presence could be due to non-specific extracellular binding, extracellular fluorescence was quenched using trypan blue and then analyzed. These results confirmed the intracellular fluorescence and the presence of DMPC inside the cells. This suggested that cells are functional despite being reduced in size.

3.3.8. Alteration in material stiffness

To better understand the influence of various 2D and 3D matrices on cell colonization, stiffness properties were evaluated. These results showed that 2D chitosan

membranes endured a longer elongation (45-60%) at break, similar to previously published results (Sarasam and Madihally 2005). With increase in MW, membranes exhibited greater strain but lesser stress at break. The stiffness decreased with increase in MW of chitosan (**Table 3.1**). There was no significant difference between the stiffness values of emulsified 2D membranes and unemulsified 2D membranes. In 3D chitosan scaffolds, stiffness decreased by three orders of magnitude and MW did not significantly affect the stiffness values. Stiffness of 3D PLGA-chitosan scaffolds could not be evaluated because handling alone affected their structural stability.

3.4. DISCUSSION

This study addressed the influence of structural design on cellular colonization of HUVECs and MEFs in 2D chitosan, 3D chitosan and PLGA-chitosan scaffolds. Thin porous 3D chitosan scaffolds with interconnected pores were obtained inside a 24-well plate or on a glass slide by controlled rate freezing and lyophilization technique (Madihally and Matthew 1999). Since 2D and 3D matrices were generated from same solutions, sterilized, neutralized and washed similarly prior to cell seeding, the complexities associated with the influence of altered solvent composition while preparing the samples was minimized. The primary differences in generating 2D and 3D matrices were the method of drying.

Different structural designs tested in this study are summarized in **Figure 3.8** along with the observed differences on cell colonization. Both HUVECs and MEFs showed a reduction in cell spreading on chitosan membranes relative to control. Similar reduction in cell spreading has also been observed on chitosan membranes (Cuy et al. 2003) despite comparable adsorption of serum proteins relative to controls. The authors eluded this

Sample	Stiffness
50-190 kD chitosan 2D membrane	6±1 MPa
>310 kD chitosan 2D membrane	2±1 MPa
Emulsified >310 kD chitosan/ 160 kD PLGA membrane	1.7±0.1 MPa
50-190 kD chitosan 3D scaffold	1.54 ± 0.16 kPa
> 310 kD chitosan 3D scaffold	1.57 ± 0.21 kPa
Emulsified >310 kD chitosan scaffold	1.06 ± 0.1 kPa
Emulsified >310 kD chitosan/ 160kD PLGA scaffold	Not detected

Table 3.1. Stiffness properties of scaffolds in different architectures.



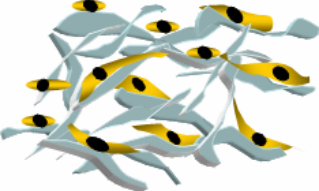
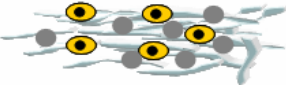
Material Architecture	Chitosan	Emulsified chitosan/PLGA
2D	 <p>Cells may spread and proliferate</p>	 <p>Cells don't spread and don't proliferate</p>
3D	 <p>Cells do spread and proliferate</p>	 <p>Cells don't spread and don't proliferate</p>

Figure 3.8. Schematic showing the cell colonization characteristics on different architectures.

observation to a strong adhesive interaction of cells and chitosan. Nevertheless, when cells were seeded onto 3D chitosan scaffolds, cell spreading significantly increased and cells grew in to the pores of chitosan matrix. Significant alterations in cell spreading were observed in 2D and 3D chitosan scaffolds although the chemical composition is the same. Therefore, the spatial architecture of scaffolds has the dominant role in directing cellular colonization even at the absence of cell-binding domain in the materials. These observations are comparable to *in vivo* implant studies condition, where scaffold microarchitecture, rather than chemical composition, is known to affect vascularization (Sieminski and Gooch 2000).

A number of factors could be contributing to the observed differences in 2D and 3D matrices. In 2D membranes, cultured cells are restricted to spread on a flat plane unlike 3D matrices which provide spatial advantages for cell adhesion. A number of studies have shown that pore size of 3D scaffolds significantly influence cellular responses and colonization (Ng et al. 2004; Salem et al. 2002; Wang and Ho 2004; Yannas et al. 1989; Zeltinger et al. 2001). Many cell types including HUVECs and fibroblasts are unable to completely colonize scaffolds with the pore sizes $>300 \mu\text{m}$ (Naughton and Applegate 2002; Ng et al. 2004) due to the difficulty in crossing large bridging distances. In this study, chitosan scaffolds used for cell colonization studies were prepared by freezing at -20°C which had a pore size distribution from 100 to 200 μm , closer to the optimum range (50 -150 μm) (Yannas et al. 1989). Thus the contribution from altered pore sizes to cell colonization was not an issue. Furthermore, HUVECs showed a faster colonization on 50-190kD chitosan scaffolds than $>310\text{kD}$ chitosan scaffolds despite having similar pore size distributions. MEFs also colonized 3D chitosan scaffolds although they may prefer

different pore sizes (Zeltinger et al. 2001). Nevertheless, further studies with pore sizes are necessary to understand the influence of microarchitecture on cell colonization.

Measured bulk mechanical properties suggested that the difference in the material stiffness could partially contribute to the observed differences in cell spreading characteristics between 2D membranes and 3D scaffolds. In 2D culture, cells are cultured on rigid glass surfaces coated with thin layer of matrices and stiffness that matrices possess may be primarily contributed by the glass surface. However, in 3D cultures, the stiffness of the scaffolds will be different than glass surfaces and may directly influence cell adhesion. Similar influence of substrate stiffness on other cellular functions has been reported (Freyman et al. 2002; Lee et al. 2001; Sieminski et al. 2004). Absence of cell spreading on 3D emulsified PLGA-chitosan scaffolds could be partially attributed to the loss of tractional forces on cells. The disassembly of FAs and stress fibers could have occurred due to loss of tractional forces and adopted a round morphology similar to cells in suspension. In this state, cells may become quiescent or cell spreading and proliferation are inhibited although they may be functional. Although endocytic activity of HUVECs was analyzed after two days, additional experiments analyzing the apoptotic pathway and other functionalities of HUVECs over a long period of time is necessary. However, the measured bulk properties are influenced by the porous structure of the 3D matrices. To better understand the influence of mechanical properties on cellular colonization, one has to evaluate the influence of porous structure on the mechanical properties of the matrices.

Altered surface texture and charge could also affect cell spreading. Cells showed less spreading area and more circular shape on 2D PLGA-chitosan membranes than

unemulsified chitosan surfaces despite having similar stiffness values. Furthermore, cell spreading decreased when MW of PLGA was increased from 19kD to 160kD PLGA, probably due to increased PLGA particles sizes which could act as hills with different net hydrophobicities. However, this could also be due to the decreased surface charge attributed to the shielding effect by PLGA since cell adhesion to chitosan could be mediated via electrostatic interactions rather than through RGD binding domain. Further studies exploring the changes in the surface charge densities are necessary to clarify this issue. Nevertheless, the existence of hills without any binding domain could constrain cell movement by restricting cytoskeletal reorganization (Clark et al. 1987) or reshape its actin filaments to fit the topography (Walboomers et al. 1999). Curtis *et al* proposed cells' "topographic reaction" to substratum in microscale through changes in cell orientation, motility, and adhesion (Curtis and Wilkinson 1999). On 2D chitosan membranes, actin was observed as bright spots in the periphery of HUVECs but was localized in the perinuclear space of MEFs. FA sites and actin maintain cell integrity in addition to acting as signaling centers to regulate cellular activity (Sastry and Burrige 2000). To better understand these observations, one has to explore the signal transduction mechanisms through which these events are communicated.

The observed differences in cell colonization could also be due to the changes in the adsorption of serum proteins on to 2D and 3D matrices. Distinctly different sets and different amounts of proteins could have adsorbed to 2D and 3D matrices contributing to the observed differences in cell spreading. Further studies profiling the adhesive serum proteins are necessary to understand the observed differences in cell colonization better. In addition, the saturation of cell proliferation in 3D chitosan scaffolds could be due to

the contact inhibition and nutrient limitation as cell seeding density was more than twice the 2D seeding density. One has to explore the role of contact inhibition and nutrient limitation by changing the seeding density, the frequency of medium changes, and the thickness of the scaffolds.

3.5. CONCLUSION

In summary, this study showed that spatial architecture significantly influences cell spreading, and proliferation. Although further studies are required, dimensionality, stiffness of the matrix, and topography of the matrix appear to regulate the cellular colonization. Thus, apart from chemical composition, scaffold architecture plays a significant role in tissue regeneration.

3.6. REFERENCES

2000. Tissue engineering. *Nat Biotechnol* 18 Suppl:IT56-8.
- Balgude AP, Yu X, Szymanski A, Bellamkonda RV. 2001. Agarose gel stiffness determines rate of DRG neurite extension in 3D cultures. *Biomaterials* 22(10):1077-84.
- Cai K, Yao K, Cui Y, Lin S, Yang Z, Li X, Xie H, Qing T, Luo J. 2002. Surface modification of poly (D,L-lactic acid) with chitosan and its effects on the culture of osteoblasts in vitro. *J Biomed Mater Res* 60(3):398-404.
- Chen CS, Mrksich M, Huang S, Whitesides GM, Ingber DE. 1997. Geometric control of cell life and death. *Science* 276(5317):1425-1428.
- Chung TW, Yang J, Akaike T, Cho KY, Nah JW, Kim SI, Cho CS. 2002. Preparation of alginate/galactosylated chitosan scaffold for hepatocyte attachment. *Biomaterials* 23(14):2827-34.
- Chupa JM, Foster AM, Sumner SR, Madhally SV, Matthew HW. 2000. Vascular cell responses to polysaccharide materials: in vitro and in vivo evaluations. *Biomaterials* 21(22):2315-22.
- Chvapil M. 1977. Collagen sponge: theory and practice of medical applications. *Journal of Biomedical Materials Research* 11(5):721-741.
- Clark P, Connolly P, Curtis AS, Dow JA, Wilkinson CD. 1987. Topographical control of cell behaviour. I. Simple step cues. *Development* 99(3):439-48.
- Curtis A, Wilkinson C. 1999. New depths in cell behaviour: reactions of cells to nanotopography. *Biochem Soc Symp* 65:15-26.
- Cuy JL, Beckstead BL, Brown CD, Hoffman AS, Giachelli CM. 2003. Adhesive protein interactions with chitosan: consequences for valve endothelial cell growth on tissue-engineering materials. *J Biomed Mater Res* 67A(2):538-47.
- Folkman J, Moscona A. 1978. Role of cell shape in growth control. *Nature* 273(5661):345-9.

- Freyman TM, Yannas IV, Yokoo R, Gibson LJ. 2002. Fibroblast contractile force is independent of the stiffness which resists the contraction. *Exp Cell Res* 272(2):153-62.
- Giancotti FG, Ruoslahti E. 1999. Integrin signaling. *Science* 285(5430):1028-32.
- Korff T, Augustin HG. 1999. Tensional forces in fibrillar extracellular matrices control directional capillary sprouting. *J Cell Sci* 112(Pt 19):3249-58.
- Lahiji A, Sohrabi A, Hungerford DS, Frondoza CG. 2000. Chitosan supports the expression of extracellular matrix proteins in human osteoblasts and chondrocytes. *J Biomed Mater Res* 51(4):586-95.
- Langer R, Vacanti JP. 1993. Tissue engineering. *Science* 260(5110):920-6.
- Lee CR, Grodzinsky AJ, Spector M. 2001. The effects of cross-linking of collagen-glycosaminoglycan scaffolds on compressive stiffness, chondrocyte-mediated contraction, proliferation and biosynthesis. *Biomaterials* 22(23):3145-54.
- Madhally SV, Matthew HW. 1999. Porous chitosan scaffolds for tissue engineering. *Biomaterials* 20(12):1133-42.
- Madhally SV, Solomon V, Mitchell RN, Van De Water L, Yarmush ML, Toner M. 2003. Influence of insulin therapy on burn wound healing in rats. *J Surg Res* 109(2):92-100.
- Mizuno K, Yamamura K, Yano K, Osada T, Saeki S, Takimoto N, Sakurai T, Nimura Y. 2003. Effect of chitosan film containing basic fibroblast growth factor on wound healing in genetically diabetic mice. *J Biomed Mater Res* 64(1):177-81.
- Mosmann T. 1983. Rapid colorimetric assay for cellular growth and survival: application to proliferation and cytotoxicity assays. *J Immunol Methods* 65(1-2):55-63.
- Naughton GK, Applegate DR. 2002. Cryopreserved dermal implants. Atala A, Langer RP, editors.

- Ng KW, Khor HL, Hutmacher DW. 2004. In vitro characterization of natural and synthetic dermal matrices cultured with human dermal fibroblasts. *Biomaterials* 25(14):2807-18.
- Oberpenning F, Meng J, Yoo JJ, Atala A. 1999. De novo reconstitution of a functional mammalian urinary bladder by tissue engineering. *Nat Biotechnol* 17(2):149-55.
- Raghavan D, Kropp BP, Lin HK, Zhang Y, Cowan R, Madhally SV. 2005. Physical characteristics of small intestinal submucosa scaffolds are location-dependent. *J Biomed Mater Res A* 73A(1):90-6.
- Rajnicek A, Britland S, McCaig C. 1997. Contact guidance of CNS neurites on grooved quartz: influence of groove dimensions, neuronal age and cell type. *J Cell Sci* 110(Pt 23):2905-13.
- Ranucci CS, Moghe PV. 2001. Substrate microtopography can enhance cell adhesive and migratory responsiveness to matrix ligand density. *J Biomed Mater Res* 54(2):149-61.
- Salem AK, Stevens R, Pearson RG, Davies MC, Tendler SJ, Roberts CJ, Williams PM, Shakesheff KM. 2002. Interactions of 3T3 fibroblasts and endothelial cells with defined pore features. *J Biomed Mater Res* 61(2):212-7.
- Sarasam A, Madhally SV. 2005. Characterization of Chitosan-Polycaprolactone Blends for Tissue Engineering Applications. *Biomaterials* (in press).
- Sastry SK, Burrige K. 2000. Focal adhesions: a nexus for intracellular signaling and cytoskeletal dynamics. *Exp Cell Res* 261(1):25-36.
- Schoen FJ, Levy RJ. 1999. Founder's Award, 25th Annual Meeting of the Society for Biomaterials, perspectives. Providence, RI, April 28-May 2, 1999. Tissue heart valves: current challenges and future research perspectives. *J Biomed Mater Res* 47(4):439-65.
- Shigemasa Y SK, Sashiwa H, Saimoto H. 1994. Enzymatic degradation of chitins and partially deacetylated chitins. *Int J Biol Macromol* 16(1):43-49.
- Sieminski AL, Gooch KJ. 2000. Biomaterial-microvasculature interactions. *Biomaterials* 21(22):2232-41.

- Sieminski AL, Hebbel RP, Gooch KJ. 2004. The relative magnitudes of endothelial force generation and matrix stiffness modulate capillary morphogenesis in vitro. *Exp Cell Res* 297(2):574-84.
- Tomihata K, Ikada Y. 1997. In vitro and in vivo degradation of films of chitin and its deacetylated derivatives. *Biomaterials* 18(7):567-75.
- Walboomers XF, Croes HJ, Ginsel LA, Jansen JA. 1999. Contact guidance of rat fibroblasts on various implant materials. *J Biomed Mater Res* 47(2):204-12.
- Wang YC, Ho CC. 2004. Micropatterning of proteins and mammalian cells on biomaterials. *Faseb J* 18(3):525-7. Epub 2004 Jan 8.
- Yannas IV, Lee E, Orgill DP, Skrabut EM, Murphy GF. 1989. Synthesis and characterization of a model extracellular matrix that induces partial regeneration of adult mammalian skin. *Proc Natl Acad Sci U S A* 86(3):933-7.
- Zeltinger J, Sherwood JK, Graham DA, Mueller R, Griffith LG. 2001. Effect of pore size and void fraction on cellular adhesion, proliferation, and matrix deposition. *Tissue Eng* 7(5):557-72.
- Zhu H, Ji J, Lin R, Gao C, Feng L, Shen J. 2002. Surface engineering of poly(D,L-lactic acid) by entrapment of chitosan-based derivatives for the promotion of chondrogenesis. *J Biomed Mater Res* 62(4):532-9.

CHAPTER 4

IN VITRO CHARACTERIZATION OF CHITOSAN-GELATIN SCAFFOLDS FOR TISSUE ENGINEERING

4.1. INTRODUCTION

Chitosan is a naturally derived polysaccharide. It has gained much attention as a biomaterial in diverse tissue engineering applications due to its low cost, large-scale availability, anti-microbial activity, and biocompatibility (Khor and Lim 2003). Chitosan scaffolds with various geometries, pore sizes, and pore orientation can be obtained using controlled rate freezing and lyophilization (Madhally and Matthew 1999). Chitosan marginally supports biological activity of diverse cell types and chitosan films are highly brittle with a strain at break of 40-50% in the wet state. Furthermore, lysozyme-dependent chitosan degradation depends on the degree of deacetylation (DD), local pH (Davies, Neuberger et al. 1969; Pangburn, Trescony et al. 1982; Shigemasa, Saito et al. 1994) and homogeneity of the source; lysozymal hydrolysis is high in acidic conditions (pH 4.5-5.5) (Nordtveit, Varum et al. 1996) and decreases with increase in deacetylation and chitosan prepared homogeneously degrades faster. Although the DD and the homogeneity of source can be controlled during polymer processing to regulate biomechanical properties, the range is marginal.

For improving the mechanical or biological properties of chitosan over a broad range, blending with other polymers is widely investigated. Less expensive gelatin is blended with chitosan to improve the biological activity. Gelatin, a fragment of collagen,

contains Arg-Gly-Asp (RGD)-like sequence that promotes cell adhesion and migration in addition to faster degradation. Chitosan and gelatin form a polyelectrolyte complex. Gelatin-chitosan scaffolds have been formed without or with cross-linkers such as glutaraldehyde (Mao, Zhao et al. 2003) or enzymes (Chen, Embree et al. 2003) and tested in regenerating various tissues including skin (Mao, Zhao et al. 2003), cartilage (Xia, Liu et al. 2004), and bone (Yin, Ye et al. 2003).

Despite these advances, not much attention is given in understanding the impact of various modifications on dynamics of tissue remodeling processes. For example, the presence of other polymers could decrease the degradation rate by limiting the lysozymal transport near the cleavable linkage. In addition, cell adhesive interactions of chitosan and morphological changes are not completely explored despite chitosan lacking a specific binding domain for integrin-mediated cell adhesion through which majority of the transmembrane signaling takes place (Hynes Ro Fau - Zhao and Zhao). Intracellular tension is modulated via focal adhesion (FA) complex, integrins, and the ECM (Chen, Mrksich et al. 1997; Galbraith and Sheetz 1998; Bhadriraju and Hansen 2002). FA-complex is comprised of many molecules including focal adhesion kinase (FAK), vinculin, and talin, (Girard and Nerem 1995) and level of FA-complex correlate with cell spreading (Chen, Alonso et al. 2003). FAK plays a vital role in FA-complex turnover (Wozniak, Modzelewska et al. 2004). Actin reorganizes with the redistribution and levels of FA-complex and alters cell shape and characteristics. When gelatin and chitosan are blended together, the structure formed can affect the spatial distribution of integrin ligands. Furthermore, polycationic chitosan interaction with the anionic cell surface could be affected. These effects influence cell adhesion, cellular bioactivity

(Heilshorn, DiZio et al. 2003; Tiwari, Kidane et al. 2003), tissue remodeling process and ultimately the quality of the regenerated tissue.

This study focused on understanding the effect of blending gelatin with chitosan on degradation properties, mechanical properties and cell-matrix interactions. 3D scaffolds of various blend ratios were formed using controlled-rate freezing technique and lyophilization. Further, human umbilical vein endothelial cells (HUVECs) and mouse embryonic fibroblasts (MEFs) were tested to understand the interactions of cells of two different origins. HUVECs that make up the luminal lining and tend to form tubular structures were tested in static culture and shear stresses. MEF are present in the connective tissue, synthesize collagen type I and III and tend to develop fibrous network (Shigemasa Y 1994) were tested in 3D and 2D cultures. Actin and FAK distribution and cell-cell junction adhesion molecule-platelet EC adhesion molecule-1 (PECAM-1, CD31) expression (Osawa, Masuda et al. 2002; Kaufman, Albelda et al. 2004) were evaluated. These results show significant influence of blending gelatin with chitosan on the tissue remodeling process.

4.2. MATERIALS AND METHODS

Chitosan of >310kD MW (DD ≈85%), type A porcine skin gelatin, 5kD MW dextran sulfate, Hen Egg White Lysozyme (46,400 U/mg) and Dulbecco's modified Eagle medium (DMEM) were obtained from Sigma Aldrich Chemical Co (St. Louis, MO). Alexa Fluor 546 goat anti-mouse IgG₁ and Alexa Fluor 488 phalloidin were obtained from Molecular Probes (Eugene, OR). HUVECs and endothelial growth medium-2 (EGM-2) BulletKit were from Cambrex Biosciences (Walkersville, MD). MEFs were from American Tissue Culture Collection (Walkersville, MD). Anti-FAK

antibody was from BD Biosciences (Franklin Lakes, NJ) and anti-human CD31 or mouse IgG1 was from Serotec (Oxford, UK).

4.2.1. Formation of 2D membranes and 3D scaffolds

Chitosan (0.5 to 1% w/v), gelatin (1.5% to 4% w/v) were dissolved in 0.5M acetic acid. To prepare sterile 1% (w/v) chitosan solution, chitosan suspension in water was first autoclaved (at 121°C in a wet cycle for 20 min) and then dissolved by adding acetic acid equivalent to 0.5M in a sterile laminar flow hood. Appropriate proportions of these solutions were mixed to obtain various blend ratios. The solutions were either used directly or refrigerated until usage. The homogenous mixtures of gelatin and chitosan were poured into petri dishes and air dried over night to obtain membranes.

Approximately 2mL of 0.5% chitosan (w/v) and 0.5% chitosan containing 1.5% (w/v) gelatin solutions were poured into 14mm diameter plastic vials. Solutions were frozen at -20°C for 24 hours from the bottom surface only by insulating all other sides with Styrofoam (even the top) to orient the pores. Some samples were cross-linked with 0.25% glutaraldehyde prior to freezing. All samples were lyophilized at -80°C for 24 hours.

4.2.2. Stabilizing Chitosan and Chitosan-gelatin Scaffolds

The formed scaffolds were neutralized in 10 mL of one of the solutions formed in water: i) 1% dextran sulfate (pH = 4.61), ii) 1% glutaraldehyde, iii) 1N NaOH, and iv) absolute alcohol. All samples were placed in sealed glass vials and in the dark till the end of the study period.

4.2.3. Mechanical testing measurement

Tensile properties of 2D membranes were measured by the method described previously (Raghavan, Kropp et al. 2005; Sarasam and Madihally 2005). In brief, large samples were neutralized in 1N NaOH for 15 min and rinsed thoroughly under tap water and immersed in phosphate buffered saline (PBS, pH=7.4) for 30min prior to testing. Rectangular strips of approximately 45 mm×7.5 mm size were cut from each sample and pulled to break at a constant cross head speed of 5 mm/min using INSTRON 5842. The slope of the linear region in the stress-strain curve gave the stiffness (or elastic modulus) values.

Three-dimensional cylindrical scaffolds were neutralized with alcohol and washed with PBS. Compression tests were performed in 37°C PBS at a rate of 5mm/min, similar to tensile tests. Compression modulus was calculated from the slope of linear region of stress-strain curve.

4.2.4. Degradation Characterization

Scaffolds were sterilized and neutralized in alcohol overnight and then washed excessively in PBS prior to incubating in 10 mL PBS with or without 10 mg/L hen egg white (HEW) lysozyme. All incubations were done in 20 mL scintillation vials with a hole drilled (~15mm diameter) in each cap. These holes were covered with 0.22 µm filters to form sterile barriers while allowing equilibration with the incubator environment (37°C and 5% CO₂/95% Air). Media was replaced weekly by freshly prepared solutions.

At regular intervals, digital photographs were obtained and analyzed for dimensional changes using image analysis software (SigmaScan Pro, Chicago, IL). Incubation media were collected for pH analysis. Every week in the beginning and every

alternate week at later time points, four scaffolds per group were ‘sacrificed’ in order to take weight measurements. For weight determination, samples were dried using a graded series of alcohol and then a brief (8 hours) vacuum drying. During this process the scaffold loses its cylindrical shape.

4.2.5. Cell culture and seeding

HUVECs were cultured in EGM-2 BulletKit medium containing 2% fetal bovine serum, hydrocortisone, fibroblast growth factor-B, heparin, vascular endothelial growth factor, insulin-like growth factor-1, ascorbic acid, human epidermal growth factor, gentamicin following vendor’s protocol. Cells between 2 and 8 passages were used in all the experiments.

MEFs were maintained in DMEM supplemented with 4 mM L-glutamine, 4.5 g/L glucose, 1.5g/L sodium bicarbonate, 100 U/mL penicillin-streptomycin, 2.5 µg/mL amphotericin and 10 % FBS (Invitrogen Corp., Carlsbad, CA).

Both cells were maintained at 37°C, 5% CO₂/ 95% air and fed with fresh medium every 48 h. Cells were dissociated with 0.01% trypsin/ 10 µM EDTA (Invitrogen Corp., Carlsbad, CA), centrifuged and resuspended in medium prior to cell seeding.

Chitosan and chitosan-gelatin (wt.1:3) scaffolds were formed inside 24-well plates, using the previously described procedure (Huang, Seiwe et al. 2005). In brief, 300 µL of polymer solutions were poured into each well, frozen at -20°C and lyophilized. Scaffolds were neutralized in ethanol and washed with PBS. 10,000 and 25,000 cells per well were seeded onto 2D and 3D scaffolds respectively and incubated with 0.5 mL of growth medium. To achieve uniform distribution of cells in 3D scaffolds, a concentrated (500,000 cells/mL) cell suspension was placed at different locations on each sample.

Viability was tested using MTT-Formazan assay (Chupa, Foster et al. 2000).

For the shear stress experiment, each the glass slides was first overlaid with 0.1% gelatin, chitosan-gelatin (weight ratio 1:1) or 0.5% chitosan solution and then air dried in the laminar flow hood. 5000-8000 cells per cm^2 were seeded on the slides and cultured for five days in static culture and the slides were taken out from petridishes, inserted into the flow chamber (described below) and exposed to various steady shear stresses.

4.2.6. Parallel-plate flow chamber system

The perfusion system (**Figure 4.1**) consisted of i) a medium reservoir, ii) a variable speed peristaltic pump (Masterflex, Cole Palmer, IL), iii) a damping vessel to maintain steady laminar flow and iv) a parallel plate reactor made of polycarbonate. The reactor (constructed in-house) consisted of a top plate, a bottom plate, and a 0.025 cm thick silicon gasket between the two plates to control the height of flow channel and to tightly seal the two parts. The top plate had connections to the inlet and outlet tubings through channels of 2 mm inner diameter coupled with propylene fittings. In the bottom plate a groove was made to insert a 7.5×2.5 cm glass slide. A slowly diverging area at the entrance and converging area at the exit were provided to facilitate the development of the flow and avoid stagnation areas. The flow rate was adjusted through the pump to reach the required shear stress, τ (dyne/cm^2), calculated using the momentum balance for a parallel-plate geometry and Newtonian fluid, $\tau = 6Q\mu/wh^2$ where Q is volumetric flow rate, μ is the viscosity of the medium ($\sim 0.01 \text{ dyne s}/\text{cm}^3$), w is the chamber width and h is the chamber height. Lower range (4.5, 8.5 dyn/cm^2) representing venous system and high range (13 and 18 dyn/cm^2) representing the arterial system were used (Malek, Alper et al. 1999).

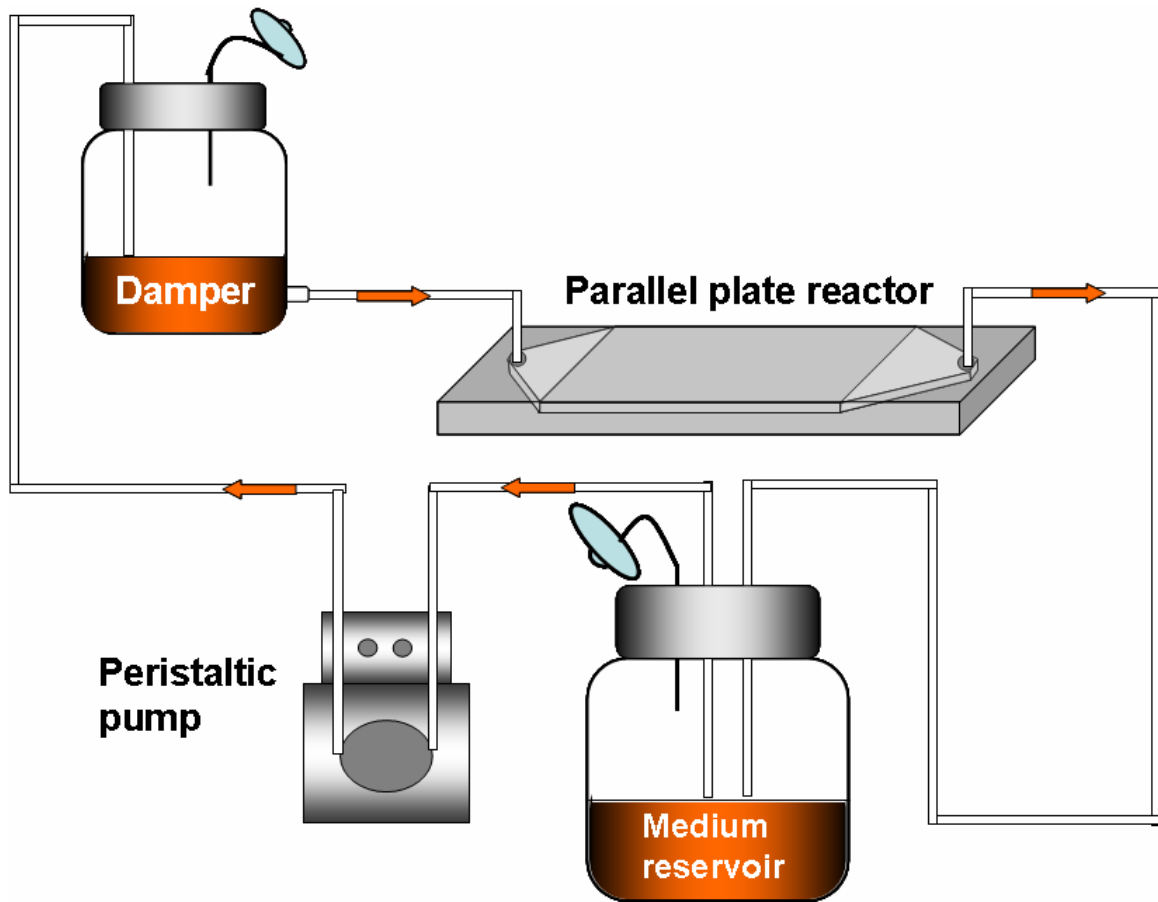


Figure 4.1. Schematic of perfusion system consisted of parallel plate chamber.

4.2.7. Morphological analysis

Morphologies were monitored using an inverted microscope (Nikon TE2000, Melville, NY) outfitted with a CCD camera. Digital micrographs were captured from different locations and analyzed for cell spreading area, pore sizes, and shape factors as described previously (Huang, Seiwe et al. 2005). For each condition, more than 50 pores or cells were analyzed. Samples were also analyzed at an accelerating voltage of 12-15 kV using scanning electron microscope (SEM, Joel JSM 6360). For this purpose, samples were dried using a series of increasing concentrations of ethanol followed by a brief vacuum drying. Dry scaffolds were sputter-coated with gold at 40 mA prior to observing under SEM.

4.2.8. Immunofluorescence staining

Cytoskeletal alterations were measured by the method described previously (Huang, Seiwe et al. 2005). Briefly, cells on different matrices were first fixed in 3.7% formaldehyde in PBS for 15 min at room temperature, and then permeabilized with ethanol (at -20°C) for 5 min after washing with PBS, and then incubated with anti-FAK for one hour at room temperature. After washing with PBS for three times, the slides were incubated with Alexa Fluor 546 goat anti-mouse IgG₁ for 40 min. For F-actin staining, the slides were then incubated with Alexa Fluor 488 phalloidin for 20 min in the dark at room temperature. Samples were observed under fluorescence microscope and digital images were obtained. Samples were also visualized using Leica TCS SP II confocal microscope (Heidelberg, Germany).

4.2.9. Flow cytometric analysis of PECAM-1

ECs were detached from slides using trypsin-EDTA and washed with PBS containing 2% FBS and incubated with mouse anti-human CD31 or mouse IgG1 (isotype control) in ice for 40-60 min. Following the incubation, ECs were washed, incubated for 30 min in ice with streptavidin conjugated R-phycoerythrin. Cells were washed again and analyzed using a FACSCalibur flow cytometer (Becton-Dickinson, San Jose, CA) by CellQuest software.

4.2.10. Statistical analysis

All experiments were repeated three or more times with triplicate samples. The pore size and cell spreading characteristics were plotted as box plots to show the distribution in the data and significant differences between measured groups. At least 50 pores or cells were analyzed for each condition. Each box encompasses 25 to 75 percentiles, extending-lines cover 90th and 10th percentiles, thin line is the median (50th percentile), and the thick line is the mean of the values. Values outside 95th and 5th percentiles were treated as outliers and are represented by dots. Significant differences between two groups were also evaluated using a one way analysis of variance (ANOVA) with 99% confidence interval. When $P < 0.01$, the differences were considered to be statistically significant.

4.3. RESULTS

4.3.1. Morphology of chitosan and chitosan-gelatin cylindrical scaffolds

Chitosan-gelatin cylindrical scaffolds of 14 mm diameter and 20 mm high were formed by controlled rate freeze-drying. Initial experiments were performed by freezing blend solutions at room temperature. These results showed two phases with increased

gelatin content in the bottom. To minimize separation of two components, solutions were refrigerated to form a gel prior to freeze-drying and the formed scaffolds showed uniform distribution of the two components. To understand the distribution of the two polymers and the microarchitecture, scaffolds were analyzed using SEM (**Figure 4.2**). No significant differences were observed between the two scaffolds except a reduction in pore sizes at high gelatin content (**Figures 4.6C and 4.6D**). Since a number of studies have formed scaffolds after cross-linking with 0.25% glutaraldehyde (Mao, Zhao et al. 2003), scaffolds formed using that techniques were also compared. These results showed microarchitecture similar to uncross-linked chitosan-gelatin scaffolds. All scaffolds were subsequently formed from refrigerated solutions without cross-linking.

4.3.2. Stabilizing chitosan and chitosan-gelatin scaffolds

Uncross-linked scaffolds were analyzed for stabilizing the scaffold while neutralizing acetic acid. After 10 min of neutralization in 100% alcohol, scaffold size did not change (**Figure 4.3**). When neutralized in 1N NaOH, size of chitosan-gelatin scaffolds did not change but chitosan samples deformed. Neutralization in 1% DS reduced the chitosan-gelatin scaffolds but not chitosan scaffolds. Cross-linking with 1% glutaraldehyde showed no size change in chitosan-gelatin scaffolds but chitosan scaffolds significant swelled.

After 24 h, all glutaraldehyde cross-linked samples turned yellow in color, and could not be held by tweezers and could not be transferred from one container to another without structural collapse. On the contrary, all chitosan scaffolds neutralized with 1% DS or 1N NaOH lost their cylindrical shape with size reduction and hard to work. Chitosan-gelatin scaffolds also shrunk significantly although cylindrical structure did not

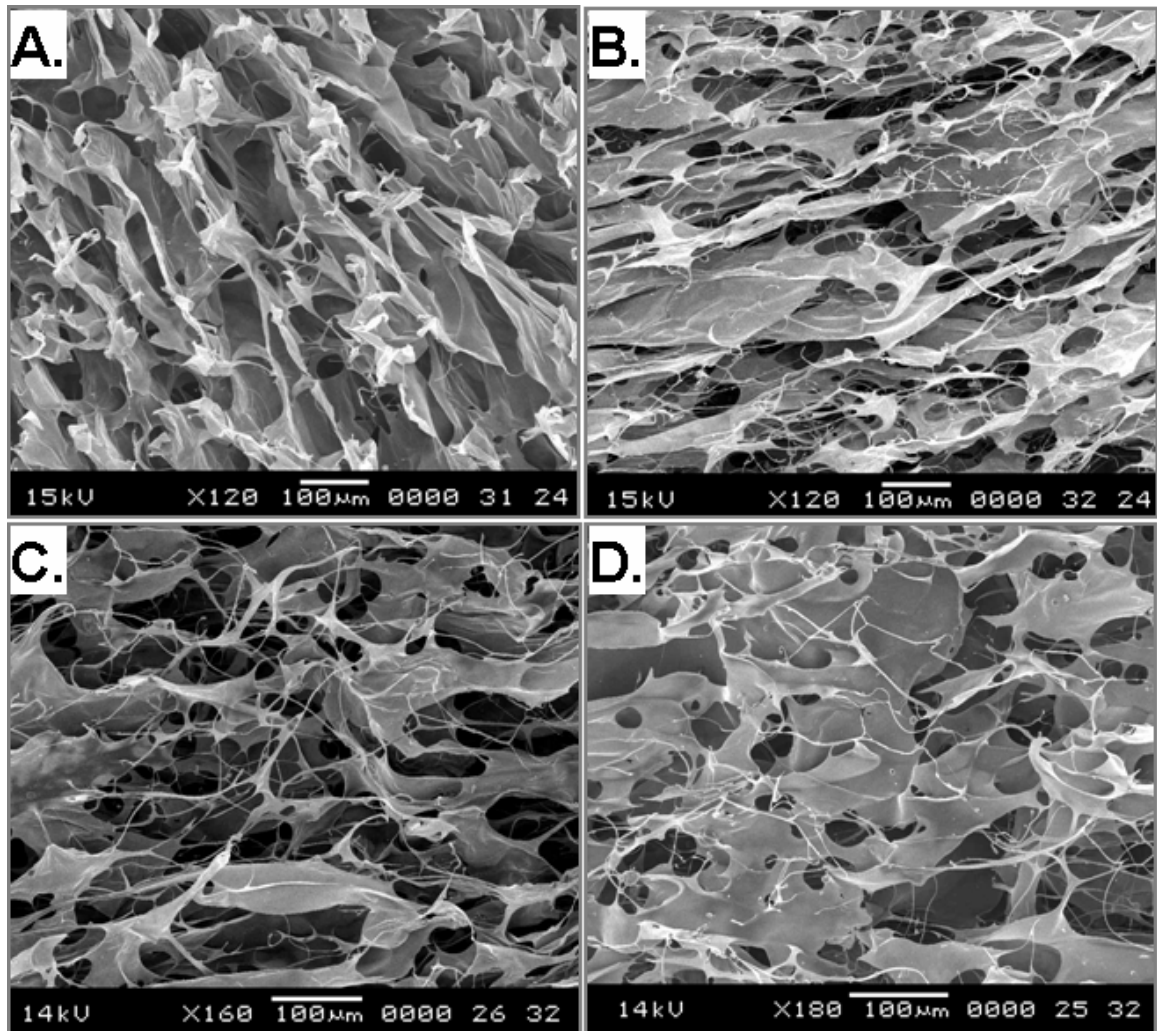


Figure 4.2. Microarchitecture of chitosan-gelatin scaffolds. All scaffolds were prepared by freezing solutions at -20°C and subsequent lyophilization. **Panel A.** Chitosan. **Panel B.** 1:3 (by wt) chitosan-gelatin without glutaraldehyde. **Panel C.** 3:1 (by wt) chitosan-gelatin after with glutaraldehyde cross-linking. **Panel D.** 1:3 (by wt) chitosan-gelatin after cross-linking with glutaraldehyde. Solutions were cross-linked prior to forming scaffolds.

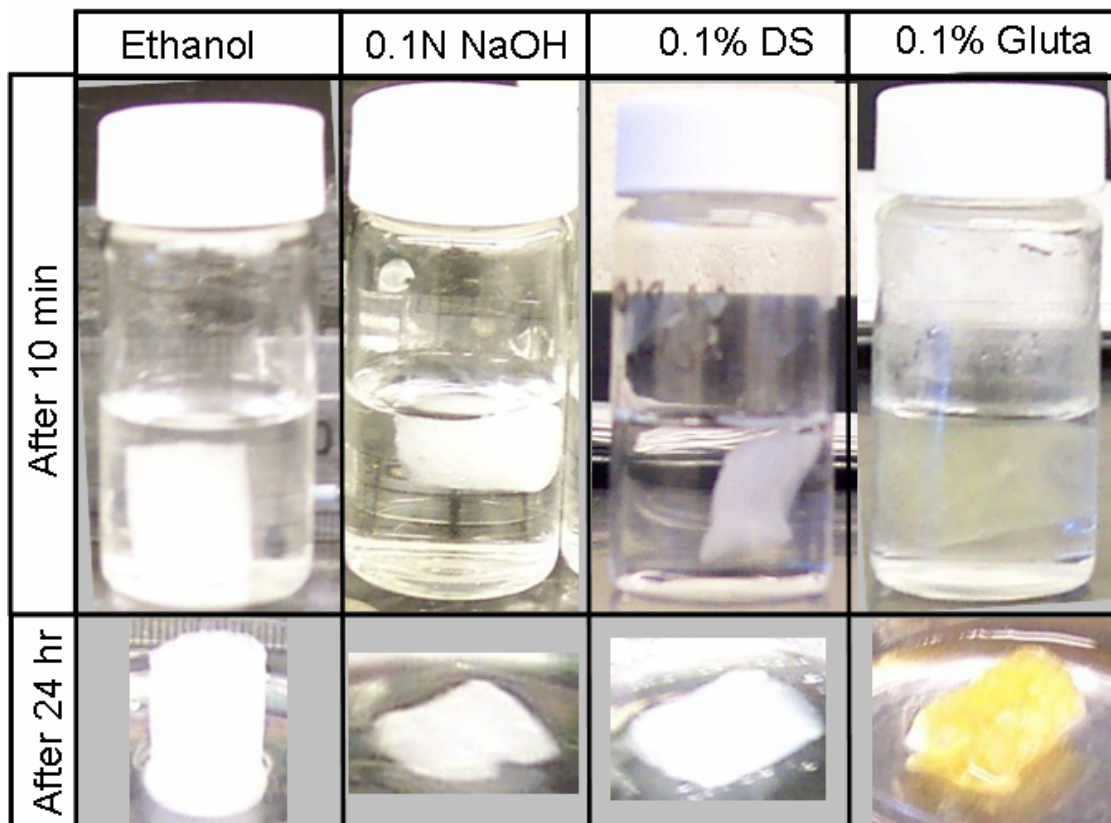


Figure 4.3. Effect of neutralization method on chitosan-gelatin scaffolds.

change, and were not difficult to handle. However, no changes in dimensions were observed in 100% ethanol and were easy to work with after 24 h. Hence, scaffolds were neutralized with 100% ethanol in all subsequent experiments.

4.3.3. Mechanical properties of chitosan-gelatin blends

Chitosan-gelatin membranes were tested for tensile properties were tested in dry and wet conditions. In dry condition, there was a significant increase in break stress with increasing gelatin content and gelatin alone had three-times the break stress of chitosan (**Figure 4.4A**). However in wet condition, an opposite trend was observed i.e., increasing gelatin content decreased break stress. In dry state, there was a decrease in the break strain with the addition of gelatin (**Figure 4.4B**). There was no clear relation between the break strain of the wet membranes and the gelatin content. When modulus values were calculated (**Table 4.1**), membranes with more gelatin had significantly increased stiffness in dry condition. On the contrary, presence of gelatin in the membranes decreased the stiffness in wet conditions and the stiffness of gelatin alone was the lowest with a 20-fold reduction relative to chitosan-gelatin (1:3) membranes.

Next, the compressive properties of cylindrical scaffolds were tested in wet conditions. These results showed (**Figure 4.4B**) a significant decrease in the stress range of chitosan and presence of gelatin increased the stress range by more than three times. However, strain range decreased in gelatin containing scaffolds. When stiffness was calculated (**Table 4.1**), a significant decrease was observed in chitosan scaffolds and the presence of gelatin increased the stiffness value by nearly 10 fold. These values were nearly twenty-five times lower than the corresponding 2D membranes (CG13) which showed the lowest stiffness values.

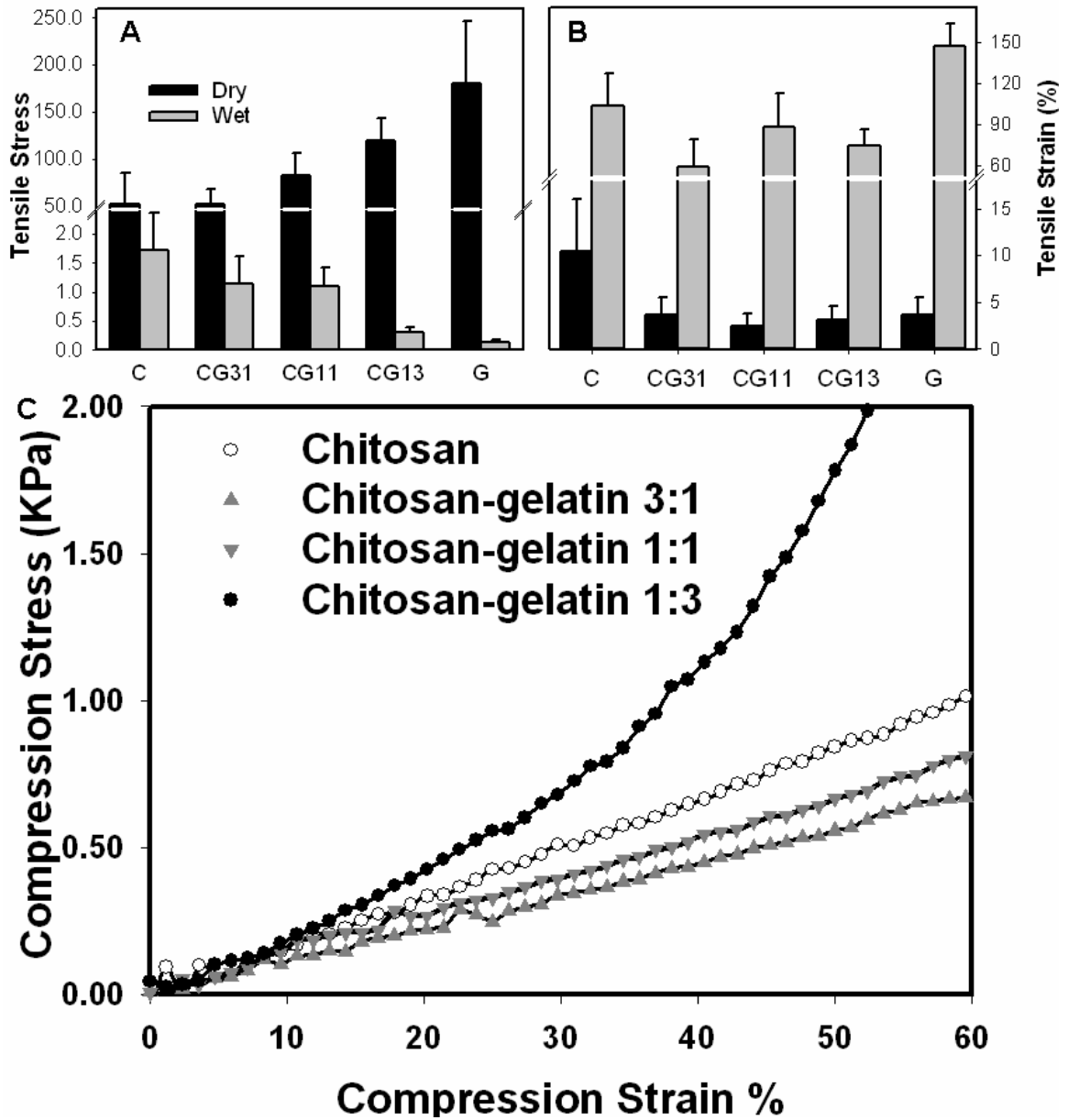


Figure 4.4. Mechanical properties. Panel A. Tensile stress of membranes. **Panel B.** Tensile strain of membranes. Cg31, cg11, cg13 refer to chitosan and gelatin blended at 3:1, 1:1 and 1:3 weight ratios. **Panel C.** Compressive stress-strain curve of 3D scaffolds.

Material	2-D Membrane (MPa)		3-D scaffolds (kPa)
	Dry	Wet	Wet
Chitosan	2054.25±1447.99	1.66±0.38	1.57±0.21
Chitosan-gelatin 3:1	1540.43±440.41	2.09±0.91	1.15±0.12
Chitosan-gelatin 1:1	7136.87±3043.78	1.22±0.20	1.31±0.05
Chitosan-gelatin 1:3	7774.89±3470.82	0.42±0.04	3.4±1.2*
Gelatin	8434.85±2804.08	0.09±0.02	

Table 4.1. Stiffness properties of blends.

4.3.4. Degradation kinetics of 3D scaffolds

To evaluate the degradation kinetics of the formed scaffolds, samples were incubated in lysozyme containing PBS with a weekly media change. The height (**Figure 4.5A**) measurements showed reduction in chitosan scaffolds incubated in lysozyme. However, presence of gelatin stabilized the reduction in size. Chitosan scaffolds incubated in PBS alone showed no significant weight changes after an initial gain of 40% within the first day (**Figure 4.5B**). Scaffolds incubated in lysozyme showed weight reduction only in the first four weeks with no significant changes in later time periods. Chitosan-gelatin scaffolds in PBS showed a reduction in weight, probably due to the loss of gelatin. However, presence of lysozyme decreased the weight further, suggesting degradation of chitosan in the blended scaffolds. At the end of eight weeks, the net weight of chitosan and chitosan-gelatin scaffolds in lysozyme were comparable. The measured pH of the incubation media indicated acidic conditions in scaffolds incubated in lysozyme containing PBS, probably due to the degraded chitosan products (**Figure 4.5C**). The maximum acidic condition occurred during the fourth week after which the pH remained closer to the initial PBS pH (=7.4).

To understand the influence on microarchitecture, scaffolds were analyzed via SEM. These results showed no significant changes in the porous structure in chitosan scaffolds with lysozyme (**Figure 4.5E**), without lysozyme (**Figure 4.5D**) and chitosan-gelatin scaffolds without lysozyme (**Figure 4.5F**). However, chitosan-gelatin scaffolds in lysozyme (**Figure 4.5G**) showed significant reduction in the material with increased porous structure.

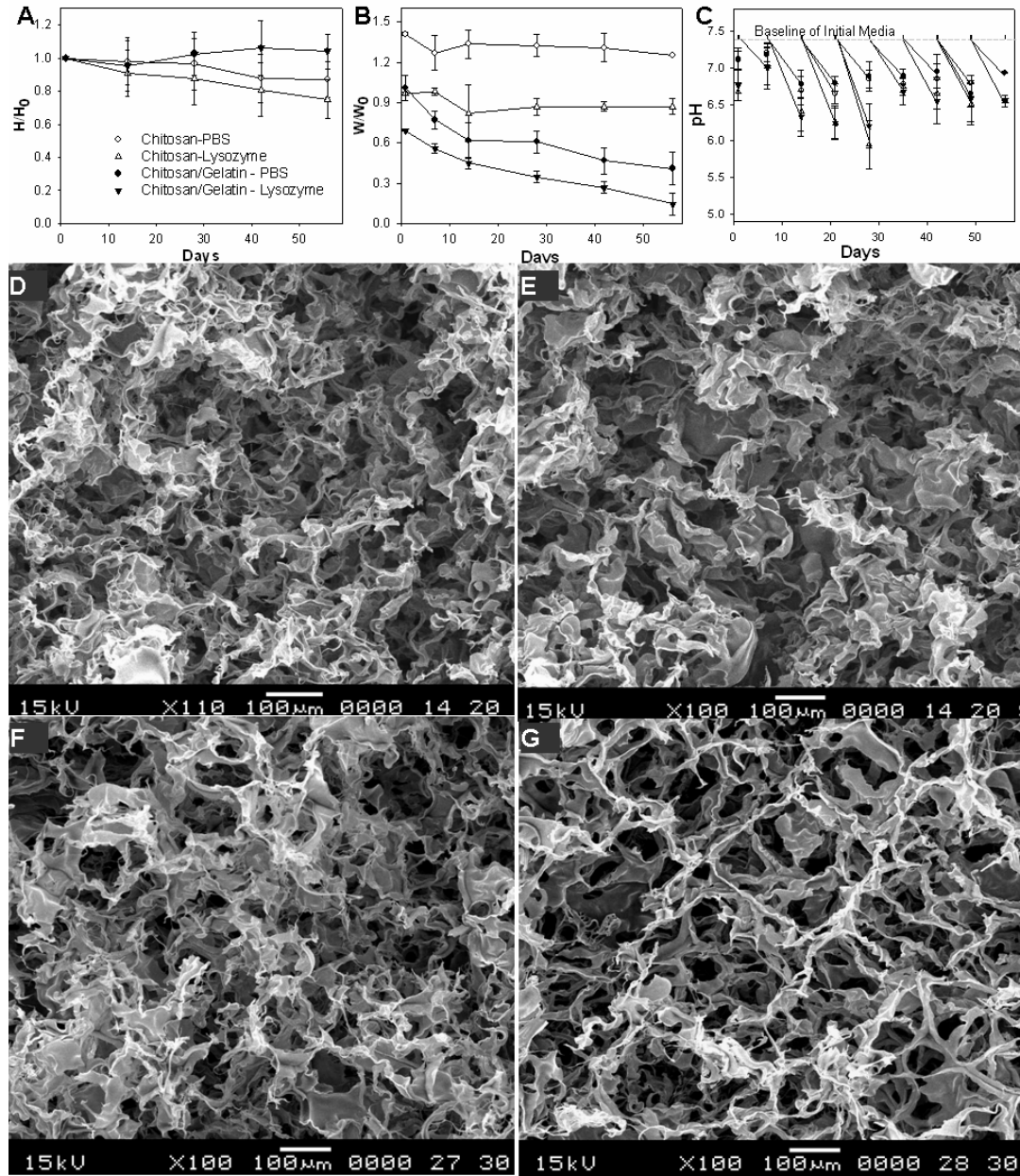


Figure 4.5. Degradation characteristics of chitosan-gelatin scaffolds. Panel A. Changes in the height relative to day zero values. **Panel B.** Changes in the weight relative to day zero values. **Panel C.** Changes in the pH of the media. After 56 days, scaffolds were analyzed for microarchitecture by SEM. **Panels D and E.** Chitosan scaffolds in in PBS or in lysozyme. **Panel E and F.** Chitosan-gelatin scaffold in PBS, or in lysozyme, respectively.

4.3.5. Evaluation of cell activity

To understand the importance of blending, MEFs were seeded onto 2D membranes and 3D scaffolds. Cell viability results showed (**Figure 4.6A**) a marginal reduction in the viability on chitosan membranes by day five. However, chitosan-gelatin (1:3) blends showed viability similar to tissue culture plastic (TCP). Viability on 3D matrices was compared by seeding cells at three times the cell density relative to 2D membranes. During these experiments, cell density on TCP surfaces were similar to 3D matrices which resulted in a very confluent monolayer after five days (**Figure 4.6B**), probably the maximum attainable in a 2D surface. Cell viability on 3D chitosan scaffolds, normalized with the confluent TCP, showed a significant increase in absorbance indicating the presence of more cells in the 3D matrix. Interestingly, no significant influence of blending high amount of gelatin was observed on the cell viability relative to chitosan scaffolds. To understand the difference in response, microstructure of the scaffold was analyzed in the wet state (**Figures 4.6C and 4.6D**) and when pore size distributions were quantified (**Figure 4.6E**), a reduction in pore sizes was observed in chitosan-gelatin (1:3) scaffolds. HUVECs were seeded into 3D chitosan and chitosan-gelatin matrices; it was found that cells had reduced microfilament spreading with increased composition of gelatin after two days of culture (**Figure 4.6F**). Especially in chitosan-gelatin (1:3) scaffolds, cells assumed round shape as bright dots without spreading as compared with chitosan scaffolds.

4.3.6. Cell adhesion on different membranes

The influence of blending in 2D configuration was evaluated by assessing HUVECs activity. Comparison of cell spreading area showed significant reduction on chitosan

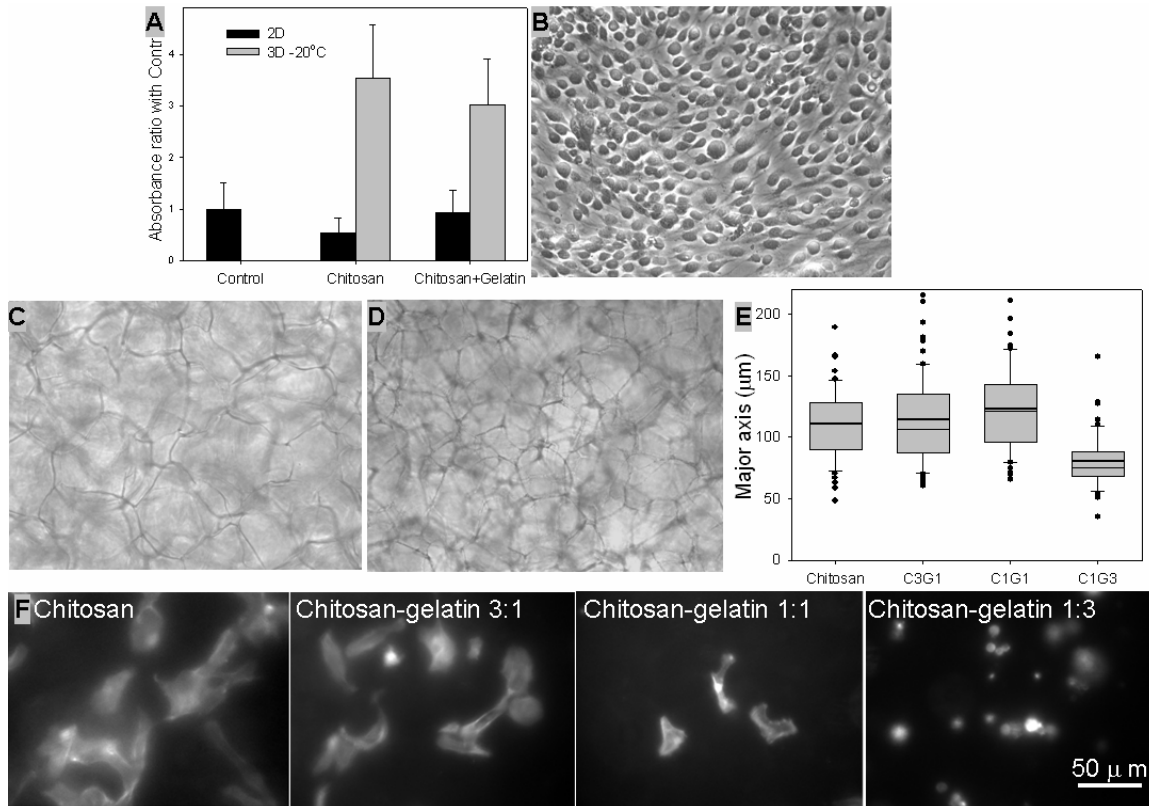


Figure 4.6. Activity of MEFs in 3-D matrices. **Panel A.** Viability after five days in culture using MTT. **Panel B.** MEF monolayer on TCP. **Panel C.** Phase contrast micrograph of chitosan scaffolds in PBS. **Panel D.** Phase contrast micrograph of chitosan-gelatin (1:3) scaffolds in PBS. **Panel E.** Box plots showing distribution of pore sizes in wet state. **Panel F.** Fluorescence micrographs of cells within chitosan and chitosan-gelatin stained with action after two days of incubation.

surfaces (**Figure 4.7A**) relative to TCP or gelatin surfaces. In addition, cells showed circular morphology rather than typical polygonal shape of HUVECs (**Figure 4.7B**), similar to other reports (Huang, Seiwe et al. 2005). Addition of equal mass of gelatin restored the HUVECs shape and size to that on gelatin surfaces.

To understand the alterations better, cytoskeletal organization of HUVECs was probed via actin staining. On chitosan membranes (**Figure 4.7C**), actin accumulated in the central region with fibers connected across the ends of the cells instead of the dense peripheral band (DPB) of actin observed on gelatin surfaces (**Figure 4.7E**). Addition of equal mass of gelatin restored the DPB of actin (**Figure 4.7D**) and inner actin accumulation was not observed, similar to gelatin surfaces. Next, the distribution of FAKs was analyzed because of the important role of FAs in regulating actin assembly. On chitosan (**Figure 4.7F**), significant accumulation of FAKs was observed within the nucleus and there was less localization of FAK near the actin fibers (**Figure 4.7I**). However, FAK was located in two parts on chitosan-gelatin (**Figure 4.7G**) membranes i) on the cell periphery and ii) around the nucleus, similar to gelatin (**Figure 4.7H**) surfaces. Superposition of the distribution of the FAK and actin on chitosan-gelatin membranes (**Figure 4.7J**) showed similarity with gelatin surfaces (**Figure 4.7K**) suggesting that the presence of gelatin plays a significant role in regulating cell spreading and size.

4.3.7. Effect of shear stress on morphological changes of ECs

To better understand the influence of blending in 2D configuration, behavior of HUVECs were analyzed under shear stress. When ECs are exposed to shear stress, ECs experience rapid changes in signaling cascades, gene regulation and cell morphologies (Azuma, Duzgun et al. 2000; Garcia-Cardena, Comander et al. 2001). The most obvious

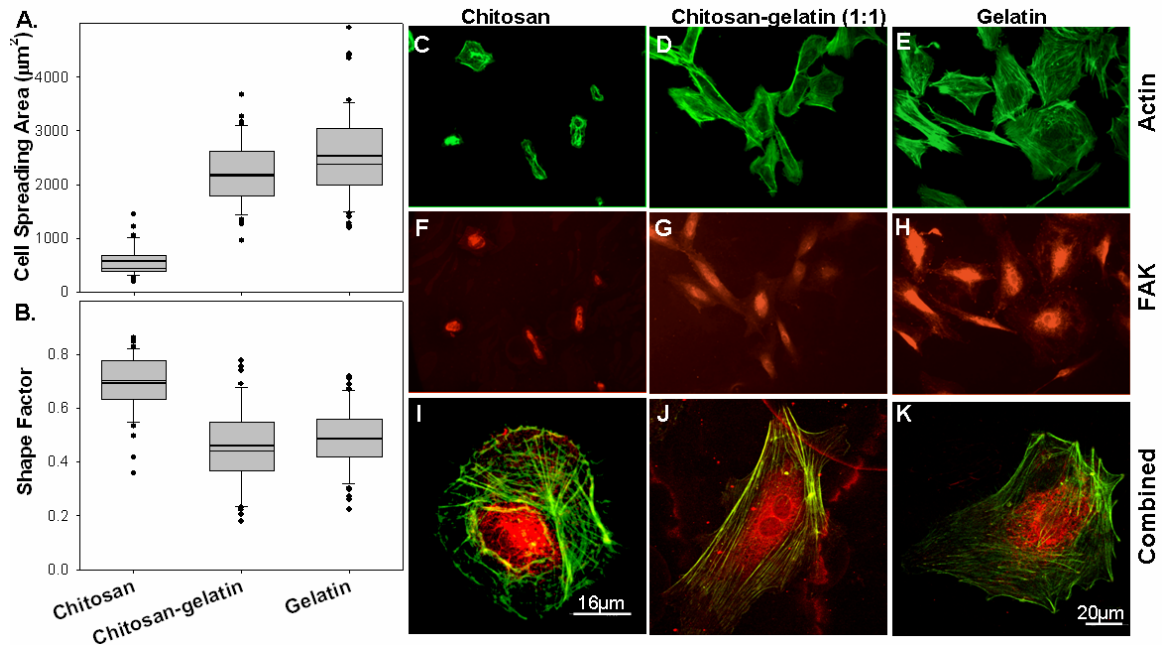


Figure 4.7. Effect of blending on the spreading of HUVECs. Cells were cultured for 2 days in on different membranes. **Panel A.** Box plots showing the distribution in the projected spreading area. **Panel B.** Box plots showing the distribution in the shape factor. **Panels C-E.** Fluorescence micrographs of cells stained for actin. **Panels F-H.** Fluorescence micrographs of cells stained for FAK. **Panels I-K.** Confocal micrographs of cells showing the combined distribution of actin and FAK.

morphological responses are elongated cell shape and alignment in the direction of flow (Davies, Barbee et al. 1997; Resnick, Einav et al. 2003). To investigate the influence of these matrices on supporting those phenomena, HUVECs were exposed to various levels of shear stress for 3 h. Interestingly, the lowest level of shear stress tested (4.5 dyn/cm^2) caused significant washout of cells on chitosan surfaces and further analysis could not be performed. However, no significant cell loss occurred in chitosan-gelatin membranes or gelatin membranes at 3 h, suggesting that addition of gelatin strengthened the cell adhesion to the matrix. In conjunction with the minimal spreading on chitosan, these results suggest that the cell adhesive forces by electrostatic interactions are weak. All subsequent experiments compared the difference between chitosan-gelatin and gelatin membranes only.

Comparison of cell spreading area (**Figure 4.8A**) on chitosan-gelatin showed marginal decrease at all shear stresses unlike gelatin surfaces where a significant increase was observed at 8.5 dyn/cm^2 shear stress and higher. However, no significant differences were observed in shape factor (**Figure 4.8B**). Next, analysis of cytoskeletal organization at 4.5 dyn/cm^2 shear stress showed DPB in both gelatin and chitosan-gelatin membranes (**Figures 4.8C and 4.8E**). However, at shear stresses 13 dyn/cm^2 and higher, disassemble of stress fibers were observed in cells present on chitosan-gelatin surfaces (**Figures 4.8D and 4.8F**).

4.3.8. Cytoskeleton reorganization

To understand the difference in response to shear stress on the two surfaces, cells were exposed to 8.5 dyn/cm^2 shear stress and monitored for changes in cell spreading characteristics for up to 48 h. These results (**Figure 4.8G**) showed that cell spreading

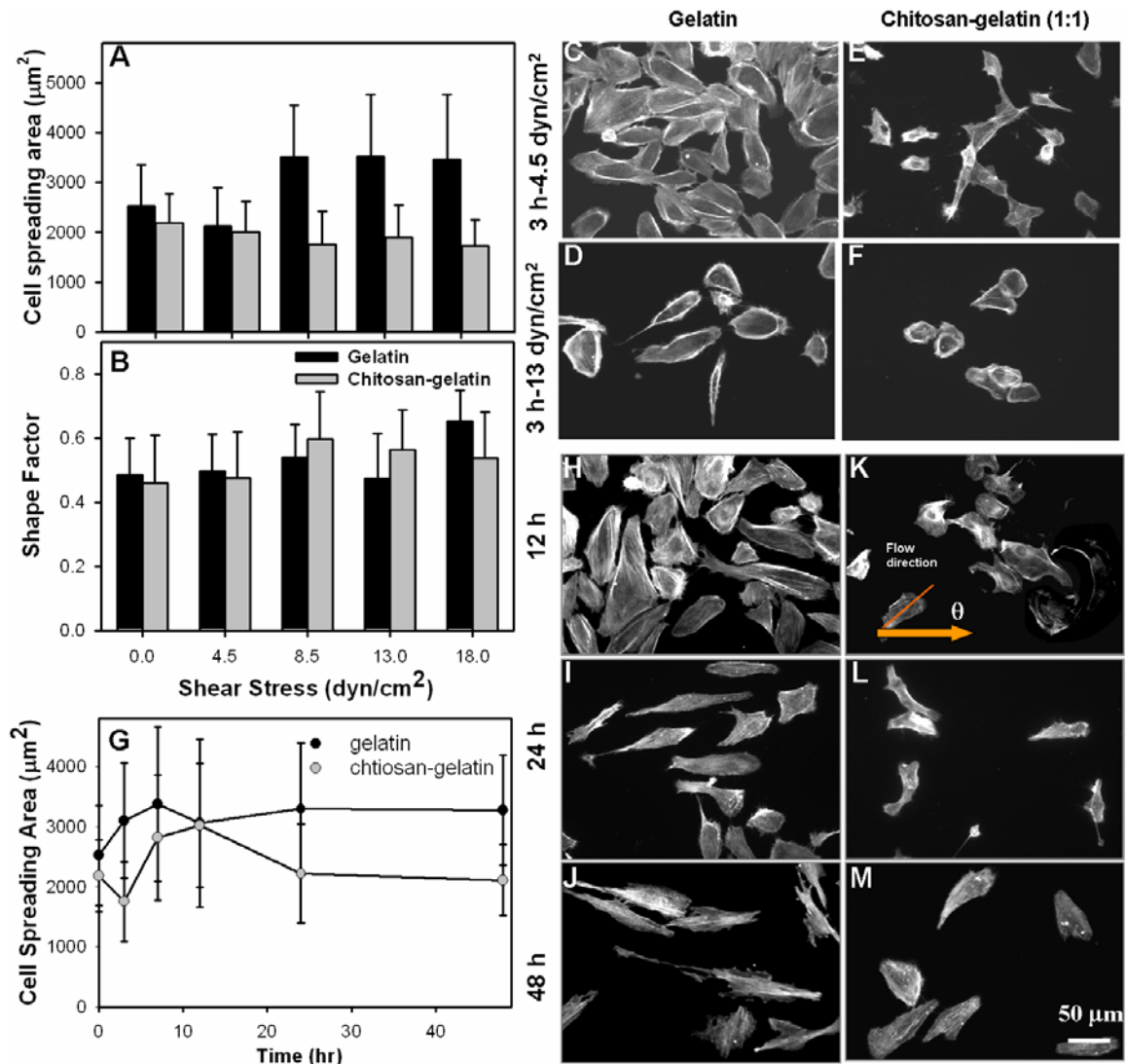


Figure 4.8. Effect of shear stress on the spreading of HUVECs. Panels A and B.

Bar graphs showing the distribution in the projected spreading area and shape factors of HUVECs exposed to various shear stresses for 3 h. **Panels C-F.** Micrographs showing the actin distribution of HUVECs exposed to shear stress of 4.5 and 13 dyne/cm^2 for 3 h. **Panel G.** Graph showing the alteration in the spreading characteristics. **Panels H-M.** Micrographs showing the actin distribution of HUVECs exposed to shear stress of 8.5 dyne/cm^2 for different periods of time. Spreading characteristics of at least 50 cells per condition were quantified.

area on both membranes stabilized after 24 h despite a difference in spreading areas. Calculated ratio of major axis length to minor axis length (**Table 4.2**) of individual cells showed no significant change on chitosan-gelatin surfaces unlike gelatin surface where HUVECs exhibited significant stretching along the major axis. In addition, angle of orientation in the direction of flow and the shape factor decreased in cells present on gelatin surfaces, suggesting that HUVECs align in the flow direction, in agreement with other reports (Sirois, Charara et al. 1998; Chiu, Chen et al. 2004). On the contrary, HUVECs on chitosan-gelatin exhibited little change in these parameters relative to static culture results.

To understand the difference between chitosan-gelatin and gelatin surfaces further, HUVECs were stained for actin. After 12 h, HUVECs on gelatin (**Figure 4.8H**) surfaces were still randomly distributed without orientation with flow direction. DPBs were visible at the edges of the cells and distributed in organized form. Longer exposure to shear stress (**Figures 4.8I and 4.8J**) on gelatin surface caused apparent cell elongation along with alignment of actin in the flow direction. However, HUVECs on chitosan-gelatin exhibited no significant changes except loss of cell population; at 8.5 dyn/cm^2 , after 24 h almost 50% of the cells were removed and at higher shear stresses, increased loss of cell population occurred at earlier time points (12 h) (**Figures 4.8K, 4.8L and 4.8M**). This is probably due to the decreased cell adhesion via the decreased RGD-binding domain per unit area of the matrix due to the presence of chitosan which could decrease the cell binding strength.

To better understand the differences, cells exposed to 13 dyn/cm^2 shear stress for 12 h were analyzed for FAK distribution. There were no significant differences between the

	Major axis length/ minor axis length	Orientation angle (°)	Shape factor
Gelatin 0h	2.22±0.78	43±28	0.49±0.11
Gelatin 24h	4.14±1.75 *	28±21 *	0.34±0.14 *
Chitosan-gelatin (1:1) 0h	2.52±1.02	51±27	0.50±0.15
Chitosan-gelatin (1:1) 24h	2.63±0.95	52±25	0.40±0.14

Asterisks indicate statistically significant differences between the two groups.

Table 4.2 Comparison of parameters describing cell morphology change in static and shear culture.

cells on gelatin surfaces (**Figure 4.9A**) to chitosan-gelatin surfaces (**Figure 4.9B**). At high resolution, the significant difference was less defined organization of actin fibers on chitosan-gelatin surface (**Figure 4.9D**) relative to gelatin surface (**Figure 4.9C**). This suggested that there could be other regulatory elements involving in changing actin distribution and cell spreading characteristics.

4.3.9. PECAM-1 expression

PECAM-1 is a cell-cell-junction molecule and establishes homophilic binding between neighboring ECs via extracellular domain in monolayered HUVECs (Albelda and Buck 1990). PECAM-1 interact with the underlying cytoskeleton and regulate assembly of F-actin at the cell periphery, in association with changes in cell shape and spreading (Osawa, Masuda et al. 2002; Newman and Newman 2003; Kaufman, Albelda et al. 2004). Since PECAM-1-mediated pathway could be involved in observed differences in cell behavior, the changes in the expression level of PECAM-1 to 8.5 dyn/cm² shear stress was analyzed via flow cytometry (**Figures 4.9E and 4.9F**). After 12 h exposure, no significant differences were observed on both the surfaces relative to respective static cultures. After 24 h, PECAM-1 expression significantly decreased on both gelatin and chitosan-gelatin surfaces. However, cells on membranes showed very low retention of shear stress. These results showed that the difference in cell response on two surfaces may not be due to PECAM-1 mediated signaling. Other cell-matrix adhesion molecules such as integrins and VE-cadherin and changes in gene expression levels of these molecules need to be investigated.

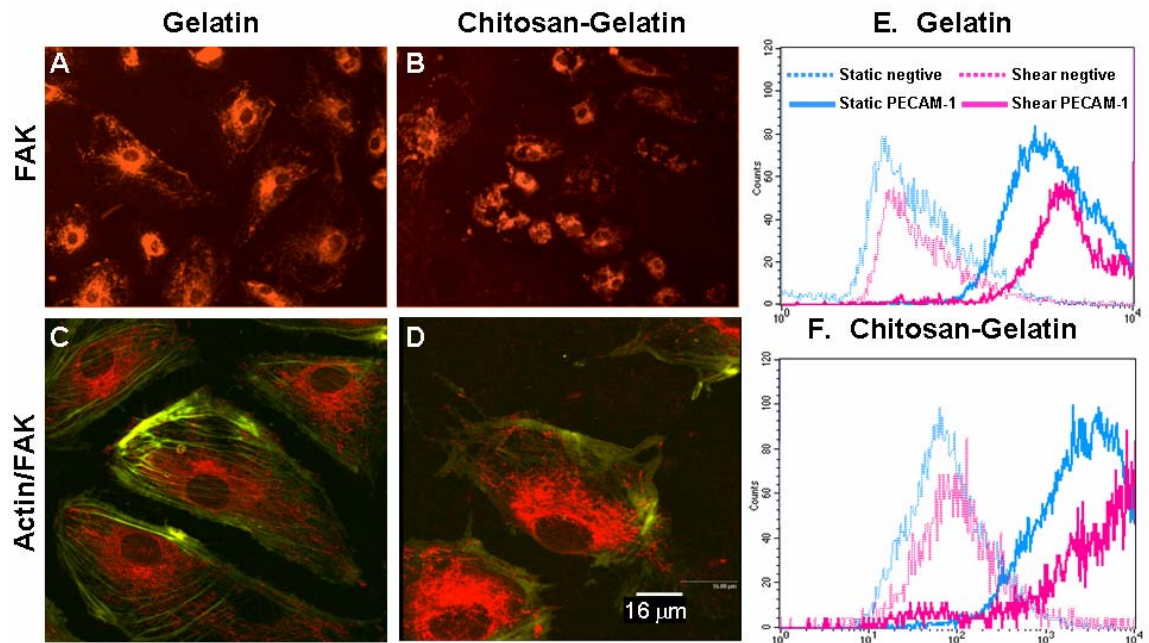


Figure 4.9. Effect of shear stress on actin assembly and PECAM-1 expression.

HUVECs were exposed to 13 dyne/cm² shear stress for 12 h. **Panels A and B.**

Fluorescence micrographs of FAK stained cells. **Panels C and D.** Confocal micrographs showing the combined distribution of actin and FAK. **Panels E and F.**

PECAM-1 histogram profiles of HUVECs exposed to shear stress of 8.5 dyn/cm² for 12 h and static culture. Cells stained with PE-conjugated isotype-matched irrelevant antibodies were used as controls.

4.4. DISCUSSION

The focus of this study was to understand the effect of blending chitosan and gelatin on various parameters important in tissue engineering in 2D and 3D scaffolds. The characterization of mechanical properties of the membranes showed that the addition of gelatin to chitosan improves the tensile stresses in dry condition. Different gelatin compositions greatly affected the membrane stiffness despite gelatin possessing very low stiffness relative to chitosan. The overall trend is similar to the published reports (Cheng, Deng et al. 2003), although the tensile properties cannot be directly correlated due to difference in strain rates. In addition, comparison of results with the published report indicates that the range of tensile stress after cross-linking is much higher than without cross-linking in both chitosan (Silva, Silva et al. 2004) and chitosan-gelatin membranes (Mao, Zhao et al. 2003).

The degradation study results showed significant weight reduction in gelatin-containing scaffolds. In addition, the degradation of uncross-linked chitosan-gelatin scaffolds is much higher than glutaraldehyde cross-linked chitosan-gelatin scaffolds, despite that double the lysozymal concentration was used relative to this study (Mao, Zhao et al. 2003). After eight weeks, the scaffold microstructure showed significant presence of chitosan in the scaffold. Probably no further degradation could occur in chitosan-based scaffolds after four weeks due to the lack of acetyl groups, necessary for lysozomal binding (Varum, Kristiansen Holme et al. 1996). Alternative techniques may be necessary for further degradation of chitosan with higher DD. However, dimensionality measurements showed no significant changes unlike *in vivo* studies where significant shrinkage of 1:1 chitosan-gelatin scaffolds was observed in the absence of

cellular components after 10 weeks (Xia, Liu et al. 2004). This could be due to the simultaneous degradation of gelatin either by matrix metalloprotease-2 (MMP-2, Gelatinase A), constitutively produced homeostatic enzyme, or MMP-9 (gelatinase B) (Makowski and Ramsby 1998), upregulated in acute and chronic inflammations. To understand the degradation kinetics of two enzyme-dependent polymers, degradation studies needs to be performed in presence of MMP-2 or MMP-9 and lysozyme.

Seeded cells showed different morphology on 2D chitosan surfaces than 3D matrices. In addition, 3D cultures showed higher cell survival relative to 2D control cultures, probably pliability and spatial structures of 3D scaffolds are more dominant in influencing cell behavior. In 2D and 3D environment, there may be different factors affecting cell behavior. In 2D substrata, cultured cells are restricted to spread on a single flat plane and the important factor affecting cellular activity is whether the substrate contains cell adhesion binding domain or not. On the contrary, 3D matrices provide spatial advantages for cell-cell and cell-matrix adhesion as well as support for cell traction. In previous chapter, it was showed that spatial architecture of scaffolds affect cell colonization (Huang, Seiwel et al. 2005) where cells exhibited different morphology in 2D and 3D scaffolds despite no change of chemical clues. In addition, many factors such as the compliance, stiffness (Harris, Wild et al. 1980; Harris, Stopak et al. 1981; Tan, Tien et al. 2003), hydrophilicity, surface topography affect various cellular processes (Ranucci, Kumar et al. 2000; Balgude, Yu et al. 2001). In 2D culture, cells are cultured on rigid glass surfaces coated with thin layer of matrices, and stiffness that matrices possess may be primarily contributed by the glass surface. However, in 3D cultures, the stiffness of the scaffolds will be different than glass surfaces and may

directly influence cell adhesion. The presence of gelatin did not affect the viability in 3D scaffolds suggesting no significant influence of cell-binding domain. However, the scaffold pore sizes were not the same and further studies are necessary to better understand the importance of cell-binding domain in 3D matrix. Furthermore, binding of serum proteins on 3D matrices could influence the observed behavior and the adhesion of serum proteins needs to be evaluated, similar to the 2D chitosan membranes which show binding of proteins comparable to TCP (Cuy, Beckstead et al. 2003).

Chitosan exhibits cell compatibility and elicit minimal immunological responses. However, it restricts cell spreading and cytoskeleton distribution (Chupa, Foster et al. 2000). The reduction in cell size is thought to be the results of strong electrostatic interactions associated with DD (Mao, Cui et al. 2004). On the contrary to this belief, attrition of cells under lowest shear stress suggests weak cell adhesion, despite high DD (85%). The difference in DD induced changes on cellular activity may not be significant relative to other cytoadhesive forces. Small observed differences in DD-induced changes could be due to indirect effects such as difference in the adsorption of serum proteins. Nevertheless, the inhibition of cell proliferation on chitosan scaffolds is due to reduced adhesion and not strong adhesion as suggested by a number of groups (Mao, Cui et al. 2004). In addition, loss of HUVECs on chitosan-gelatin at high shear stress and difference in response to shear stress further confirms the weakened cell adhesion in presence of chitosan. The strong binding characteristics of cell-matrix can prevent cells from detaching under mechanical stimuli as well as provide resistive force for cell traction thereby stabilizing the nucleo-cytoskeletal lattice(Chen, Mrksich et al. 1997). Therefore, cells on gelatin may anchorage to the direction of flow, find new binding sites,

protrude and adhere to the substratum through integrins and FA complexes due to the presence of multiple cell-binding domains. On the contrary, cells on chitosan-gelatin have less adhesive strength; they can either lose current binding while they can not recognize and anchor to new binding sites. Thus, cells showed less adaptation to the flow and they lose their cytoskeleton integrity. The analysis of actin, FAK and PECAM-1 showed no significant differences between chitosan-gelatin (1:1) and gelatin, it can not be concluded that cells demonstrate similar function on these membranes. To better understand the difference in response, one has to evaluate the changes in the expressions of other FA-elements such as paxilline (Panetti, Hannah et al. 2004), and signal transduction cascades leading to altered gene expression profiles and functional changes (Papadaki, Eskin et al. 1999).

4.5. CONCLUSION

The effects of blending gelatin with chitosan on scaffold stiffness properties and degradation kinetics were characterized in this study. The addition of gelatin greatly affected the stiffness of 2D and 3D scaffolds. Also, the presence of gelatin in chitosan facilitated the degradation rate and maintained the dimension stability in the presence of lysozyme. Evaluation of cell adhesive interactions showed decreased cell spreading area on chitosan membranes, accumulated actin and localized FAK inside HUVECs in static culture. Exposure to shear stress showed weak cell adhesion on chitosan surfaces. By adding gelatin to chitosan, HUVECs exhibited morphology similar to gelatin in static culture. However, the weaker binding strength was observed when higher shear stresses applied, conforming cell-chitosan adhesion is not very strong and the presence of cell-binding ligands can play crucial role in maintaining cell adhesion under forces in 2D

culture. In 3D culture, the influence of gelatin becomes more complex in respect to spatial effects. Although chitosan-gelatin scaffolds showed some promising perspectives in tissue engineering, mechanisms exploring 3D cell-matrix interaction need further investigated.

4.6. REFERENCES

- Albelda, S. M. and C. A. Buck (1990). "Integrins and other cell adhesion molecules." Faseb J **4**(11): 2868-80.
- Azuma, N., S. A. Duzgun, et al. (2000). "Endothelial cell response to different mechanical forces." J Vasc Surg **32**(4): 789-94.
- Balgude, A. P., X. Yu, et al. (2001). "Agarose gel stiffness determines rate of DRG neurite extension in 3D cultures." Biomaterials **22**(10): 1077-84.
- Bhadriraju, K. and L. K. Hansen (2002). "Extracellular Matrix- and Cytoskeleton-Dependent Changes in Cell Shape and Stiffness." Experimental Cell Research **278**(1): 92-100.
- Chen, C. S., J. L. Alonso, et al. (2003). "Cell shape provides global control of focal adhesion assembly." Biochem Biophys Res Commun **307**(2): 355-61.
- Chen, C. S., M. Mrksich, et al. (1997). "Geometric control of cell life and death." Science **276**(5317): 1425-1428.
- Chen, T., H. D. Embree, et al. (2003). "Enzyme-catalyzed gel formation of gelatin and chitosan: potential for in situ applications." Biomaterials **24**(17): 2831-41.
- Cheng, M., J. Deng, et al. (2003). "Study on physical properties and nerve cell affinity of composite films from chitosan and gelatin solutions." Biomaterials **24**(17): 2871-80.
- Chiu, J. J., L. J. Chen, et al. (2004). "A model for studying the effect of shear stress on interactions between vascular endothelial cells and smooth muscle cells." J Biomech **37**(4): 531-9.
- Chupa, J. M., A. M. Foster, et al. (2000). "Vascular cell responses to polysaccharide materials: in vitro and in vivo evaluations." Biomaterials **21**(22): 2315-22.
- Cuy, J. L., B. L. Beckstead, et al. (2003). "Adhesive protein interactions with chitosan: consequences for valve endothelial cell growth on tissue-engineering materials." J Biomed Mater Res **67A**(2): 538-47.

- Davies, P. F., K. A. Barbee, et al. (1997). "Spatial relationships in early signaling events of flow-mediated endothelial mechanotransduction." Annu Rev Physiol **59**: 527-49.
- Davies, R. C., A. Neuberger, et al. (1969). "The dependence of lysozyme activity on pH and ionic strength." Biochim Biophys Acta **178**(2): 294-305.
- Galbraith, C. G. and M. P. Sheetz (1998). "Forces on adhesive contacts affect cell function." Current Opinion in Cell Biology **10**(5): 566-571.
- Garcia-Cardena, G., J. I. Comander, et al. (2001). "Mechanosensitive endothelial gene expression profiles: scripts for the role of hemodynamics in atherogenesis?" Ann N Y Acad Sci **947**: 1-6.
- Girard, P. R. and R. M. Nerem (1995). "Shear stress modulates endothelial cell morphology and F-actin organization through the regulation of focal adhesion-associated proteins." J Cell Physiol **163**(1): 179-93.
- Harris, A. K., D. Stopak, et al. (1981). "Fibroblast traction as a mechanism for collagen morphogenesis." Nature **290**(5803): 249-51.
- Harris, A. K., P. Wild, et al. (1980). "Silicone rubber substrata: a new wrinkle in the study of cell locomotion." Science **208**(4440): 177-9.
- Heilshorn, S. C., K. A. DiZio, et al. (2003). "Endothelial cell adhesion to the fibronectin CS5 domain in artificial extracellular matrix proteins." Biomaterials **24**(23): 4245-52.
- Huang, Y., M. Seiwe, et al. (2005). "Effect of Spatial Architecture on Cellular Colonization." Biotechnology/ Bioengineering **Under revision**.
- Hynes Ro Fau - Zhao, Q. and Q. Zhao "The evolution of cell adhesion." (0021-9525).
- Kaufman, D. A., S. M. Albelda, et al. (2004). "Role of lateral cell-cell border location and extracellular/transmembrane domains in PECAM/CD31 mechanosensation." Biochem Biophys Res Commun **320**(4): 1076-81.

- Khor, E. and L. Y. Lim (2003). "Implantable applications of chitin and chitosan." Biomaterials **24**(13): 2339-49.
- Madhally, S. V. and H. W. Matthew (1999). "Porous chitosan scaffolds for tissue engineering." Biomaterials **20**(12): 1133-42.
- Makowski, G. S. and M. L. Ramsby (1998). "Identification and partial characterization of three calcium- and zinc-independent gelatinases constitutively present in human circulation." Biochem Mol Biol Int **46**(5): 1043-53.
- Malek, A. M., S. L. Alper, et al. (1999). "Hemodynamic shear stress and its role in atherosclerosis." Jama **282**(21): 2035-42.
- Mao, J., L. Zhao, et al. (2003). "Study of novel chitosan-gelatin artificial skin in vitro." J Biomed Mater Res **64A**(2): 301-8.
- Mao, J. S., Y. L. Cui, et al. (2004). "A preliminary study on chitosan and gelatin polyelectrolyte complex cytocompatibility by cell cycle and apoptosis analysis." Biomaterials **25**(18): 3973-81.
- Mao, J. S., L. G. Zhao, et al. (2003). "Structure and properties of bilayer chitosan-gelatin scaffolds." Biomaterials **24**(6): 1067-74.
- Newman, P. J. and D. K. Newman (2003). "Signal transduction pathways mediated by PECAM-1: new roles for an old molecule in platelet and vascular cell biology." Arterioscler Thromb Vasc Biol **23**(6): 953-64. Epub 2003 Apr 10.
- Nordtveit, R. J., K. M. Varum, et al. (1996). "Degradation of partially N-acetylated chitosans with hen egg white and human lysozyme." **29**(2): 163-167.
- Osawa, M., M. Masuda, et al. (2002). "Evidence for a role of platelet endothelial cell adhesion molecule-1 in endothelial cell mechanosignal transduction: is it a mechanoresponsive molecule?" J Cell Biol **158**(4): 773-85. Epub 2002 Aug 12.
- Panetti, T. S., D. F. Hannah, et al. (2004). "Extracellular matrix molecules regulate endothelial cell migration stimulated by lysophosphatidic acid." J Thromb Haemost **2**(9): 1645-56.

- Pangburn, S. H., P. V. Trescony, et al. (1982). "Lysozyme degradation of partially deacetylated chitin, its films and hydrogels." Biomaterials **3**(2): 105-8.
- Papadaki, M., S. G. Eskin, et al. (1999). "Fluid shear stress as a regulator of gene expression in vascular cells: possible correlations with diabetic abnormalities." Diabetes Research and Clinical Practice **45**(2-3): 89-99.
- Raghavan, D., B. P. Kropp, et al. (2005). "Physical characteristics of small intestinal submucosa scaffolds are location-dependent." J Biomed Mater Res A **73A**(1): 90-6.
- Ranucci, C. S., A. Kumar, et al. (2000). "Control of hepatocyte function on collagen foams: sizing matrix pores toward selective induction of 2D and 3D cellular morphogenesis." Biomaterials **21**(8): 783-93.
- Resnick, N., S. Einav, et al. (2003). "Hemodynamic forces as a stimulus for arteriogenesis." Endothelium **10**(4-5): 197-206.
- Sarasam, A. and S. V. Madihally (2005). "Characterization of Chitosan-Polycaprolactone Blends for Tissue Engineering Applications." Biomaterials (**in press**).
- Shigemasa, Y., K. Saito, et al. (1994). "Enzymatic degradation of chitins and partially deacetylated chitins." Int J Biol Macromol **16**(1): 43-9.
- Shigemasa Y, S. K., Sashiwa H, Saimoto H (1994). "Enzymatic degradation of chitins and partially deacetylated chitins." Int J Biol Macromol **16**(1): 43-49.
- Silva, R. M., G. A. Silva, et al. (2004). "Preparation and characterisation in simulated body conditions of glutaraldehyde crosslinked chitosan membranes." Journal of Materials Science: Materials in Medicine **15**(10): 1105.
- Sirois, E., J. Charara, et al. (1998). "Endothelial cells exposed to erythrocytes under shear stress: an in vitro study." Biomaterials **19**(21): 1925-34.
- Tan, J. L., J. Tien, et al. (2003). "Cells lying on a bed of microneedles: an approach to isolate mechanical force." Proc Natl Acad Sci U S A **100**(4): 1484-9. Epub 2003 Jan 27.

- Tiwari, A., A. Kidane, et al. (2003). "Improving endothelial cell retention for single stage seeding of prosthetic grafts: use of polymer sequences of arginine-glycine-aspartate." Eur J Vasc Endovasc Surg **25**(4): 325-9.
- Varum, K. M., H. Kristiansen Holme, et al. (1996). "Determination of enzymatic hydrolysis specificity of partially N-acetylated chitosans." **1291**(1): 5.
- Wozniak, M. A., K. Modzelewska, et al. (2004). "Focal adhesion regulation of cell behavior." Biochim Biophys Acta **1692**(2-3): 103-19.
- Xia, W., W. Liu, et al. (2004). "Tissue engineering of cartilage with the use of chitosan-gelatin complex scaffolds." J Biomed Mater Res **71B**(2): 373-80.
- Yin, Y., F. Ye, et al. (2003). "Preparation and characterization of macroporous chitosan-gelatin/beta-tricalcium phosphate composite scaffolds for bone tissue engineering." J Biomed Mater Res A **67**(3): 844-55.

CHAPTER 5

INFLUENCE OF MATRIX ARCHITECTURE ON ES CELL DIFFERENTIATION

5.1. INTRODUCTION

ES cells are pluripotent cells with the capacity of unlimited self-renewal and differentiation potential. ES cells represent a promising source for cell transplantation due to their unique characteristic of differentiation into cell lineages including endodermal, ectodermal and mesodermal cells (Keller 1995). Many somatic cell types have also been derived from mES cells or hES cells, such as neuronal cell (Rolletschek, Chang et al. 2001; Schuldiner, Eiges et al. 2001), hematopoietic cells (Kaufman, Hanson et al. 2001), cardiomyocytes (Sachinidis, Fleischmann et al. 2003), ECs (Levenberg, Golub et al. 2002; McCloskey, Lyons et al. 2003; Kaufman, Lewis et al. 2004). ECs have been derived from ES cells through the formation of embryoid bodies (EB) (Levenberg, Golub et al. 2002) or direct differentiation through 2D monolayer (Nishikawa, Nishikawa et al. 1998).

The ECM components and soluble factors play a significant role in affecting ES cell differentiation. By varying different substrata that cells are attaching, the differentiation process can be regulated. When mES cells are cultured on dishes coated with gelatin, fibronectin, type I collagen and type IV collagen, type IV collagen would support Flk-1⁺ cell (EC precursor cell) differentiation most efficiently (Nishikawa, Nishikawa et al.

1998). In addition, VEGF has been found to promote the differentiation of Flk1⁺ cells (Nishikawa, Nishikawa et al. 1998). Material used in that study contained cell-binding domain and thus facilitated cell adhesion on those substrates. However, it is not clearly understood how the ES cells differentiate or proliferate when cultured on materials that do not contain cell-binding domain and present in multiple forms. Chitosan, a naturally derived polysaccharide, does not contain cell-binding domain, has been shown to affect cellular behavior of mature cell types significantly when presented in different architectures and blending with different materials (as demonstrated in previous chapters). Especially 3D scaffolds, which can provide physical cues of porous structures and mechanical strength to guide cell colonization as well as chemical cues of cell-binding sites to support cell attachment and spreading. The goal of this study was to understand the influence of matrix components that do not have cell-binding domain on ES cell differentiation.

Murine CCE cell line has been modified to grow on gelatin-coated surface in the presence of leukemia inhibitory factor (LIF). In this study, we circumvented the EB formation method and attempted to directly differentiate ES cells in 2D monolayer in a more efficient way. The effect of EC medium on ES cell differentiation into EC was studied, conditioned medium and combined cytokines showed ES cell differentiation to EC. Further, the influence of chitosan on ES cell differentiation was evaluated in 2D and 3D configuration. Cells exhibited different differentiation morphology on gelatin, chitosan and chitosan-gelatin substrates. The presence of chitosan did not support ES cell attachment. To compare the differentiation difference in 2D and 3D culture, ES cells

were cultured in 3D scaffolds in the presence of VEGF. ES cells in 3D matrices exhibited significant variances compared with ES cells in 2D forms.

5.2. MATERIALS AND METHODS

Chitosan of >310kD MW (DD ≈85%), type A porcine skin gelatin, goat anti- Flk-1 and monothioglycerol (MTG) were obtained from Sigma Aldrich Chemical Co (St. Louis, MO). Murine ES (CCE cell lines) derived from 129/sv mouse strain (Robertson, Bradley et al. 1986; Keller, Kennedy et al. 1993) and fetal bovine serum (FBS, ES tested) were obtained from StemCell Technologies Inc. (Vancouver, Canada). EDTA, glutamine, and knockout Dulbecco's Modified Eagle's Medium (DMEM) were from Invitrogen Corp. (Carlsbad, CA). Mouse LIF (ESGRO), mouse monoclonal anti-SSEA-1 and VEGF were purchased from Chemicon (Temecula, CA). EGM-2 BulletKit was from Cambrex Biosciences (Walkersville, MD). Goat anti-mouse IgG, anti-rabbit IgG (H+L) and goat anti-mouse IgM were obtained from Biomeda Corp. (Foster City, CA). FITC labeled rabbit anti-goat IgG was from ICN Biomedicals Inc. (Aurora, OH). RPE-conjugated goat anti-mouse IgM and sheep anti-rabbit IgG were from Serotec (Oxford, UK). Monoclonal mouse CD31-FITC was obtained from Immunotech (Westbrook, ME) and rabbit polyclonal IgG Oct-4 was from Santa Cruz Biotechnology Inc. (Santa Cruz, CA). Alexa Fluor 488 AcLDL and Alexa Fluor 488 phalloidin were from Molecular Probes (Eugene OR).

5.2.1. Scaffold formation

Chitosan scaffolds were formed and characterized as described previously (chapter 3). In brief, 300 μ L 0.5% chitosan solutions was added into 24-well plate which were frozen at -20°C (in a freezer) followed by lyophilization for 24 h. The scaffolds were

sterilized with 100% isopropanol overnight and washed four times in PBS prior to cell seeding.

5.2.2. Cell culture

Undifferentiated mES cells were maintained in knockout DMEM supplemented with 15% fetal bovine serum (FBS, ES tested), 100 U/mL penicillin, 100 µg/mL streptomycin, 0.1mM non-essential amino acids, 2mM L-glutamine, 100 µM MTG, and 1000 U/mL LIF. Undifferentiated ES cells were cultured on gelatin coated flasks and passaged every two or three days following vendor's protocol.

To study ES differentiation on different substrata, 1×10^6 /mL cells were seeded to 6-well plates coated with gelatin, chitosan-gelatin (wt. 1:1) and chitosan in the ES maintenance medium without LIF. For the EC differentiation, ES cells were transferred to gelatin coated 6-well plate and fed with EGM-2 medium containing 2% FBS with the following supplements: hydrocortisone, fibroblast growth factor, insulin like growth factor-1, ascorbic acid, epidermal growth factor, vascular endothelial growth factor, GA-1000 (gentamicin/amphotericin) and heparin (EGM-2 BulletKit). The other cell samples were fed with EGM-2 with additional 30 ng/mL VEGF. The cultures were maintained at 37 °C, 5% CO₂ /95% air for two weeks and fed with fresh medium every four days. For 3D cell culture, 1×10^6 /mL cells were seeded into twenty four well plates filled with chitosan scaffolds. Sufficient shaking was performed to allow uniform cell seeding.

5.2.3. Morphological analysis

Morphologies were evaluated using an inverted microscope (Nikon TE2000, Melville, NY) outfitted with a CCD camera. Digital micrographs were captured from different locations.

5.2.4. Flow cytometry

At certain time intervals (day 6, 16), differentiated ES cells were dissociated with 0.01% trypsin/ 10 μ M EDTA, centrifuged and resuspended in PBS containing 2% FBS. For cell surface marker expression analysis, cells were incubated with goat anti-mouse IgG (1:100) for 20 min at 4°C to block nonspecific antibody binding. Cells analyzed for Flk-1 (VEGF R2) and SSEA-1 were first incubated with relevant primary antibodies: goat anti- Flk-1 and mouse monoclonal anti-SSEA-1 at 4 °C for 1h followed by incubation with secondary antibodies for 40 min at 4 °C. The secondary antibodies were FITC labeled rabbit anti-goat IgG and RPE-conjugated goat anti-mouse IgM. Goat anti-mouse IgG and goat anti-mouse IgM were used as isotype controls, respectively. For analysis of CD31, cells were incubated with monoclonal mouse CD31-FITC for 1h at 4 °C; cells that were not stained were used as control. Cells to be stained with intracellular Oct-4 were first fixed in 1% formaldehyde in PBS at room temperature (RT) for 20 min and then permeabilized with 1% saponin in PBS for 10 min at RT. Cells were incubated either with anti-rabbit IgG (H+L) as isotype control or rabbit polyclonal IgG Oct-4 for 1h at 4 °C followed by staining with RPE conjugated sheep anti-rabbit IgG for 40 min at 4 °C. Cells were washed again and analyzed using a FACSCalibur flow cytometer (Becton-Dickinson, San Jose, CA) by CellQuest software.

5.2.5. Immunostaining

Analysis for the acetylated LDL (AcLDL) receptor was performed by incubating cells in serum-free EGM-2 medium containing 10 μ g/mL Alexa Fluor 488 AcLDL for 4h at 37 °C. The samples were fixed with 3.7% formaldehyde for further observation. For

F-actin staining, cells were incubated with Alexa Fluor 488 phalloidin for 20 min in the dark after fixing at room temperature.

Flk-1 expressions were detected by first fixing cells in 3.7% formaldehyde and incubating with goat anti-mouse IgG (1:100) for 20 min at RT to block nonspecific antibody binding. After washing with PBS, cells were incubated with anti- Flk-1 for 1 h followed by incubation with FITC labeled rabbit anti-goat IgG for 30 min at RT. For CD31 staining, cells were stained with CD31-FITC for 1 h at RT. Samples were observed under fluorescence microscope and digital images were obtained.

5.2.6. Statistical analysis

All experiments were repeated three or more times with triplicate samples. Significant differences between two groups were also evaluated using a one way analysis of variance (ANOVA) with 99% confidence interval. When $P < 0.01$, the differences were considered to be statistically significant.

5.3. RESULTS

5.3.1. EC differentiation in conditioned medium

mES were grown in EGM-2 medium containing combined growth factors (VEGF, bFGF, EGF and IGF) which are shown to support EC growth and adhesion. First, the effects of the medium were tested on the differentiation of ES cells. One set of cell sample was fed with EGM-2 and another set was fed with EGM-2 + 30 ng/mL VEGF. Unlike other published reports, the promoting effect of VEGF on ES cells differentiation into EC was not observed. Attached cells exhibited a heterogeneous cell population with no EC-like cells by day 4 (**Figure 5.1A**). With more cells proliferating, alteration in morphology occurred. Cells gradually assumed a uniform elongated or stellate-shaped

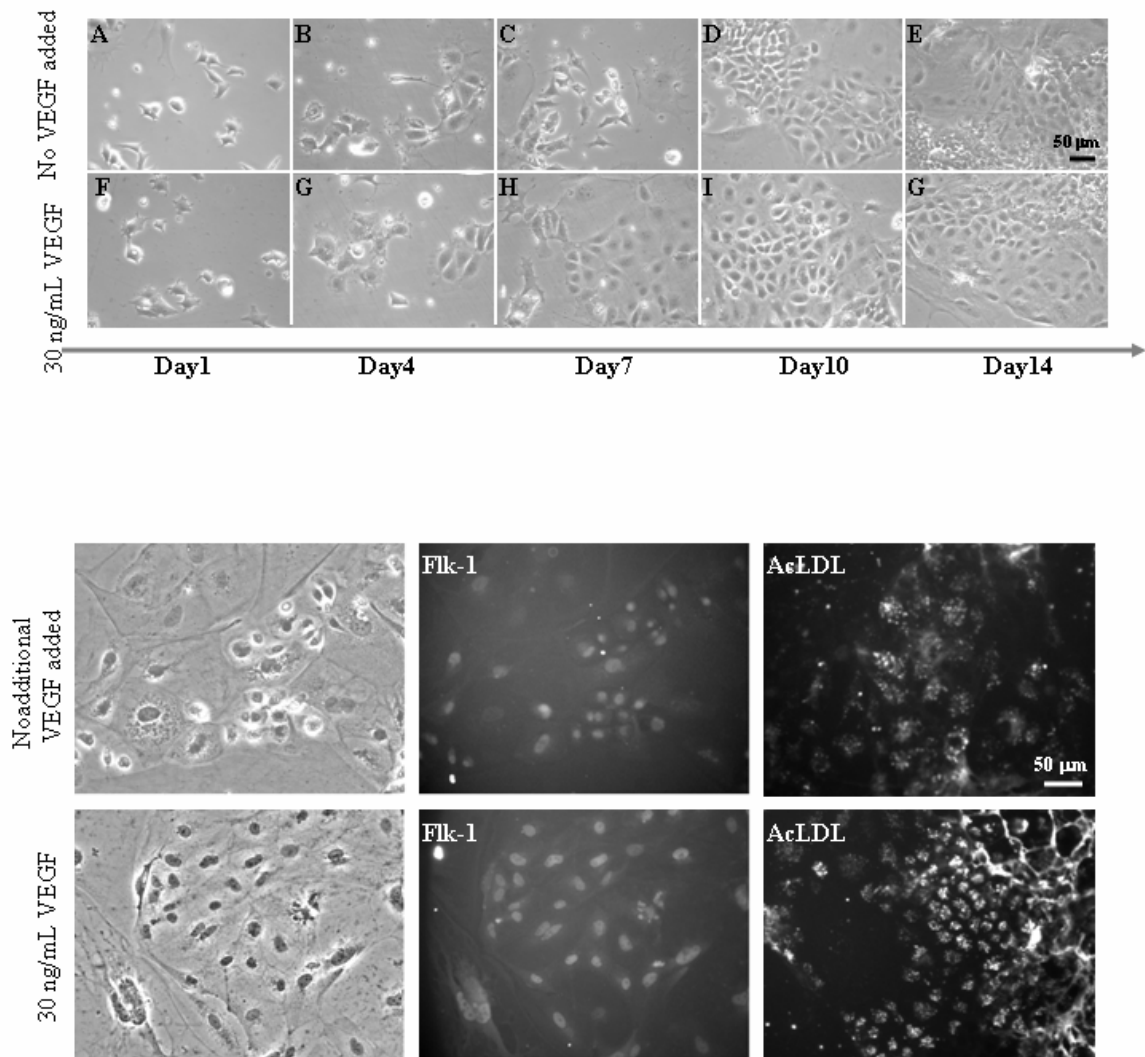


Figure 5.1. Effect of EC medium on ES cell differentiation after two weeks of incubation. Panel A. Phase contrast graphs showing changes in cell morphology during two weeks of culture. **Panel B.** Phase contrast and fluorescence micrographs of cells stained for Flk-1 and AcLDL. Cultures were performed with the additional VEGF added or not.

morphology and become flattened with characteristics of ECs (**Figure 5.1A**). Different from EC proliferation where cells divide equally, ES derived cells formed small colonies first, more cells grow from the centre of the colonies and the outskirt cells spread out and became flattened. After two weeks of incubation, cells in EGM-2 medium almost reached confluency with cells still proliferating inside the colonies. The ES-cell-derived cells showed positive staining for uptake of AcLDL, especially in the proliferating cells located inside colonies (**Figure 5.1B**). Flk-1 expression, however, exhibited uniform distribution in all the cells. CD31 expression was not detected in all the ES derived cells. Absence of CD 31 expression throughout the culture period was further confirmed by flow cytometry results (**Figure 5.2**). For Flk-1 expression, however, cells exhibited a positive shift compared with the early period where no expression was detected. These results showed that ES cells grew in conditioned EC medium undergo steps to differentiate into EC-like cells, exhibiting some features of EC cells.

5.3.2. Differentiation of ES cell on different 2D substrates

Murine CCEs can be maintained in undifferentiated state on gelatin coated flasks without mouse embryonic fibroblast feeder layer in the presence of LIF. To investigate how the ES cells differentiate in the absence of LIF, ES on gelatin, chitosan-gelatin and chitosan coated plates were cultured in ES maintenance medium in the absence of LIF. On day 1, ES cells formed small aggregates consisting of 5~6 cells on gelatin surfaces with few of them attached to the substrate (**Figure 5.3A**). Presence of chitosan decreased the aggregates size to 2~3 cells and chitosan alone showed individual cells suspended in the medium (**Figure 5.3B, Figure 5.3C**). After two days of culture, cells on gelatin attached with visible spreading, showed significant increase in cell

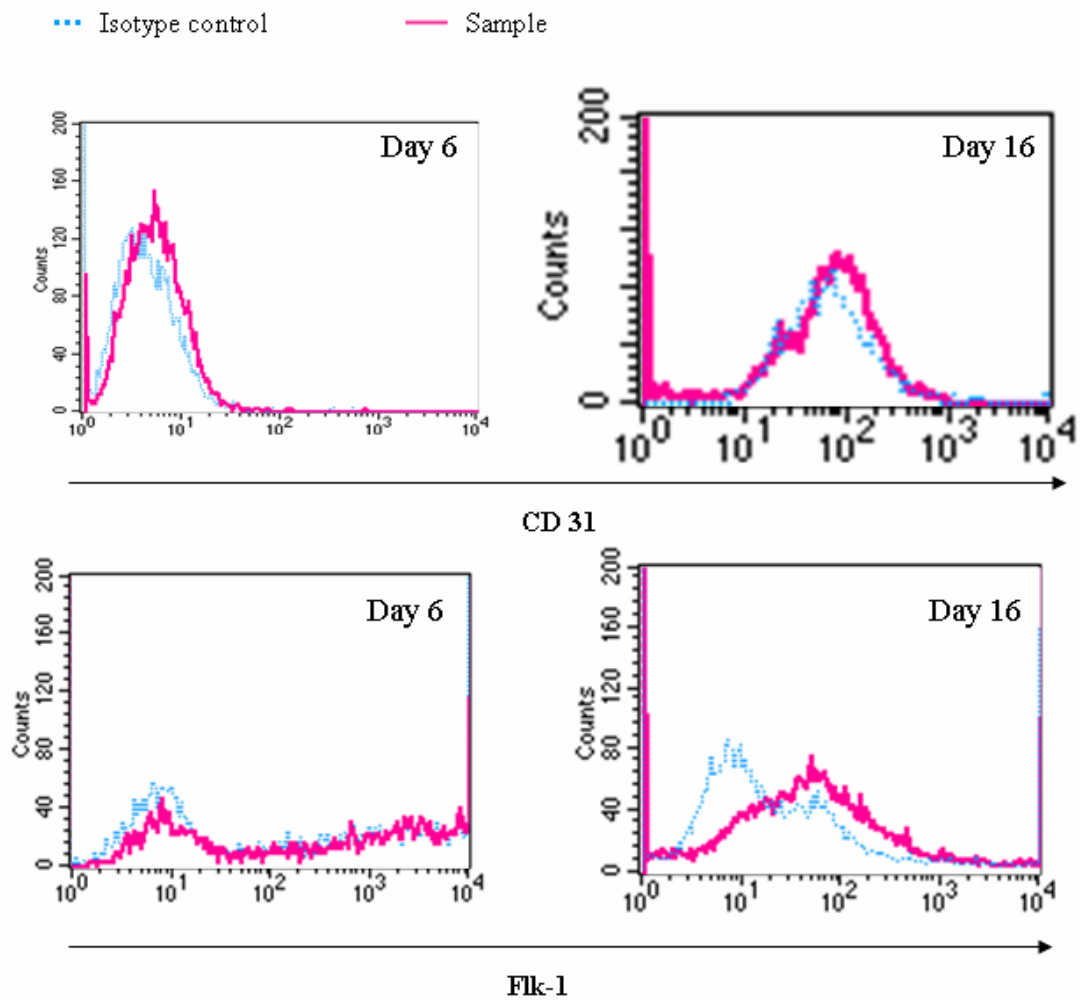


Figure 5.2. Histogram profiles of CD31 and Flk-1 expression showing ES differentiation after sixteen days incubation in EC medium.

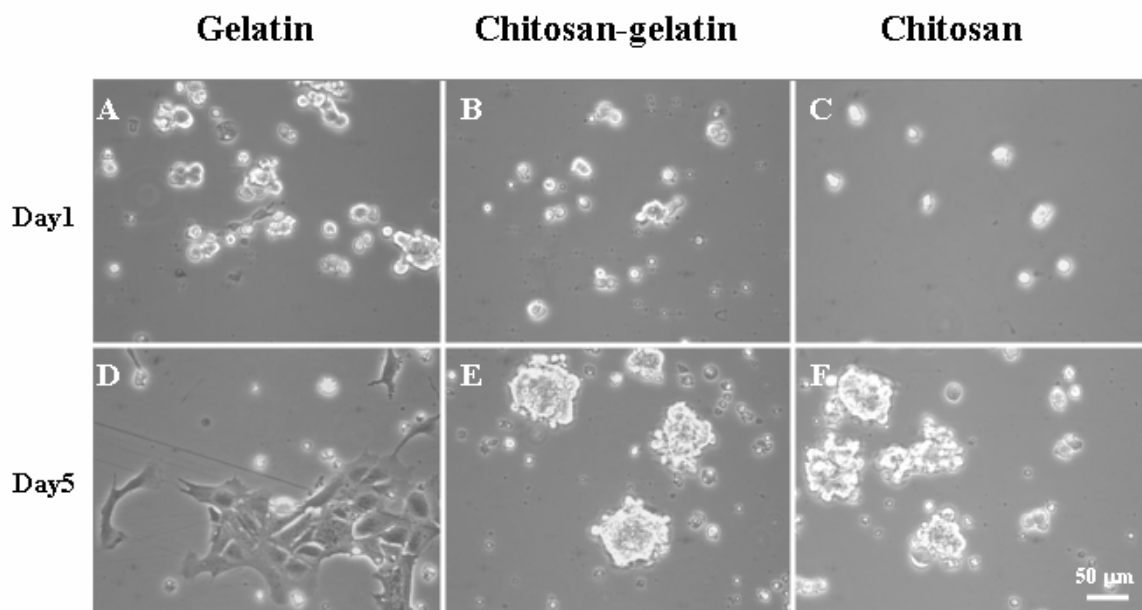


Figure 5.3. ES cells were differentiated on different substrates with the absence of LIF.

population, and reached confluency on day 5 (**Figure 5.3D**). Unlike cells exhibited flattened and adherent morphology, the granular colonies where single cells were not distinguishable in the undifferentiated state. Cells on both chitosan-gelatin and chitosan coated plates showed no adherent morphology; however, more cell aggregates were formed (**Figures 5.3E, 5.3F**).

Undifferentiated mES have both SSEA-1 and Oct-4 expression, confirmed by the flow cytometry results (**Figure 5.4A**). To understand the differentiation process further, differentiated ES cells on gelatin, chitosan-gelatin and chitosan surfaces were analyzed for SSEA-1 expression. These results showed that ES cells lost their SSEA-1 expression on day 3 on all three substrates (**Figure 5.4B**). Further analysis of endothelial marker Flk-1 in the cells showed that no expression in all the three cell populations (**Figures 5.4B, 5.5B**), demonstrating no EC differentiation. Cells on chitosan-gelatin and chitosan exhibited two populations on day 12 with one population having smaller cell size and high granularity (**Figure 5.5A**), but not on day 3. The percentages of the cell populations were analyzed. It was interesting to find that cells on gelatin surfaces showed biggest percentage of about 64% in gated area compared with cells on chitosan-gelatin surfaces of about 12%.

5.3.3. Influence of 3D architecture on mES cell differentiation

When ES cells were incubated with 3D porous chitosan scaffolds for two weeks, these cells showed different morphology than 2D differentiation. Instead of attaching and spreading on the substrate in 2D system, small cell groups distributed inside the pores and aggregates according to the pore structures without spreading (**Figure 5.6**). AcLDL and Flk-1 staining showed positive expression in 2D differentiation, however,

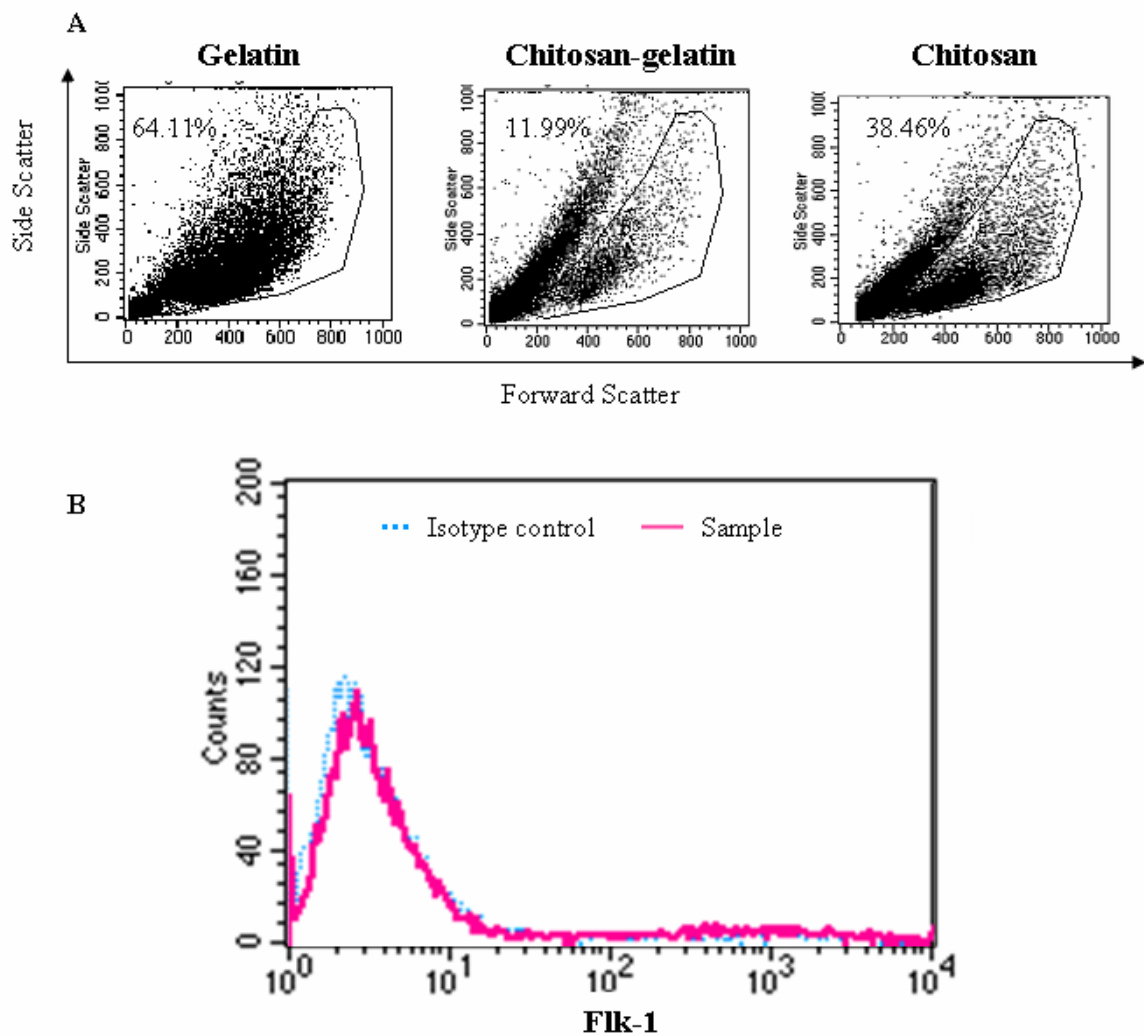


Figure 5.5. Flow cytometric analysis of ES cells on different substrates after twelve days of differentiation. Panel A. Dots plots showing the distribution of cell size and granularity. **Panel B.** Flk-1 expression of ES cell derived cells grew on gelatin.

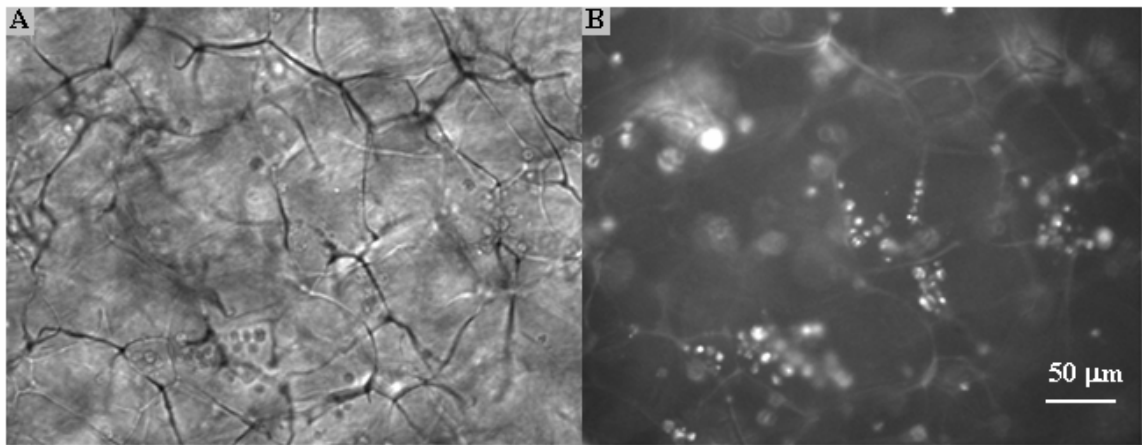


Figure 5.6. Phase contrast (A) and fluorescence micrographs stained with actin (B), showing ES cells within 3D chitosan matrices. ES cells were cultured for two weeks in EC medium.

were not detected using fluorescence microscope either due to the interference of chitosan background or no expression on these two markers in these cells.

5.4. DISCUSSION

This study focused on understanding the influence of growth factor cocktails and matrix architecture on ES cell differentiation.

Soluble factors play an important role in directing ES cells differentiation to ECs. The growth factors present in the medium include VEGF, IGF-1, FGF, EGF; these factors have been shown to stimulate EC proliferation and long-term maintenance *in vitro*. Additional 30 ng/mL of VEGF in the medium did not show significant differences in ES cell differentiation, probably due to the presence of VEGF already in the medium. The level might be saturated in affecting ES cell differentiation. The synergistic regulation of growth factors may have more important role in promoting EC differentiation than VEGF alone. The ES-cell-derived cells were characterized by expression of Flk-1 and uptake of AcLDL, which were consistent with EC phenotype. However, the ES-derived cell populations failed to express CD31, which is similar to other report (Kaufman, Lewis et al. 2004). The authors attributed the reasons for the lack of CD31 expression to the diversity of EC types from various tissues. Studies have shown that there are EC populations which don't express CD31 (Cines, Pollak et al. 1998; Balconi, Spagnuolo et al. 2000). Nevertheless, more studies are needed to understand the functional differences between ES-derived ECs and from matured ECs.

In 2D system, the presence of chitosan did not allow ES cell attachment, similar to previous reports on mature cells (i.e. HUVEC, MEF). Chitosan restricted cell spreading, probably due to weak cell adhesion attributed to the lack of cell-binding domain. In the

absence of adherent substrata, ES cells spontaneously formed 3D structures of EB consisted of cell aggregates in suspension, a method to induce ES cell differentiation *in vitro* (Keller 1995). The cell aggregate formation could be due to the dominant cell-cell adhesive force relative to cell-matrix adhesion. In ES cells, cell-cell adhesion could be stronger than in matured cells. If cell-matrix interaction is strong enough, cells are more likely to settle to the substratum; when such interaction is not available or very weak to allow cell set, cells can have interaction with each other to aid cell growth in suspension (i.e. the role of cadherin in promoting differentiation). Differentiated ES cells within EB have difference in morphologies from adherent cells on gelatin, featuring more granularity and smaller size as shown by the dot plots. The proliferation rate of ES derived cells is also different. On gelatin coated substratum, cells did not proliferate much in the first three days of culture. Once the cells were adherent, proliferation was very significant. Compared with adherent cells, non-adherent cells had a much slower growth. But the cells developed within cell aggregates need further investigation to characterize specified lineages.

In 3D chitosan matrices, cell colonies consisted of non-spread cells. This behavior is different from cells on 2D chitosan membranes, where small cell aggregates formed in suspension. It is also unlike ECs in 3D culture where cells spread within the pore structures, ES-derived cells did not spread within matrices. Compared with 2D differentiation, 3D scaffolds can provide spatial template to guide ES differentiation and thus 3D differentiation process may undergo different mechanisms in response to spatial effects. A higher level of 3D cell aggregates structure can be developed. For example, specified organization of human ES cell-derived-cells with 3D vessel-like network was

observed in PLGA/PLLA scaffolds (Levenberg, Huang et al. 2003). In addition, the formed cell aggregates within the matrices could be very different with EB formed in 2D culture in inner structures and cell homogeneity. Further, ES-derived ECs had the ability to develop complex tubular structures on collagen or Matrigel (Levenberg, Golub et al. 2002; McCloskey, Lyons et al. 2003; Kaufman, Lewis et al. 2004), suggesting functional similarity with matured ECs. However, further studies are needed exploring the mechanisms underlying ES cell differentiation in a 3D environment.

5.5. CONCLUSION

In vitro differentiation potential of mES cells were studied in 2D and 3D culture. Under the synergistic stimulus of EC medium components containing defined cytokines, ES cells showed EC differentiation even in the absence of EB formation. Without spreading within 3D chitosan matrices, ES cells formed cell aggregates distributed under the guidance of pore structures. The function of ES derived ECs and more mechanisms on 3D differentiation need further investigation.

5.6. REFERENCES

- Balconi, G., R. Spagnuolo, et al. (2000). "Development of endothelial cell lines from embryonic stem cells: A tool for studying genetically manipulated endothelial cells in vitro." Arterioscler Thromb Vasc Biol **20**(6): 1443-51.
- Cines, D. B., E. S. Pollak, et al. (1998). "Endothelial cells in physiology and in the pathophysiology of vascular disorders." Blood **91**(10): 3527-61.
- Kaufman, D. S., E. T. Hanson, et al. (2001). "Hematopoietic colony-forming cells derived from human embryonic stem cells." Proc Natl Acad Sci U S A **98**(19): 10716-21. Epub 2001 Sep 04.
- Kaufman, D. S., R. L. Lewis, et al. (2004). "Functional endothelial cells derived from rhesus monkey embryonic stem cells." Blood **103**(4): 1325-32. Epub 2003 Oct 16.
- Keller, G., M. Kennedy, et al. (1993). "Hematopoietic commitment during embryonic stem cell differentiation in culture." Mol Cell Biol **13**(1): 473-86.
- Keller, G. M. (1995). "In vitro differentiation of embryonic stem cells." Curr Opin Cell Biol **7**(6): 862-9.
- Levenberg, S., J. S. Golub, et al. (2002). "Endothelial cells derived from human embryonic stem cells." Proc Natl Acad Sci U S A **99**(7): 4391-6. Epub 2002 Mar 26.
- Levenberg, S., N. F. Huang, et al. (2003). "Differentiation of human embryonic stem cells on three-dimensional polymer scaffolds." Proc Natl Acad Sci U S A **100**(22): 12741-6. Epub 2003 Oct 15.
- McCloskey, K. E., I. Lyons, et al. (2003). "Purified and proliferating endothelial cells derived and expanded in vitro from embryonic stem cells." Endothelium **10**(6): 329-36.
- Nishikawa, S. I., S. Nishikawa, et al. (1998). "Progressive lineage analysis by cell sorting and culture identifies FLK1+VE-cadherin+ cells at a diverging point of endothelial and hemopoietic lineages." Development **125**(9): 1747-57.

Robertson, E., A. Bradley, et al. (1986). "Germ-line transmission of genes introduced into cultured pluripotential cells by retroviral vector." Nature **323**(6087): 445-8.

Rolletschek, A., H. Chang, et al. (2001). "Differentiation of embryonic stem cell-derived dopaminergic neurons is enhanced by survival-promoting factors." Mech Dev **105**(1-2): 93-104.

Sachinidis, A., B. K. Fleischmann, et al. (2003). "Cardiac specific differentiation of mouse embryonic stem cells." Cardiovasc Res **58**(2): 278-91.

Schuldiner, M., R. Eiges, et al. (2001). "Induced neuronal differentiation of human embryonic stem cells." Brain Res **913**(2): 201-5.

CHAPTER 6

CONCLUSIONS AND RECOMMENDATIONS

6.1. CONCLUSIONS

This research focused on the fundamental concepts of tissue engineering where the cells interact with biodegradable materials constructed as 2D membranes or 3D networks resembling natural ECM. Three elements were found to be key factors in regulating cellular behavior *in vitro*: i) cell-binding domain, ii) spatial architecture (2D and 3D forms) and iii) scaffold stiffness (the surface where cell contact with the scaffold).

The presence of cell-binding domain in the materials plays an important role in regulating cell adhesion on 2D matrices and the cell-binding strength is stronger than non-receptor mediated cell-material binding; however, role of cell binding domain may not be critical in 3D environment since cells can utilize spatial structures to facilitate cell adhesion to the matrix as well as to other cells. Thus, the pore structures and sizes of the scaffolds assume very dominant roles in guiding cell organization and activity in 3D matrix. Another important influencing factor is the stiffness of 3D scaffold which provides strength to withstand the cell tractional forces generated by the assembling cytoskeleton as well as binding sites. However, this issue is not important in 2D culture since membranes are on rigid tissue culture plastic or glass slides. Some of the conclusions from the three studies are as below.

6.1.1. Influence of architecture in the absence of cell-binding domain

2D and 3D chitosan and PLGA scaffolds were formed without varying inherent chemical composition. These two polymers don't have specific cell-binding domain. In 2D culture, both HUVECs and MEFs had significantly reduced spreading area and disassembly of actin distribution on chitosan and PLGA-chitosan membranes compared with TCP control due to the absence of cell-binding domain in the materials.

Emulsification of chitosan with chloroform further reduced the cell spreading area.

Changes in surface wettability may cause different adsorption of proteins/peptides on the surface due to the emulsification process. Further, cell spreading reduced on PLGA-chitosan membranes with increased MW of PLGA which revealed the effect of surface texture on cell behavior. The presence of different size of non-adhesive PLGA particles may form obstacles to cell movement and restrict cell spreading. Although all the factors combined to affect cellular behavior, the absence of adhesive component in the materials is the dominant factor for reduced cell spreading in 2D culture.

Compared with 2D system, actin filaments of HUVECs and MEFs spread in 3D chitosan matrices with brighter DPB distributed in the periphery of cells. However, cells did not spread in emulsified chitosan and PLGA-chitosan scaffolds. The variation in pore structures, decreased 3D scaffold stiffness, and lack of interconnectivity resulting from emulsification affect cell behavior. These results showed that the spatial structures can help and guide cellular reorganization *in vitro* despite the absence of cell-binding domain in 3D scaffolds. Cell behavior is markedly influenced by 3D architecture.

6.1.2. Influence of architecture in the presence of cell-binding domain

Cell matrix interaction was explored in 2D and 3D forms by adding gelatin, which contains cell-binding domain. In static 2D condition, the effect of gelatin was dominant in HUVECs cultured on chitosan-gelatin membranes. However, under mechanical stimulus, the presence of chitosan weakened cell adhesive strength. Further, cells exposed to chitosan-gelatin did not show elongation, alignment, and increased spreading area in response to shear stress, unlike cells on gelatin membranes. These results confirmed that cell interactions with chitosan is not very strong and the interaction is via electrostatics rather than direct integrin-binding. For the characterization of 3D scaffolds, addition of gelatin to chitosan greatly affected the mechanical properties of 2D and 3D scaffolds. The degradation study results showed significant weight reduction in gelatin-containing chitosan scaffolds than chitosan scaffolds. Presence of gelatin decreased the membrane stiffness or “softened” the membranes relative to chitosan. However, bulk stiffness of scaffolds increased. Nevertheless, the measured stiffness values may not correctly represent the tractional forces that individual pore surfaces provide. Weak surface stiffness may be the reason for decreased cell spreading in chitosan-gelatin scaffolds. However, small pore size ($<100\mu\text{m}$) in 1:3 chitosan-gelatin scaffolds could also affect cell ingrowth within pores. Thus the presence of cell-binding domain in 3D scaffolds, the architecture and stiffness of scaffold surface seem more important in regulating cellular behavior.

6.1.3. Influence of matrix on ES cell differentiation

mES cells were investigated to understand the influence of spatial architecture on cellular differentiation and proliferations. The substratum that ES cells adhere and the

growth factors contained in the conditioned medium play critical roles in regulating ES cell differentiation. In the absence of cell-adhesive component (gelatin) in the substratum, ES cells formed suspended EBs instead of adhering to the chitosan coated substratum. In EC medium, ES cells differentiated to ECs, as indicated by the presence of positive Flk-1 expression and uptake of AcLDL markers. After growing within 3D chitosan matrices, ES cells did not spread within the porous structures, showing different differentiation process from 2D system.

6.2. RECOMMENDATIONS

6.2.1. Study on the adsorption and deposition of ECM components

Significant differences were observed between 2D and 3D chitosan scaffolds. A possible explanation is the altered adsorption of ECM molecules onto the material surface from the serum of the culture media or deposited by cells (e.g., vitronectin, fibronectin, collagen, laminin). Cuy et al. (Cuy, Beckstead et al. 2003) measured the adsorption of various ECM proteins on the chitosan surfaces. Their results showed that the quantities of proteins adsorbed were similar to TCP. However, these proteins did not affect cell spreading characteristics. Nevertheless, to understand the influence of spatial architecture, one has to quantify the adsorption of some ECM molecules and compare the adsorption profiles on 2D and 3D scaffold surfaces, this will provide more insight into the observed differences (**Figure 6.1A**).

6.2.2. Evaluation of stiffness of material in the surface

Alterations in the mechanical properties were evaluated in this study. Although there was a correlation between cell spreading and stiffness, these measured properties are bulk properties. To better understand the influence of material stiffness on cell

behavior, it is more important to characterize individual fiber stiffness. AFM based measurements could be performed at physiological conditions. To understand the influence of stiffness in 2D configurations, membranes have to be formed on weak substrates rather than glass or TCP. To understand stiffness of fibers in 3D scaffolds, one can construct substrates with various stiffness (i.e. agarose gel, collagen gel) and then form chitosan membranes on the top (**Figure 6.1B**). Cells then can be seeded on top with the support of the substrates. The influence of stiffness on cell adhesion can be detected reflecting the interface characteristics between cells and substrates.

6.2.3. Cell behavior study on spatially well-defined patterns in 3D system

The scaffolds were fabricated by freeze drying method in this study, the pore sizes and orientation can be controlled by varying the pre-freezing temperature. However, more complex architectures were not produced in micro-scale features. Cell-binding domain should be spatially distributed in various patterns in the 3D environment and then the influence of the architecture on cell function should be tested. This would be very beneficial to understand cell colonization in 3D environment.

6.2.4. Characterization of surface wettability and charge

Characterization of basic physicochemical properties of the material surface, which is important for protein adsorption and cell-material interaction such as surface charge and wettability, have to be explored to better understand the observed differences between 2D and 3D architecture. Due to the negative charge of cells, they can attach the positively charged material surface by electrostatic interaction. Although electrostatic interaction is not very strong relative to receptor mediated cell-material interactions, it

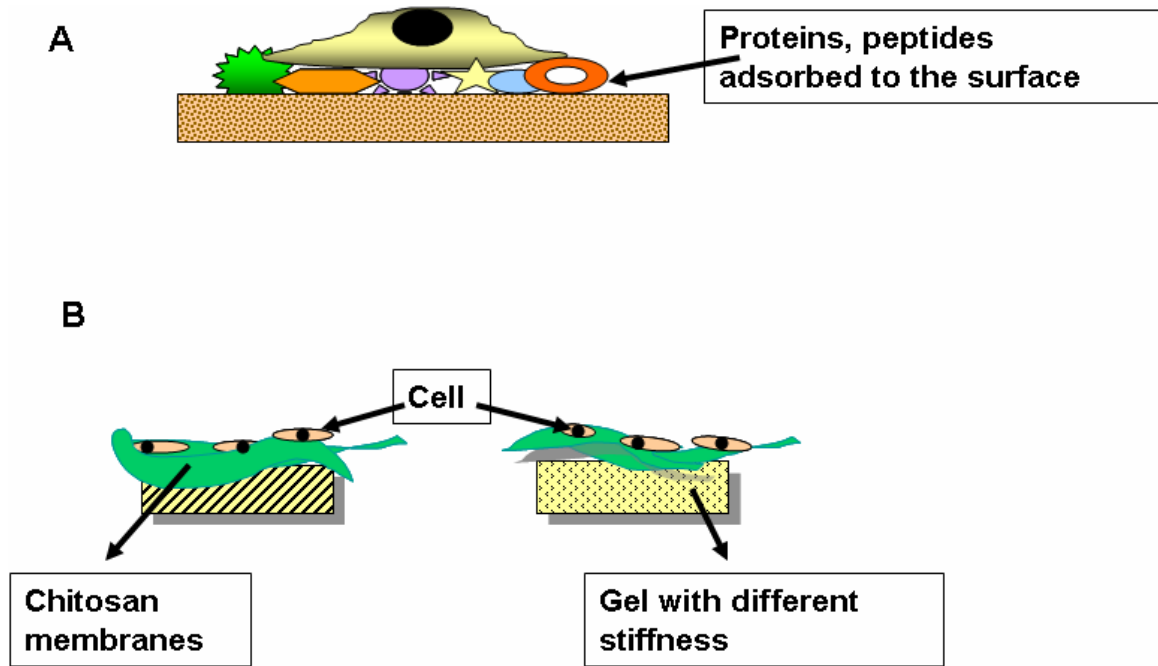


Figure 6.1. Schematic showing the adsorption of proteins to the surfaces (A) and evaluation of influence of scaffold stiffness on cell behavior.

plays a role in affecting adsorption of proteins to the material surface. In addition, cells generally favor hydrophilic surfaces because optimum protein absorption is usually achieved at hydrophilic conditions. Most biodegradable polymers have water adhesive tension (τ) in the hydrophobic/hydrophilic boundary ($\tau= 30$ dyne/cm), thus little modification on the surface can facilitate cell adhesion (Lim, Liu et al. 2004). The adjustment of wettability can be achieved using physical methods as well as chemical treatments. For example, treatment of PLGA, PLA and PGA with chloric acid can increase the surface wettability and lead to enhanced cell adhesion and proliferation (Lee, Khang et al. 2002; Lim, Liu et al. 2004).

6.2.5. Exploration on cellular signal transmitting structures in 3D culture

Cells interact with ECM at FA via integrins. The leading role of integrins in regulating cell-matrix interaction should be explored. Various combinations of α and β units can have preferential affinity to certain ECM molecules (Bacakova, Filova et al. 2004). Thus studying certain amino acid sequences integrin receptors bind can help understand the underlying mechanism in regulating cell adhesion. After ligand binding, integrin receptors are recruited into FA complexes by cytoskeleton. The FA associated proteins need to be studied such as talin, paxillin or vinculin due to their important role in linking integrin with cytoskeleton, influencing molecule transport, cell proliferation, differentiation and apoptosis (Ingber, Prusty et al. 1995). In addition, 3D cell-matrix differs with 2D interaction in cell adhesion, size, shape and distribution/spreading of FA plaques need to be investigated in 3D scaffolds.

6.3. REFERENCES

- Bacakova, L., E. Filova, et al. (2004). "Cell adhesion on artificial materials for tissue engineering." Physiol Res **53**(Suppl 1): S35-45.
- Cuy, J. L., B. L. Beckstead, et al. (2003). "Adhesive protein interactions with chitosan: consequences for valve endothelial cell growth on tissue-engineering materials." J Biomed Mater Res **67A**(2): 538-47.
- Ingber, D. E., D. Prusty, et al. (1995). "Cell shape, cytoskeletal mechanics, and cell cycle control in angiogenesis." J Biomech **28**(12): 1471-84.
- Lee, S. J., G. Khang, et al. (2002). "Interaction of human chondrocytes and NIH/3T3 fibroblasts on chloric acid-treated biodegradable polymer surfaces." J Biomater Sci Polym Ed **13**(2): 197-212.
- Lim, J. Y., X. Liu, et al. (2004). "Systematic variation in osteoblast adhesion and phenotype with substratum surface characteristics." J Biomed Mater Res A **68**(3): 504-12.

VITA

Yan Huang

Candidate for the Degree of

Doctor of Philosophy

Thesis: INFLUENCE OF SCAFFOLD PROPERTIES ON CELLULAR
COLONIZATION FOR TISSUE ENGINEERING

Major Field: Chemical Engineering

Biographical:

Personal Data: Born in Hubei, China, on January 17, 1975, the daughter of Xianti Huang and Boju Liu.

Education: Graduated from Zhijiang First High School, Zhijiang, Hubei in July 1992; received Bachelor of Science degree in Biochemical Engineering from Beijing Technology and Business University, Beijing, China in July 1996; obtained Master of Science degree in Applied Chemistry from Beijing University of Chemical Technology, Beijing, China in June 1999. Completed the requirements for the Doctor of Philosophy degree with a major in Chemical Engineering at Oklahoma State University in May, 2005.

Experience: Employed by Beijing Institute of Botany of Chinese Academy of Sciences as research assistant from 1999 to 2001; employed as a graduate research assistant by Oklahoma State University from 2001 to 2005.

Name: Yan Huang

Date of Degree: May, 2005

Institution: Oklahoma State University

Location: Stillwater, Oklahoma

Title of Study: INFLUENCE OF SCAFFOLD PROPERTIES ON CELLULAR
COLONIZATION FOR TISSUE ENGINEERING

Pages in Study: 161

Candidate for the Degree of Doctor of Philosophy

Major Field: Chemical Engineering

Scope and Method of Study: Scaffolds properties play crucial roles in regulating the cell-matrix interaction. To understand how the scaffolds architecture (i.e. pore structures), the presence of cell-binding domain and stiffness affect cell colonization within the scaffolds, 2D and 3D chitosan and poly (lactide-co-glycolide) (PLGA)-chitosan scaffolds without cell-binding domain were synthesized through controlled rate freezing and lyophilization. Cytoskeletal organization, morphology, and proliferation of Human umbilical vein endothelial cells (HUVECs) and mouse embryonic fibroblasts (MEFs) seeded on 2D, 3D chitosan, PLGA-chitosan scaffolds were characterized. Next, gelatin which contains cell-binding domain was blended with chitosan to investigate cell adhesion characteristics through receptor-mediated binding under static and shear conditions. Murine embryonic stem (mES) cells were used as model to study the differentiation process under the influence of substratum and medium components (i.e. cytokines).

Findings and Conclusions: Both HUVECs and MEFs showed circular morphology with reduced spreading area on 2D scaffolds while increased spreading and connected cell organization within 3D chitosan matrices. 2D and 3D emulsified chitosan and PLGA-chitosan scaffolds did not support spreading of HUVECs and MEFs. In gelatin-chitosan membranes, effect of gelatin was dominant; actin and focal adhesion kinase (FAK) distribution were comparable to gelatin in static culture. However, at higher shear stresses, presence of chitosan inhibited shear-induced increase in cell spreading and weakened cell adhesive strength. More composition of gelatin in the 3D chitosan scaffolds inhibited cell spreading within the porous structures. Similarly, the presence of chitosan in the membranes did not support mES attachment. These results support the hypothesis that the presence of cell-binding domain in the materials assumes the most important roles in regulating cell adhesion on 2D matrix whereas microarchitecture and stiffness are more important in 3D scaffolds on influencing cellular colonization.

Advisor's Approval: _____